Asymmetric extension and subsequent unroofing of the Pohorje pluton at the western margin of the Pannonian basin, Slovenia.

Tycho Z. de Bie, Inge E. van Gelder & E. Willingshofer

Master thesis, Utrecht University, Mei 2014

Abstract

The Pohorje pluton, an Early Miocene tonalitic to granodioritic intrusion close to the transition of the eastern Alps to the Pannonian Basin in northern Slovenia underwent rapid exhumation from mid crustal levels to the surface within 3 Ma. The timing of crystallization as well as of the exhumation path are well constrained by various isotope systems. However, the mechanism by which the Pohorje Pluton was exhumed is still unknown. In this study we use structural fieldwork and the analysis of microstructures to shed light on the processes, which led to the exhumation of the Pohorje Mountains in the frame of Miocene Alps-Adria convergence and coeval Pannonian Basin extension.

The new field data reveal three stages of deformation: D1 is characterized by isoclinally folded quartz veins and a penetrative foliation (S1), D2 by recumbent, tight folds, with axial planar foliation (S2) and are interpreted to represent nappe stacking and associated metamorphism within Austroalpine units surrounding the Pohorje pluton. D3 also affects the pluton and thus constrains the Early Miocene age of deformation. D3 is associated with the formation of E-W oriented stretching lineations, and top-to-East sense of shear within mylonitic zones under retrograde, lower greenschist metamorphic conditions. D3 deformation localized at former nappe contacts and led to the omission of part of the metamorphic succession. This asymmetric East-directed shear suggests exhumation of the pluton along an east-dipping low-angle detachment, which also provides an explanation for the differential exhumation (higher in the east) of the pluton. Detachment faulting was coeval with N-S shortening probably contributing to the doming of the structure as well as to folding and tilting of adjacent Lower Miocene sediments, which was amplified by later convergence during the Pliocene to Quarternary. The style of deformation is similar to other regions at the transition of the Alps to the Pannonian basins suggesting that footwall exhumation along low-angle detachments is strongly linked to the Pannonian Basin extension.

Table of contents

Introduction

The Pohorje and Kozjak mountains are small mountain ranges in NE-Slovenia. Together they comprise the easternmost part of the Alps (figure 1). The mountain ranges are bounded by Miocene age sedimentary basins on three sides: the Styrian basin to the north and the Mura basin to the south east and east. Both are subbasins of the larger Pannonian basin, a landlocked basin between the Alpine, Carpathian and Dinaric mountains. Thus, the Pohorje area is located at the critical transition zone where mountain building due to Adria-Europe convergence and mountain destruction due to extensional basin formation interferes.

The Pohorje and Kozjak mountains consist of various metamorphic and igneous rocks. Structurally, the metamorphic rocks are part of different Austroalpine nappes (Janak et al., 2004). The W to NW-directed nappe stacking occurred during the Cretaceous and is likely to be associated with the closure of an embayment of the Neotethys ocean (Schmid et al., 1996, Schmid et al., 2008). The metamorphism related to this event is referred to as Eoalpine, as it predates the metamorphism in other parts of the Alps, where the metamorphic overprint typically is of Paleogene age. The lower nappe in the Pohorje area records regional amphibolite facies metamorphism containing slivers of high pressure to ultra-high pressure (UHP) rocks (Vrabec et al., 2012, Janak et al., 2004, Janak et al., 2006). The upper nappe consists of low-grade metamorphic basement and a non-metamorphic cover.

The Austroalpine basement of the Pohorje and Kozjak Mountains has been intruded by the Pohorje Pluton, an elongate, granodiorite-tonalite intrusion. The age of the pluton is analysed by U-Pb zircon dating, and a Miocene crystallization age of 18.64 ± 0.11 Ma was determined (Fodor et al., 2008). This crystallization age distinguishes the Pohorje pluton from Oligocene age tonalite intrusions, which are located along the Periadriatic lineament. Therefore, a genetic link with these Periadriatic intrusions is highly questionable.

The pluton intruded at average depths of 14 km, and was subsequently exhumed to the surface in approximately 3 My, as is indicated by Karpatian sediments of ~16,5 Ma that contain tonalite pebbles, eroded from the pluton (Steininger et al., 1988, Fodor et al., 2008). The proposed rapid exhumation is in good agreement with cooling ages of the Pohorje pluton. Cooling ages derived from K/Ar whole rock and mineral dating (~18-16 Ma) as well as from zircon fission track analysis (~17,7-15,6 Ma), also imply rapid cooling after emplacement of the pluton (Fodor et al., 2008). Thus, the crystallization age of the igneous rocks and the subsequent rapid cooling of the pluton and surrounding host rocks are well constrained. It is well established that intrusion and subsequent cooling of the Pohorje pluton was synchronous with the subsidence in the Pannonian basin. However, the mutual relationship between basin formation and exhumation of the Pohorje and Kozjak mountains is unknown. In particular, detailed structural work describing structures and mechanisms that have accommodated Miocene exhumation of the Pohorje pluton are largely lacking.

In this research, the main emphasis is on collecting outcrop- and micro-scale structural and kinematic data from the igneous and metamorphic rocks in the Pohorje and Kozjak mountains. These data are used to identify structures and their kinematics, which can be related to the exhumation of the Pohorje mountains. Based on the new data set we discuss possible exhumation mechanisms and the link of rock exhumation to Pannonian basin formation.

Geological background

Polyphase deformation driven by the convergence of two major plates, the European plate to the north and the African plate to the south, has resulted in multiple orogens, such as the Alps, the Carpathians and the Dinarides (figure 1). The Pannonian basin is a back arc basin that is situated between these mountain ranges.

The Pohorje mountains are located at the contact between the Eastern Alps and the Pannonian basin (figure 1). The following sections provide the tectonic frame for the discussion of the structural evolution of the Pohorje Mountains at the transition of the Alps to the Pannonian Basin.

Figure 1: *The Mediterranean area with multiple mountain ranges and sedimentary basins which evolution is governed by the relative plate motions of the European plate in the north and the African plate in the south, and associated micro plates. The Alps are the central mountain range in this image. Directly east is the Pannonian basin. The fieldwork area (indicated by the red box is situated at the boundary of these two regions.*

The Alps

The Alps form an arcuate, elongated mountain belt that stretches from the Italian Ligurian coast, across France, Switzerland to the Eastern parts of Austria and Slovenia.

The Alps are formed by the closure of oceanic domains during convergence of the African and European plates, followed by continental collision. They are the product of two orogenies, one of Cretaceous and one of Tertiary age. The Cretaceous orogeny is related to the closure of an embayment of the Meliata ocean (figure 2). The Tertiary orogenic phase is the result of the closure of the Alpine Tethys between Europe and Apulia (Schmid et al., 2004).

Cretaceous (Eo-Alpine) orogeny

In the late Triassic the Neotethys ocean separated the African from the Eurasian plate. An embayment of this ocean protrudes westward, enclosed by continental domains. This embayment is referred to as the Meliata ocean (figure 2).

In the Cretaceous this embayment started to close. The closure of this embayment is related to W to NW directed nappe stacking of Austroalpine units that initiated at 135 Ma (Schmid et al., 2008). The degree of metamorphism related to this phase increases from the NW to the SE, and culminates in Eclogite facies metamorphism in the south eastern part of the present day Alps (Janak et al., 2004). Continental subduction towards the E to SE has been inferred from this metamorphic field gradient.

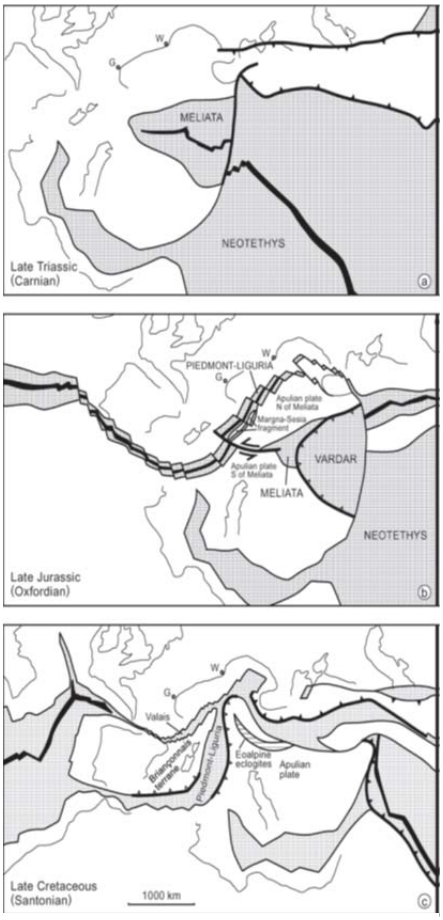

Figure 2: *Plate tectonic reconstruction of the Mesozoic evolution of the Mediterranean region. The development of oceanic domains related to different phases of mountain building is described. After Schmid et al., 2004.*

Cretaceous eclogite facies metamorphism has been recognized by Schmid et al. (2008) as evidence for deep subduction during the first orogenic stage in the Alps. The timing of this phase is determined by Sm-Nd dating of garnets in eclogites, to be ~91 Ma (Thöni et al., 2002).

Cretaceous extension

After deep subduction and associated (U)HP metamorphism during the early Late Cretaceous, extension affected the Austroalpine units during the middle to late Late Cretaceous. This stage is marked by the development of deep intracontinental basins, the so called Gosau basins, that were actively subsiding between 86 and 75 Ma (Willingshofer et al., 1999 and references therein). N-S extension also led to exhumation of high grade metamorphic rocks in the Koralm complex (Kurz et al., 2002) and to the exhumation of Austroalpine basement in the Eastern Alps, at approximately 80 Ma (Willingshofer et al., 1999 and references therein). Further to the NE, near the Rechnitz window, $^{40}Ar/^{39}Ar$ cooling ages reveal a Late Cretaceous (82-76 Ma) exhumation history for the Austroalpine units as well (Cao et al., 2013).

Tertiary orogeny

Already in the Jurassic Period the Piedmont Liguria or Alpine Tethys Ocean starts to open from the west. It is kinematically related to the opening of the Atlantic ocean. The resulting ocean separates the European and Apulian/Adriatic plates. In the Cretaceous another oceanic branch opens between Iberia and the European plate, the Valais Ocean.

This oceanic branch links up with the Piedmont-Liguria Ocean and the northern part of the Neotethys (figure 2). This oceanic domain will be collectively called the Alpine Tethys and separates Apulia/Adria from the European plate. The closure of this oceanic domain and resulting continental collision gave rise to the second orogenic phase recorded in the Alps (figure 2). Subduction beneath the Adriatic microplate, started around the Cretaceous-Paleogene boundary (Schmid et al., 1996) and resulted in continent-continent collision in the Eocene (Neubauer et al., 2000).

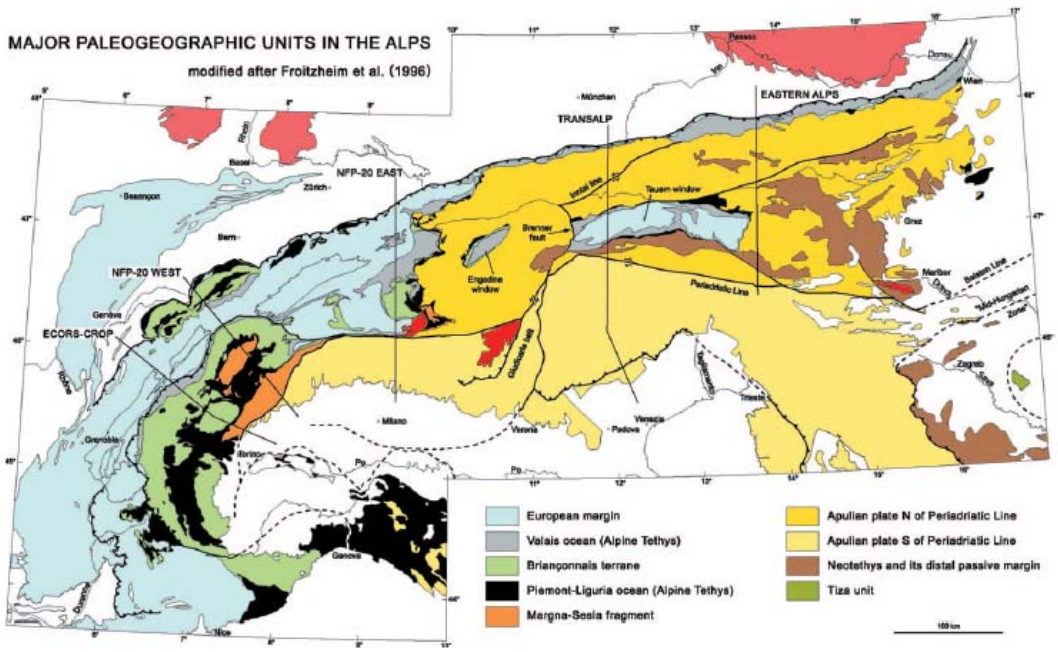

Figure 3: *Subdivision of the Alps into major tectonic units on the basis of paleogeographical origin. Schmid et al. 2004, modified after Froitzheim et al. 1996.*

An indication for this continental collision and the emplacement of Austroalpine units onto the European plate, is the metamorphic overprint of Penninic nappes and parts of the European foreland at 45 Ma. (Schuster et al., 1998 and references therein). The thrusting of Austroalpine nappes onto the European foreland had ceased by the late Oligocene (Schmid et al., 1996). During this orogeny the European plate subducted to the south to southeast beneath the Adriatic micro continent. Several super units in the Alps are distinguished in the Tertiary nappe stack (figure 2). The Helvetic nappes are derived from the European plate and the continental margin. These nappes are structurally in the lowermost position. The Penninic nappes (European distal margin and Alpine Tethys) are structurally below the Austroalpine nappes (Adriatic distal margin and Alpine Tethys) as is evidenced by their relative positions, for instance at the Tauern window (figure 3).

In the Eastern Alps the Austroalpine nappes are the dominant units exposed at the surface (figure 2). The nappes are generally subdivided into three main groups; the Lower Austroalpine (LA), the Lower Central Austroalpine (LCA) and the Upper Central Austroalpine (UCA) (Janak et al, 2004). The LCA consists largely of Variscan basement with only locally some of the cover preserved. This unit has experience the most high-grade Eo-Alpine metamorphism and subducted below the low grade metamorphic UCA during the Cretaceous (Janak et al., 2004 & Kirst et al., 2011). Furthermore, this model could explain the absence of sedimentary rocks as they could be scraped off during subduction. The present day configuration of these nappes in the Eastern Alps is shown in figures 3 & 4.

After the Eocene-Oligocene continental collision and nappe stacking, N-S compression did not cease, but was accommodated along other structures (Schmid et al, 1996). One of these structures emphasized here is the Periadriatic lineament (figure 3 & figure 4). The Peridadriatic lineament is the collective name for a system of large faults at the contact between the Adriatic microplate and the European plate and thrust nappes derived from Adria (Schmid et al, 1996, Schmid et al, 2008.). This major fault zone developed during the early Oligocene, around 32 Ma (Schmid et al., 1996). Parts of the fault system indicate significant uplift of the European side of the fault, but in the Eastern Alps the main kinematic expression of the fault is dextral strike slip (Luth et al., 2013). The faults were mainly active during the Oligocene, coeval with intrusions along this lineament. Known as the Periadriatic intrusions (sensu Fodor et al., 2008). Together these strike slip faults separate the Western, Central and Eastern Alps from the Southern Alps (figure 2). Ar/Ar ages of newly formed muscovite and dating on pseudotachylytes revealed that the Periadriatic lineament was reactivated during the Early Miocene.

Lateral extrusion

The Miocene evolution of the Alps is characterized by ongoing N-S shortening, mainly in the Southern Alps (Schmid et al., 1996). Coeval with this N-S shortening, lateral extrusion of the Eastern Alps towards the east occurred (Ratschbacher et al., 1989, Frisch et al., 2000). Blocks of Austroalpine nappes bounded by strike-slip faults moved towards the East. Typically, sinistral strike slip faults striking NE and dextral strike slip faults striking SE, form the northern and southern limits of these blocks, respectively (Frisch et al., 2000, Froitzheim et al., 2008). This simple geometry is a good first order approximation for the more complex patterns of fault (shear) zones found in the Eastern Alps. Strike slip faults bordering the Tauern window are the sinistral Salzachtal fault to the north and the dextral Mölltal fault zone to the south. Further to the East the sinistral Mur-Mürz fault system and

the dextral Pöls-Lavanttal system form another conjugate pair of faults, accommodating extrusion of crustal blocks to the east (Frisch et al., 2000).

The extrusion of Austroalpine blocks was associated with the unroofing of Penninic nappes, resulting in the formation of windows like the Tauern window metamorphic core complex and the Rechnitz window metamorphic core complex (Frisch et al., 2000, Dunkl & Démeny, 1997, Cao et al., 2013). Unroofing in the Tauern window is accommodated by low angle shear zones at its Western and Eastern margins; the Brenner and Katschberg low-angle extensional shear zones (Frisch et al., 2000).

Dating of the exhumation, by analysis of mineral cooling ages yields consistent ages of ~17 Ma for the Tauern and Rechnitz windows (Dunkl & Démeny, 1997, Frisch et al., 2000 and references therein). This period corresponds well with the formation of intramontane basins, alpine magmatism and displacement along strike slip faults during the Early Miocene, ~23-13 Ma (Frisch et al., 2000).

The driving force for ongoing N-S shortening in the Eastern Alps and associated lateral extrusion remains somewhat enigmatic, despite of extensive research in this region. Some of the most prominent features that distinguish the Eastern Alps from the Central and Western alps are the large extend of the Southern Alps retro wedge in the east and a tomographic cold anomaly, which are believed to indicate that the polarity of subduction is reversed in the Eastern Alps (Luth et al., 2013, Ustaszewski et al., 2008). The Adriatic plate is the lower plate and subducts below the European plate (figure 4). Deriving the key mechanisms behind this process requires a more regional approach and is beyond the scope of this research.

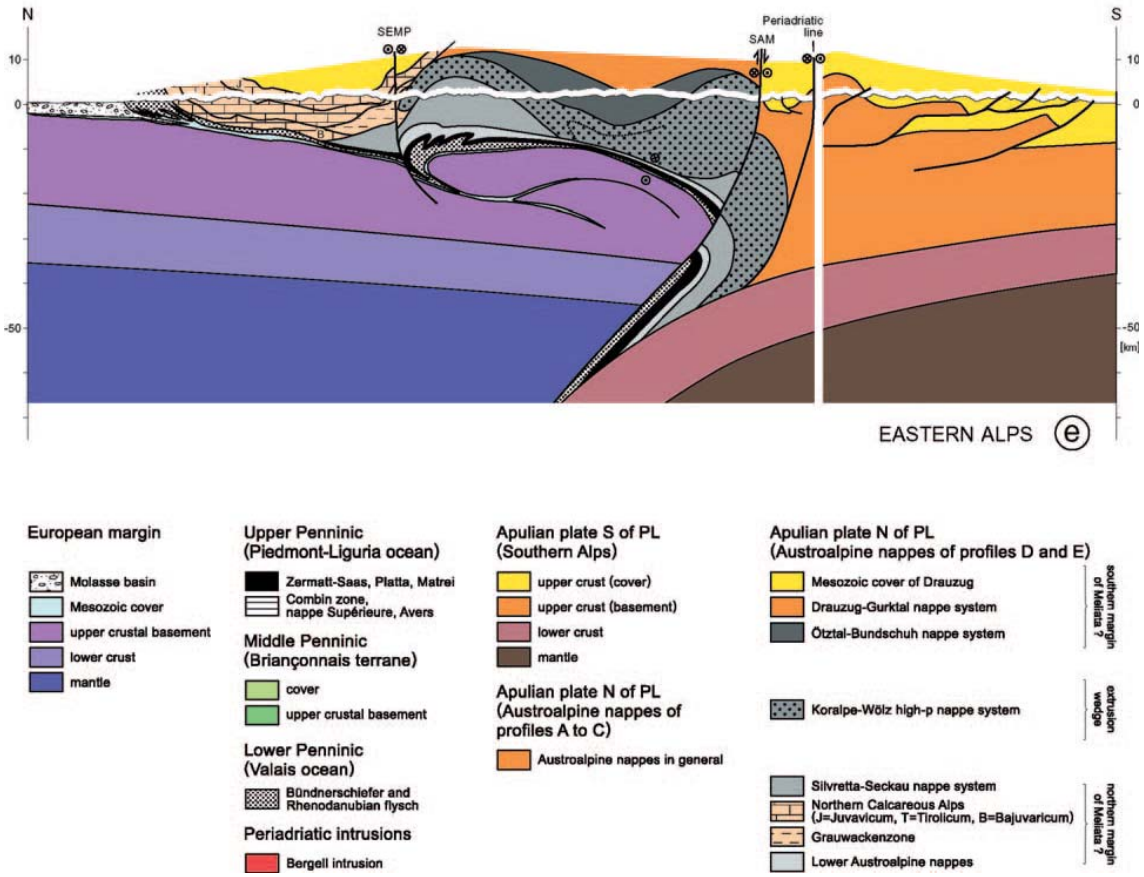

Figure 4: Cross section of the Eastern Alps. The Adriatic plate subducts beneath the European plate towards the North. The Koralpe-Wölz nappe system corresponds to the Lower Central Austroalpine nappes. The Ötztal-Bundschuh nappe, the Drauzug-Gurktal nappe and its Mesozoic cover represent the Upper Central Austroalpine nappes.

The Pannonian basin

The Pannonian basin is, as previously described, a landlocked basin between three mountain ranges: the Alps, the Carpathians and the Dinarides. Horvath et al. (2006) stated that the formation of the Pannonian basin is the result of extensional collapse of a thick Alpine crust. It is believed that this thick orogenic crust resulted from nappe stacking in the Alps during the Paleogene. This lead to gravitational instability and eventually orogen-parallel extension and thinning of the crust (Ratschbacher et al., 1989). Extension is assisted by the rollback of the Carpathian slab providing an unconstrained margin, or a so called 'free surface', which has accommodated the lateral extrusion of crustal blocks to the east.

The formation of the Pannonian basin occurred in the Early Miocene and is marked by the unconformity between pre-rift strata and the lower Miocene deposits. Exact dating of this unconformity is difficult, however a tuff horizon in the lowermost sediments is dated at 20 Ma (Hamor et al., 1980).

Deformation in the upper crust is characterized by sinistral shear along large ENE striking faults in the Northern part of the Pannonian basin, while in the Southern part of the basin large east striking dextral strike slip faults are present. The parts between these faults move to the East with respect to the Northern and Southern margins of the basin (figure 5). The areas between these large strike-slip faults however do not behave as coherent blocks. Normal and low angle normal faulting with a N-S orientation reveal lots of internal deformation. Two terranes can be identified within the eastward extruding orogenic wedge, the Alcapa terrane in the north and the Tisza-Dacia terrane in the South (figure 5). A set of strike slip faults along the Balaton line separates both terranes. The Balaton line is the Eastern extension of the Periadriatic lineament. Extrusion of these terranes took place from the Late Oligocene to the Early Miocene.

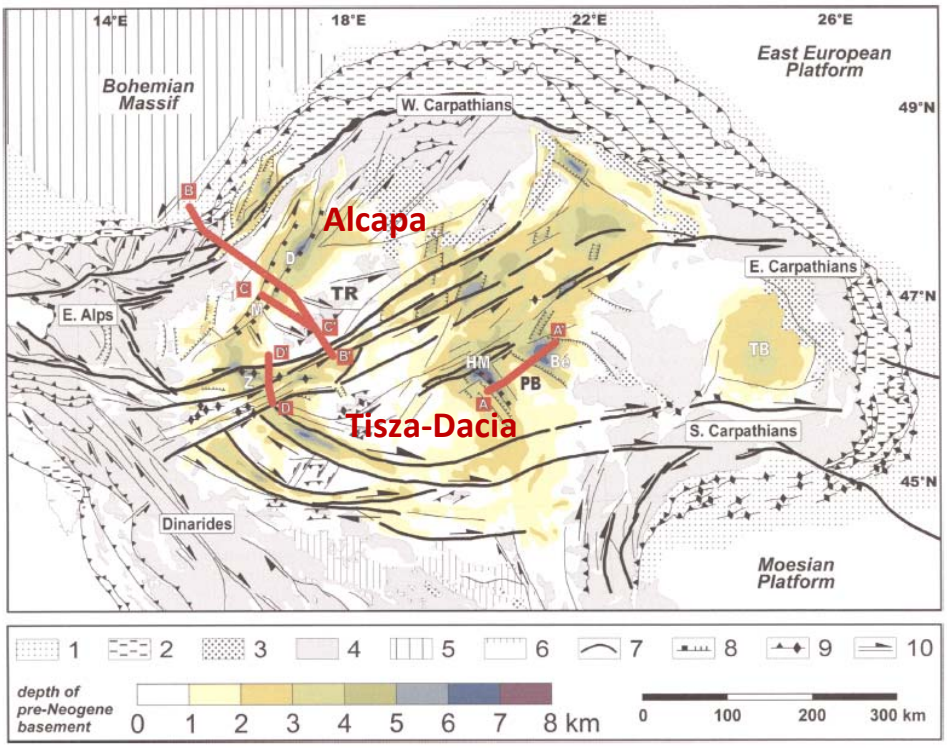

Figure 5: *Main tectonic structures of the Pannonian basin that accommodate extrusion towards the east (Horvath et al., 2006).*

Two phases of extension are recognized within the Pannonian basin, that both have very different styles of deformation (Tari et al., 1999). The first phase is characterized by asymmetric extension and locally the formation of metamorphic core complexes. The second phase of extensional deformation affected a much wider area, and is characterized by a back arc rift style of deformation.

Metamorphic core complex formation

The crustal extension in the area reached values between 50% and 120% (Horvath et al., 2006). Lithospheric mantle extension was up to an order of magnitude greater. The crustal strain localized along older structures, which are probably pre-existing weakness zones such as nappe contacts. Flat lying foliations resulting from earlier deformation phases might be reused as slide planes, accommodating the shearing. The structures that accommodate extension in this area are dominantly low angle normal faults (Tari et al., 1999, Ratschbacher et al., 1989, Dunkl & Démeny, 1997, Cao et al., 2013). These structures flatten at mid crustal depths, probably near the brittle-ductile transition (Tari et al., 1999).

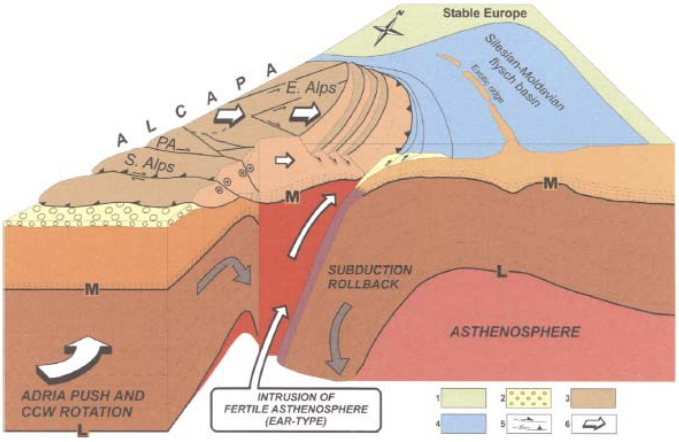

Figure 6: *The model on the formation of the of the Pannonian basin and lateral extrusion of the Eastern Alps (Horvath et al., 2006). The rotational movement of Adria towards the European plate drives shortening in the Eastern Alps, simultaneously subduction rollback beneath the Carpathian mountains causes tensile stresses and associated normal faulting in the overriding plate. In the Eastern Alps, the combination of the external stresses causes crustal blocks to move towards the east between large strike-slip fault systems.*

The low-angle normal faults result in core complexes; high grade metamorphic rocks are exhumed from beneath lower grade metamorphic rocks. The core complexes are characterized by mylonitic shear zones with retrograde metamorphic overprint. Multiple areas with these deformation characteristics have been recognized: The Rechnitz window (Dunkl & Démeny, 1997, Cao et al., 2013), The Algyö high (Tari et al., 1999) and the Medvenica mountains (Beniest et al., 2013). Some of these areas, such as the Rechnitz window, qualify for the term Cordilleran type metamorphic core complex (sensu Lister & Davis, 1984). Cordilleran type metamorphic core complexes (MCC's) are characterized by an antiformal shape with the same direction of shear on both sides. Furthermore they are characterized by overprinting structures representing progressively shallower environments, ranging from ductile structures formed under amphibolite facies conditions to discrete faults formed near the surface. Finally, metamorphic core complexes are intimately connected with granitic plutons (Lister & Davis, 1984).

Fission track data by Tari et al. (1999) indicate Miocene cooling and exhumation of the metamorphic Algyo block (Located in the Tisza-Dacia unit, at the Romanian-Hungarian border). Similar ages of ~17 Ma were derived from zircon fission track ages and K/Ar ages of muscovite for the cooling in the Rechnitz window (Dunkl & Démeny, 1997).

Multiple processes are believed to have taken place providing the proper circumstances for this orogen parallel extension to take place (Ratschbacher et al, 1989). Firstly, the Alpine orogenic crust is

believed to be thermally weakened, making the area prone for strain localization. Secondly, the eastward retreat of the Carpathian subduction zone led to tensional stresses in the overriding plate, as a result of which space is created for extruding blocks (Ratschbacher et al, 1989) (figure 6).

Wide rifting and inversion

Tari et al. (1999) suggest that after an initial phase of core complex formation in the Karpatian, later extension is governed by back arc rifting, which is characterized by steep normal faulting. This later phase did not occur isochronous throughout the basin, but the end is marked by an unconformity typically of Early Badenian age (14,8 Ma). Contrary to typical narrow rift zones, the back arc rifting in the Pannonian region affected a broad zone in which several subbasins developed. This type of rifting is termed the wide rifting style (Tari et al., 1999). Only during the Sarmatian and lowermost Pannonian deformation localized, and a narrow rift style dominates specific regions leading to the formation of deep subbasins underlain by thin crust and very thin lithosphere (< 45 km) that are often associated with magmatism (Tari et al., 1999).

At 11 Ma the latest nappe stacking was recorded in the Carpathians. By this time all oceanic lithosphere had been subducted and rollback has stopped (Matenco et al., 2010). This Pannonian age coincides with the latest extension in the basin. Shortly after, from 11-8 Ma, inversion of extensional structures occurred locally, marking a compressional phase (Horvath et al., 2006, Bada et al., 2001). Uplift in the western parts of the Pannonian basin, the Vienna and Styrian basins, occurred slightly earlier, during the Sarmatian, between 12,3 and 12,1 Ma (Harzhauser & Piller, 2004).

For Late Pliocene to recent times, a more intensive compressional event is well documented (Horvath et al., 2006, Bada et al., 2001). Inversion of extensional structures is still active today.

The Pohorje Mountains

The Pohorje and Kozjak Mountains of NE Slovenia are the eastern most parts of the Alps exposing crystalline rocks. They are part of the Eastern Alps at the margin of the Pannonian basin, in close proximity to the Northern Dinarides. The hilly, forest mountain range has peaks up to just over 1500 m, and typically gentle slopes. Steeper slopes border the incised valley of the Drava river, a main tributary to the Danube, that makes its way through the Kozjak mountains. The ranges are separated by an E-W trending topographical low, named the Ribnica-Selnica trough. To the north and to the east the Styrian and Mura basins are found. These represent the easternmost subbasins of the Pannonian basin. The Lavanttal/Labot fault borders the Pohorje mountain to the SW. This dextral strike slip fault displaces the Periadriatic lineament which trends E-W and is located south of the Pohorje mountains (figure 7).

The Pohorje mountains are part of the Eastern Alps and consist of rocks from the Austroalpine nappes, originally derived from the Apulian plate. The major part of the Pohorje and Kozjak mountains consist of high grade metamorphic rocks (Gneisses, micaschists and amphibolites with lenses of marble, quartzite and eclogite) that reflect upper amphibolite facies metamorphism. This unit represents the basement of the Lower Central Austoalpine nappe (Kirst et al., 2011).

In the NW of the area low grade metamorphic, Paleozoic rocks and associated Mesozoic unmetamorphosed sedimentary rocks are found, that represent the Upper Central Austroalpine basement and cover, respectively (Mioc & Znidarcic, 1987, Kirst et al., 2011).

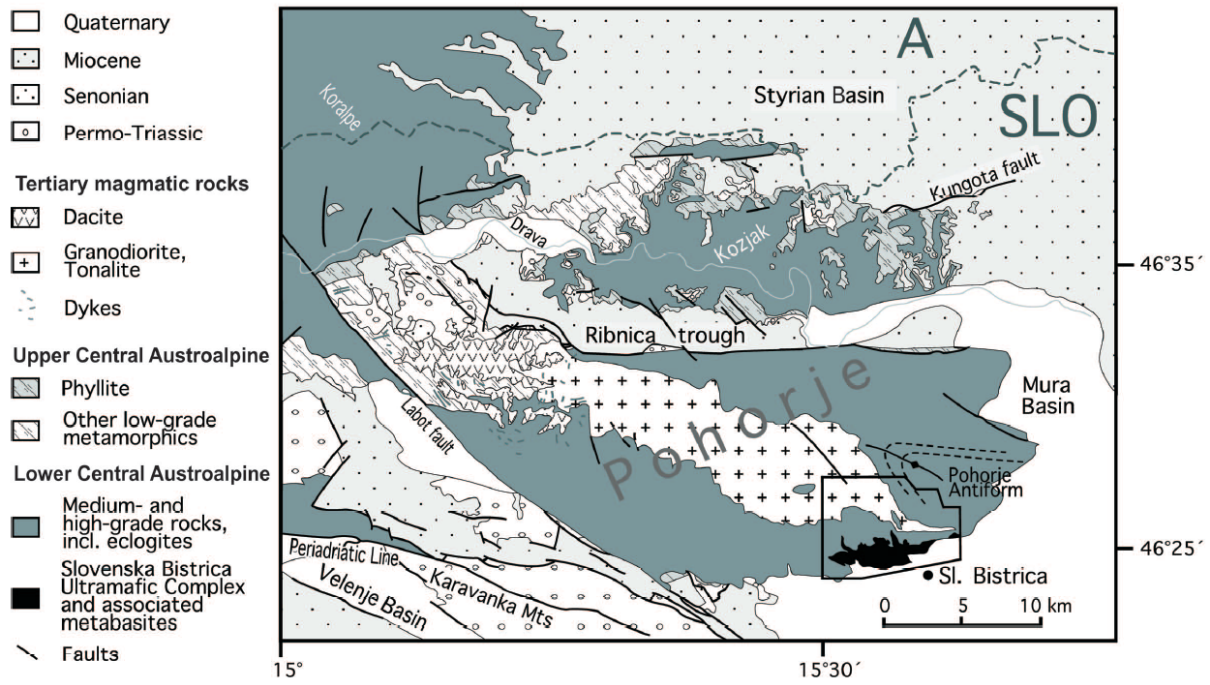

Figure 7: *Simplified geological map of the Pohorje mountains (Kirst et al., 2011). The metamorphic rocks are divided in the Lower and Upper Central Austroalpine nappes. Igneous and sedimentary rocks make up the rest of the map.*

Multiple phases of metamorphism are recorded in the rocks of the LCA nappe. The first phase comprises (U)HP metamorphism that is observed in eclogite lenses, peridotites and serpentinites in a complex of ultramafic rocks, named the Slovenska Bistrica Ultramafic Complex (SBUC), in the SE of the Pohorje mountains (Kirst et al., 2011).

Different studies of metamorphic conditions of kyanite eclogites suggest different peak metamorphic conditions. A maximum pressure between 1.8 and 2.5 GPa was found by Sassi et al. (2004), while Janak et al. (2004) measured peak pressures of up to 3.1 GPa. An UHP metamorphic history of these rocks therefore is disputed. Thermobarometric research on garnet peridotites from Janak et al. (2006) however supports the evidence for a Cretaceous UHP metamorphic event. Pressures of up to 4 GPa were calculated from garnet-olivine and garnet-pyroxene Fe-Mg thermometers.

The Cretaceous UHP metamorphic event is best explained by subduction in Cretaceous times, probably related to the closure of the Meliata oceanic embayment Schmid et al. (2004). The host rocks of the lenses for which UHP metamorphism has been established, reveal upper amphibolite facies metamorphism that is most likely related to the same subduction event.

Amphibolite facies gneisses and schists have been affected by strong chloritisation during retrograde metamorphism. Rocks that display this type of metamorphism were mapped as diaphthorite (Mioc & Znidarcic, 1977) and are found mainly in the western parts of the Pohorje and Kozjak mountains and in some areas in the Easternmost parts of these ranges.

A pluton of granodiorite to tonalite composition is found in the center of the Pohorje mountains, The pluton is exposed as an elongated body of 40 km, oriented WNW-ESE (figure 7) with an age of intrusion, determined by U-Pb dating on zircons, of 18.6 ± 0.11 Ma (Fodor et al., 2008). Dacitic volcanics and subvolcanics, thought to be genetically linked to the pluton show slightly younger ages. Biotite K-Ar data and and Zircon fission track data show very similar ages in the range of 18 to 15 Ma (Fodor et al., 2008, Trajanova et al., 2008). Their similarity is interpreted to indicate that these ages

are close to the emplacement age of the Dacite, so a Karpatian age is postulated for these volcanics (Fodor et al., 2008). The youngest volcanics intruded Karpatian sediments, providing a maximum Karpatian age for these volcanics. Pyroclastic intercalations in Karpatian sediments (17,3-16,5 Ma) also record volcanic activity during the Karpatian (Steininger et al., 1988).

Thermobarometric calculations revealed that the Eastern part of this pluton, now at the surface, crystallized at depths of approximately 16-19 km, whereas the Western part crystallized at shallower depths around 8-11 km. Different amounts of exhumation must have affected the Eastern and Western part of the Pohorje mountains in order to expose the entire body at the surface. Research has shown that the Pohorje pluton has experienced rapid cooling shortly after its emplacement (Fodor et al., 2008). Supporting this model of rapid exhumation shortly after the emplacement of the pluton are $^{40}Ar/^{39}Ar$ cooling ages of biotite, which yield ages between 17,9 and 16,3 Ma (Hendrickx et al., 2010).

Granodiorite pebbles and blocks that are found in deformed Miocene sediments have features indicating a proximal source. Dating of the biotite cooling ages in these pebbles yielded ages similar to those found in the Pohorje pluton (Fodor et al., 2008). Therefore, these pebbles are believed to be derived from the Pohorje pluton. The age of the sediments is only 3 My younger than the U-Pb age of the pluton, indicating rapid exhumation to the surface. Sachsenhofer et al. (1998) also showed that the sediment was derived from the local outcrops of Austroalpine basement rocks and the Tonalite pluton. Apatite ages of the metamorphic and igneous basement and detrital apatite ages show similar ages. These detrital apatite ages were not overprinted by later reheating after deposition, as vitrinite reflectance data show that these sediments only reached a maximum temperature of 70°C which can only slightly affect apatite fission track ages. Both show an Eggenburgian (~19 Ma) age, that is only 1-2 My older than the age of the Karpatian sediments. This serves as another evidence for rapid exhumation of the Kozjak and Pohorje mountains (Sachsenhofer et al., 1998).

What mechanism has caused this rapid cooling and exhumation during the Miocene is not yet well understood. Understanding this mechanism and the relation with Miocene regional processes such as the opening of the Pannonian basin and the lateral extrusion of the Eastern Alps is the main goal of this research.

Tectonostratigraphy and lithology

In this chapter the several lithologies found in the Pohorje and Kozjak mountains in eastern Slovenia are described. Lithological descriptions of previous work (e.g. Mioc & Znidarcic, 1977) are supplemented with new observations by the author. Based on the rocktype and degree of metamorphism, a basic subdivision can be made, that is closely related to the different nappes in the region. 5 major units are distinguished:

1) High grade metamorphics (LCA)
2) Low grade metamorphics (UCA)
3) Sedimentary rocks associated with low grade metamorphics (UCA)
4) Igneous rocks
5) Miocene and younger sediments

Based on this subdivision a simplified version of the map by Mioc & Znidarcic (1977) has been constructed, which shows the distribution of these units and highlights the major tectono-stratigraphic contacts (figure 8).

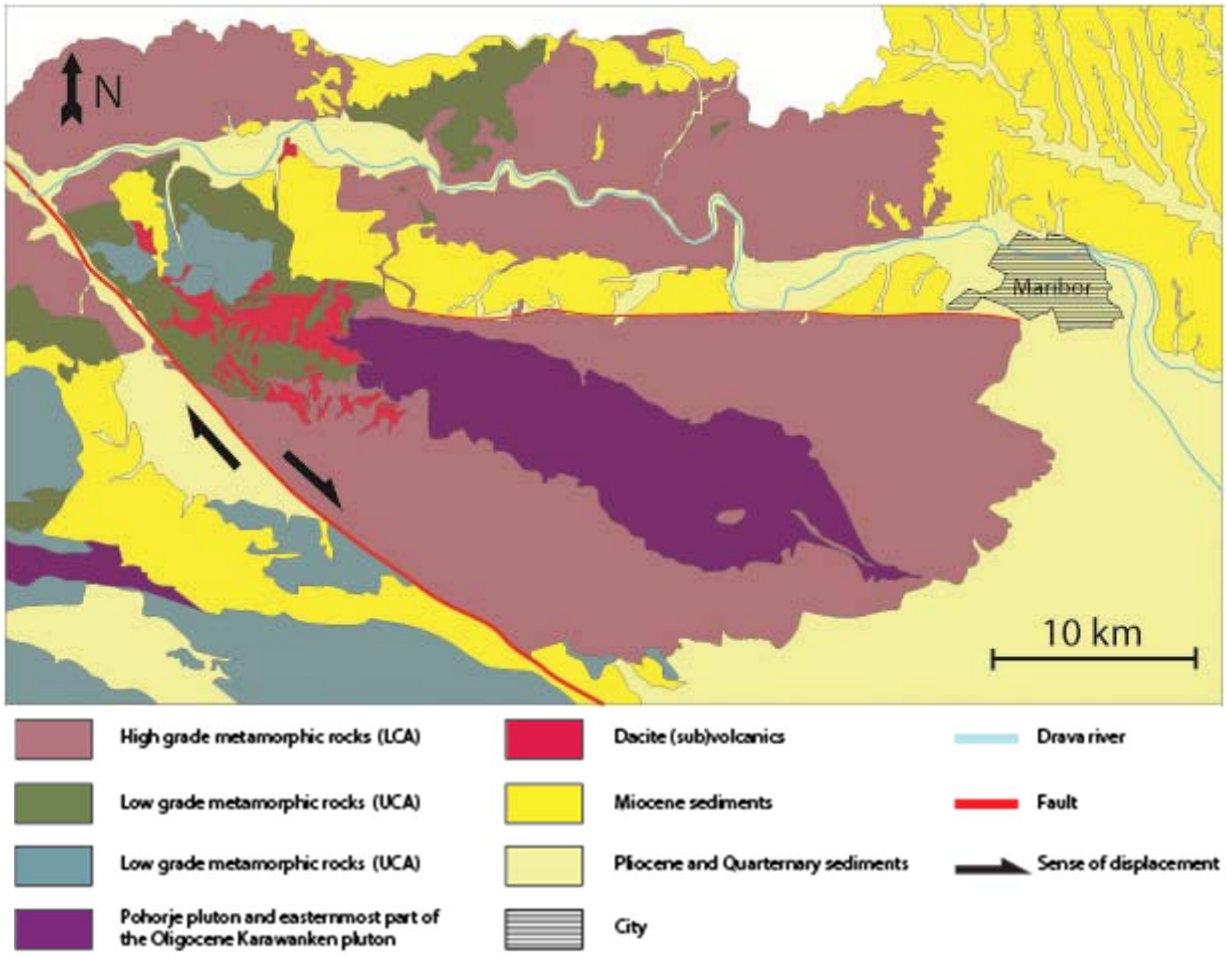

Figure 8: *Simplified geological map of the Pohorje and Kozjak Mountains, highlighting the different tectonic units (modified after Mioc & Znidacic, 1977). The colors correspond to the color coding shown in figure 18: Tectonostratigraphic column. Lenses of different rock types in the high grade metamorphic rocks were not shown for the reason of maintaining simplicity.*

In this section, first the main lithologies of every unit will be described. Than the significance of the contacts is discussed as well as the absolute ages of the rocks, in order to arrive at a composite tectono-stratigraphic column. At last a correlation between the units in the Pohorje area to the larger scale structural units of the Eastern Alps will be made.

Lithologies

The description of the lithologies largely follows the classification of Mioc and Znidarcic (1977), however only those units that were encountered during this fieldwork are included in this report. Close agreement exists between the findings of Mioc & Znidarcic and our findings. This section combines the observations of both works to establish a complete but concise overview of the rocks in the fieldwork area. The descriptions are based on field observations and thus exclude microstructures. More information on microstructures and more extensive mineralogical compositions can be found in chapter 5: Microstructural and Petrological analysis.

1. High grade metamorphics

The first group comprises medium to high grade (upper amphibolite facies) metamorphic rocks, making up the largest part of these small mountain ranges (figure 8). These high grade metamorphic rocks of the Pohorje Mountains consist mainly of gneisses and schists, which include lots of lenses of different lithologies. Especially amphibolite lenses are widespread. Occasionally smaller lenses of eclogite, serpentinite, marble and orthogneiss are observed. Phyllonites and chlorite rich amphibolite are found only in the north of the Pohorje mountains and throughout the Kozjak mountains and represent the highest units of this nappe.

1.1 Gneisses and schists

The bulk of the metamorphic rock consists of light colored gneisses, containing high percentages of quartz and feldspar. Both muscovite and biotite are generally present as is garnet.

The mineralogical content and the appearance of the gneisses varies locally. Augengneisses consist of high percentages of 0,5-5 cm large augen of feldspar and or folded quartz veins (figure 9a and 9b). These augengneisses contain large (>1 cm) garnets, with a typical pink colour. This variety of gneisses also shows distinctively large minerals of muscovite (figure 9c).

Micaschists containing large crystals of muscovite are frequently observed. These foliated rocks contain, besides muscovite, also biotite, feldspar, quartz and occasionally small garnets.

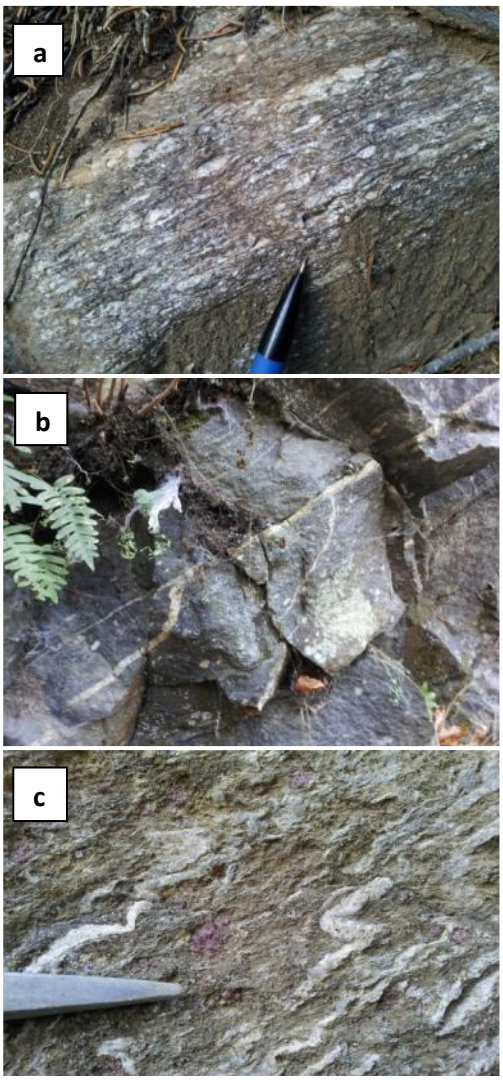

Figure 9: *Several types of gneisses.* ***A)*** *Light coloured augengneiss, location 98.* ***B)*** *Dark augengneiss, location 130.* ***C)*** *Gneiss with garnets and quartzbands, location 57.*

At most locations quartz veins are present within the high grade metamorphic rocks. Small white veins with large amphiboles are abundantly present within these gneisses (figure 10a).

On some locations the rocks contain significant amounts of chlorite, which indicates a lower degree of metamorphism (figure 10b). Otherwise these rocks are very similar to the other gneisses and schists and are therefore thought to result from retrograde metamorphism. These rocks are found mostly higher up in the high grade metamorphic sequence of the Lower Central Austroalpine nappe.

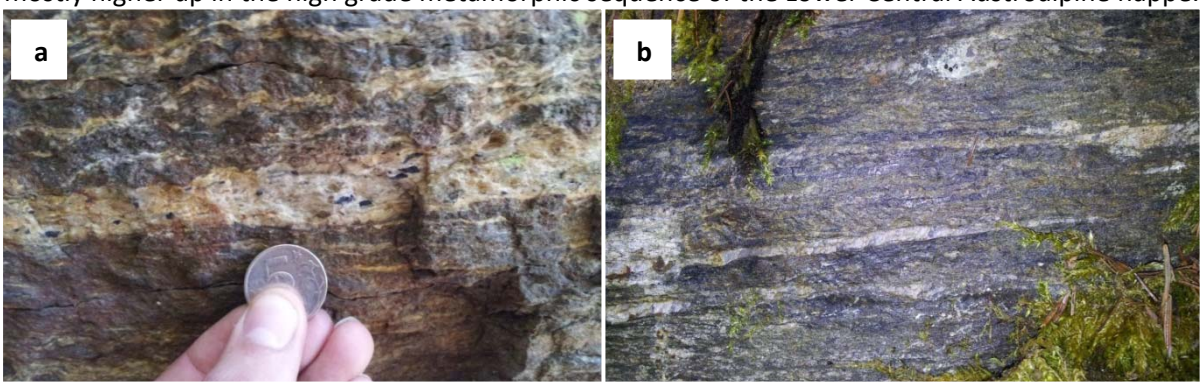

Figure 10: A) *White veins with large amphiboles in garnet rich gneiss, location 47.* ***B)*** *Chlorite rich gneiss typical for the upper parts of the gneisses and schists, location 39. Width of view is 25 cm.*

1.2 Lenses

Lenses of several different rock types are present within the series of gneisses and schists. The origin of these lenses varies, some rock types are likely to have a sedimentary protolith, such as the marbles, whereas the eclogites, orthogneisses and serpentinites resulted from metamorphism of magmatic rocks.

Amphibolites occur as lenses throughout the gneisses and schists, but are especially abundant towards the north of the Pohorje mountains and within the Kozjak mountains. In the Kozjak Mountains the occurrence of amphibolite is also more dominant, lenses are up to several kilometers in width. Amphibolites typically have a dark green appearance. Most amphibolites have a characteristic wavy, irregular foliation consisting of alternating white and green bands (figure 11a). The green bands contain mainly amphiboles, especially hornblende, whereas the white bands consist mainly of feldspars and quartz. In these samples typical mineral sizes are 1-3 mm and individual crystals are easily detected. Often larger (2 cm)amphiboles occur within the finer matrix. Other amphibolites are finer grained and individual crystals are hard to distinguish, however we recognized that the alternation of dark colored amphiboles and light feldspars often create a ‘salt and pepper’-structure.

Marbles occur as lenses within the gneisses and schists. The marbles have a very light, off-white colour, white bands alternate with dark grey bands. Zoisite minerals, typically 1 mm across, are present throughout the marble but are more abundant within the darker bands. It is recognized that these minerals often have a dark reaction rim (figure 11b).

Lenses of eclogite consisting of omphacite, garnet, kyanite and quartz occur mostly within the southeastern part of the Pohorje mountains. The mineral assemblage gives these rocks a typical colour composition of white, bright green and red (figure 11c). The outcrops of eclogite often have rims of amphibolite, and sometimes the entire outcrops of eclogite are amphibolitized.

Finely banded gneisses are found locally as lenses within biotite and muscovite rich gneiss. The minerals are smaller within these lenses and they have a characteristic light yellow colour with a fine lamination. Small amphiboles and biotite are present within the light coloured bulk rocks. These

small lenses are thought to represent the orthogneisses derived from the metamorphism of old pegmatite intrusions (Mioc & Znidarcic, 1977).

Locally, occurrences of serpentinite are found. An exceptionally large body of serpentinite is situated at the south-eastern edge of the Pohorje mountains. This body is termed the Slovenska Bistrica Ultramafic Complex (Kirst et al., 2010). The dark bodies of serpentinite consist mainly of serpentine (figure 11d) and lack any structure. The surfaces are weathered into chaotic shapes.

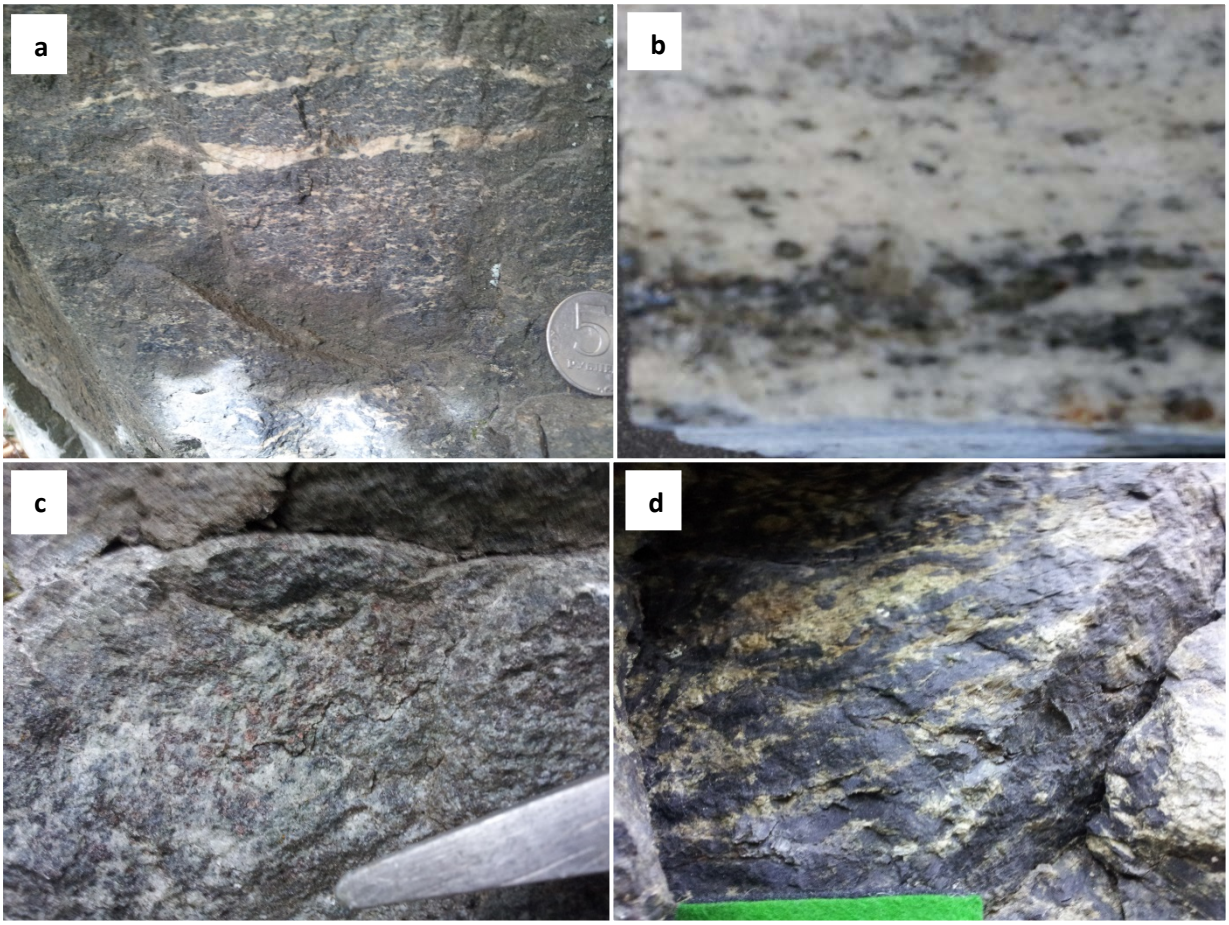

Figure 11: *Rock types of various lenses in the high grade metamorphic schists and gneisses.* ***A)*** *Amphibolite, amphiboles and plagioclase feldspar with a distinct wavy foliation pattern.* ***B)*** *Marble, typical green minerals with dark reaction rims.* ***C)*** *Partially amphibolitized eclogite.* ***D)*** *Serpentinite*

1.3 Phyllonites and chlorite rich amphibolite

As described by Mioc & Znidarcic (1977), chloritized amphibolite and phyllonite are structurally the highest levels of the high grade metamorphic unit.

On the northern side of the Pohorje Mountains, south of the Selnica-Ribnica trough a sliver of chloritized amphibolite is found. In the western part of the Kozjak mountains this type of rock is abundantly present. The appearance of the rock is different for every location, but every outcrop shares a pale gray-greenish colour of the rock. Sometimes features, such as a wavy foliation, characteristic for amphibolite are recognized within this rock type. At some locations dark green vitreous spots are observed that are typically associated with quartz veins. Also, large amphiboles are present. The rock consist mainly of amphibole, feldspar, chlorite and quartz.

Phyllonites are mainly found in to the north of Pohorje, within the Kozjak mountains. These very light colored, foliated rocks often have a rusty appearance. The main minerals are feldspar and mica

(muscovite), which are often separated into thin bands. In some cases the mica's appear to be organized into small aggregates of several crystals in a groundmass of feldspar. In some samples muscovite minerals are relatively large, up to 0,5 cm. Quartz veins are regular features, as are occurrences of small to medium sized garnets.

2. Low grade metamorphics

The second unit consists of low grade metamorphic rocks, which are found almost exclusively in the northwestern part of both the Pohorje and Kozjak mountain ranges (figure 12). These low grade rocks are structurally in a higher position than the high grade metamorphic rocks.

They include a dark coloured, almost black phyllite consisting largely of small mica and chlorite containing large quartz clasts (figure 12a), and dark carbonitic micaschist with quartz and small mica. Lenses of laminated marble are incorporated in the phyllites and schists. At location 114 an outcrop with marble is found, with possibly inclusions of chert. This particular outcrop is strongly foliated (figure 6b).

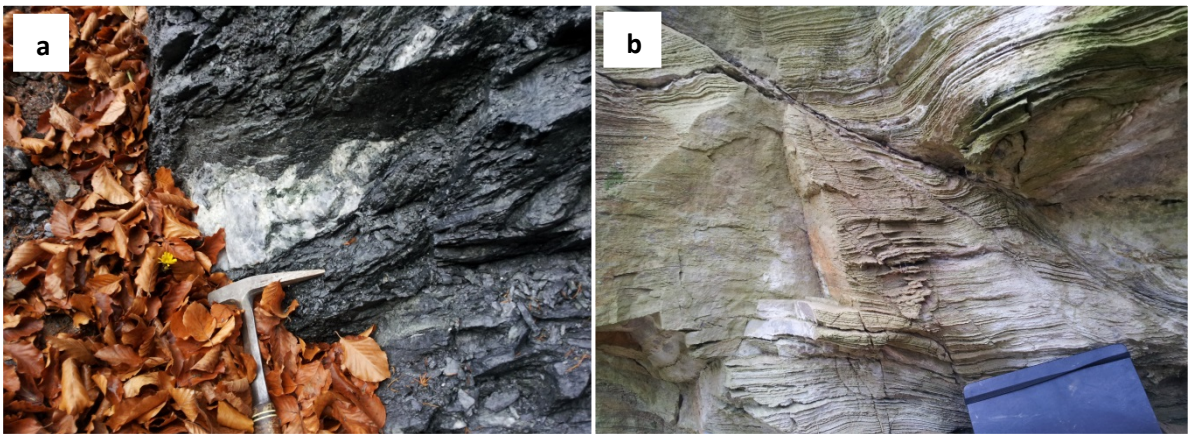

Figure 12: *Low grade metamorphic rocks.* ***A)*** *Black phyllites with quartz veins.* ***B)*** *Laminated meta-limestone*

3. Mesozoic sedimentary rocks associated with low grade metamorphics

In the north westernmost part of the Pohorje mountains a unit composed of sedimentary rocks is observed. Their presence is limited to areas surrounded by low grade metamorphic rocks. Structurally these sediments are above the low grade metamorphic rocks.

Figure 13: *These sedimentary rocks form part of the succession of weakly metamorphosed sediments associated with the low grade metamorphic basement rocks. The grey colored rock on the right, is mudstone with numerous quartz veins. In the center of the image, violet colored debris is derived from the phyllite layer directly above the mudstone.*

The succession includes from the base up: mudstones, containing chlorite and several generations of quartz veins, violet-red phyllite and violet-red, fine-grained sandstones. Coarse, red colored conglomerates are found as loose blocks in mountain creeks. Possibly several alternations of this rock succession exist within the entire unit.

4. Igneous rocks

In the core of the Pohorje mountains a large pluton intruded into the metamorphic rocks. Other igneous rocks are subvolcanics closely related to the pluton. Together they constitute the fourth unit of rocks.

The Pohorje pluton has a granodioritic-tonalitic composition. Next to plagioclase and quartz, the tonalite consists of hornblende and biotite (figure 14). Along the edges of the pluton a foliation can be observed, whereas the inner part of the pluton shows no preferred orientation of crystals and no foliation.

Figure 14: *Granodiorite sample with typical mineral assemblage (Plagioclase, amphibole, K-feldspar and biotite). After Haalboom & van Greuningen (2013).*

Dykes crosscut the metamorphic host rocks around the pluton. Most dykes are light coloured and consist almost exclusively of feldspar and quartz, sometimes with small amounts of mafic minerals. A type locality is found just south of the easternmost part of the pluton (location 7), here most intrusions occur parallel to the foliation of the host rock (figure 15b), however some veins clearly crosscut the foliation (figure 15a).

In the Northwestern part of the Pohorje mountains, at the western margin of the pluton a region with scattered but abundant outcrops of Dacite is found. These rocks may have a volcanic or subvolcanic origin, and most probably represent the (near)surface expression of the magmatism that resulted in the tonalite pluton. The Dacite consists of pinkish feldspars of up to 0,5 cm, quartz, muscovite and small mafic minerals which are either biotite, amphiboles or pyroxenes or a combination of these minerals. Little or no foliation developed within these volcanics.

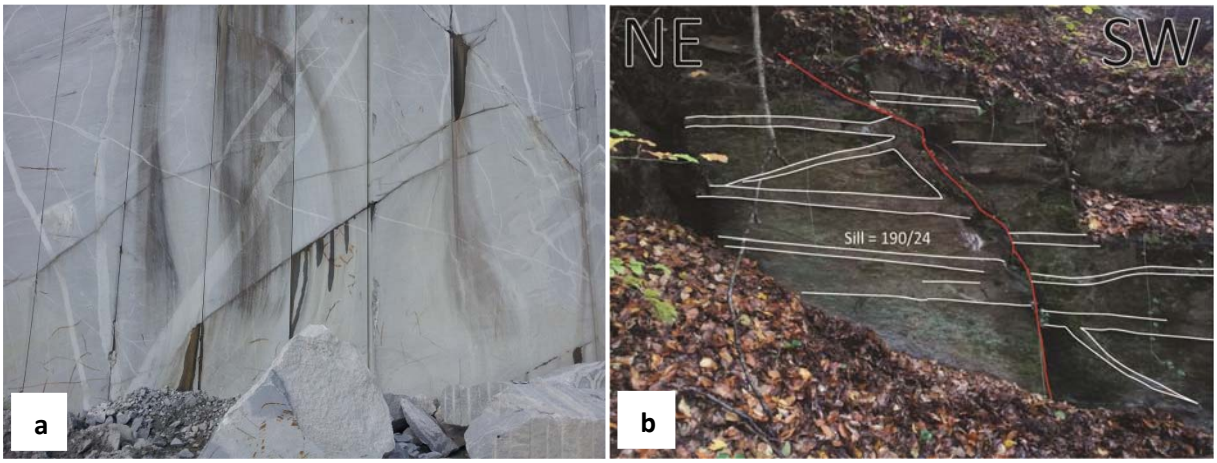

Figure 15: *Igneous rocks of the Pohorje mountains. A) Tonalite in quarry with numerous cross cutting dykes B) Sills and dykes in metamorphic rocks surrounding the pluton*

5. Sedimentary rocks and sediments

The fourth group consists of unmetamorphosed sediments. These are found mostly in the lower lying areas surrounding the ranges. Along the southern margin of the Pohorje mountains the metamorphic rocks are juxtaposed to sedimentary rocks, separated by the Lavantall strike slip fault (figure 8).

The oldest of these sedimentary rocks are Triassic limestones. These limestones consist of alternating white and grey beds of limestones and occasional marly intervals. These outcrops are part of extensive Triassic reef systems.

Figure 16: *Tilted beds of Triassic limestone, south of the Lavantall fault. Bands, 20 cm thick, of alternating white limestone, greyish limestone and marls are common for this Triassic reef deposit . Normal faults with up to 40 cm offset are observed.*

Miocene sedimentary rocks are found south of the Lavantall fault, in an East-West oriented zone separating the Pohorje and Kozjak mountains and to the north and east of the Kozjak mountains. The main lithologies include conglomerates and sandstones and marls. Most conglomerates are located in the area North East of the Pohorje mountains between Ruse and Maribor.

Some conglomerates contain large boulders of tonalitic material (figure 17a). The angular shape of clasts indicates that these boulders come from a proximal source. Some beds consist of tonalitic material for more than 90%, in between shaly, organic rich intervals are found.

Figure 17: *Miocene age sedimentary rocks.* ***A)*** *Large boulders of Tonalite in Miocene conglomerate,* ***B)*** *Alternation of carbonitic sandstone and marl,* ***C)*** *Crinoid fossils,* ***D)*** *fine grained sandstone*

To the North East of the Kozjak mountains the Miocene sediments comprise predominantly carbonitic sandstones with a lot of detrital mica, alternating with marly intervals (figure 17b & 17d). Coarse arenites containing fossilized crinoids (figure 17c) indicate a shallow marine deposition environment. Scour marks are also observed within these sediments. The youngest deposits are fluvial deposits, related to the Drava river system. These unconsolidated sediments cover large parts of the Mura basin east of the Pohorje and Kozjak mountains.

Structural relations and ages

The medium to high grade metamorphic rocks that are thought to have Precambrium sedimentary protoliths (Mioc & Znidarcic, 1977), represent the basement rocks of the lowermost nappe. This nappe which includes high pressure metamorphic rocks is also termed the Pohorje nappe (Janak et al., 2006, Vrabec et al., 2010). It is part of the Lower Central Austroalpine nappe, which does not include Mesozoic cover rocks in the Pohorje area.

The low grade metamorphic rocks, in the north and east of the Pohorje and Kozjak mountains, are assigned to Paleozoic (Ordivician, Silurian and Devonian) ages by Mioc & Znidarcic. These rocks comprise the metamorphic rocks of the nappe structurally above the Pohorje nappe, and belongs to the Upper Central Austroalpine nappe.

Relatively small occurrences of unmetamorphosed Mesozoic rocks are found on top of the low grade metamorphic rocks. Some authors describe these rocks as a separate nappe, structurally above the low grade metamorphic basement rocks. (Vrabec et al., 2008). However, in this report they are treated as a Mesozoic cover, being an integral part of the Upper Central Austroalpine. With these tectonic relations, a composite tectono-stratigraphic column is constructed (figure 18). The Miocene pluton and (sub)volcanics crosscut nappe contacts. A nonconformity exists between the rocks belonging to the thrust nappes and the Miocene to recent sediments.

A simplified map highlighting the main structures of the Pohorje and Kozjak mountains is present in figure 8. In this map colors do not refer to specific rock types but to structurally different domains, such as the above described nappe system.

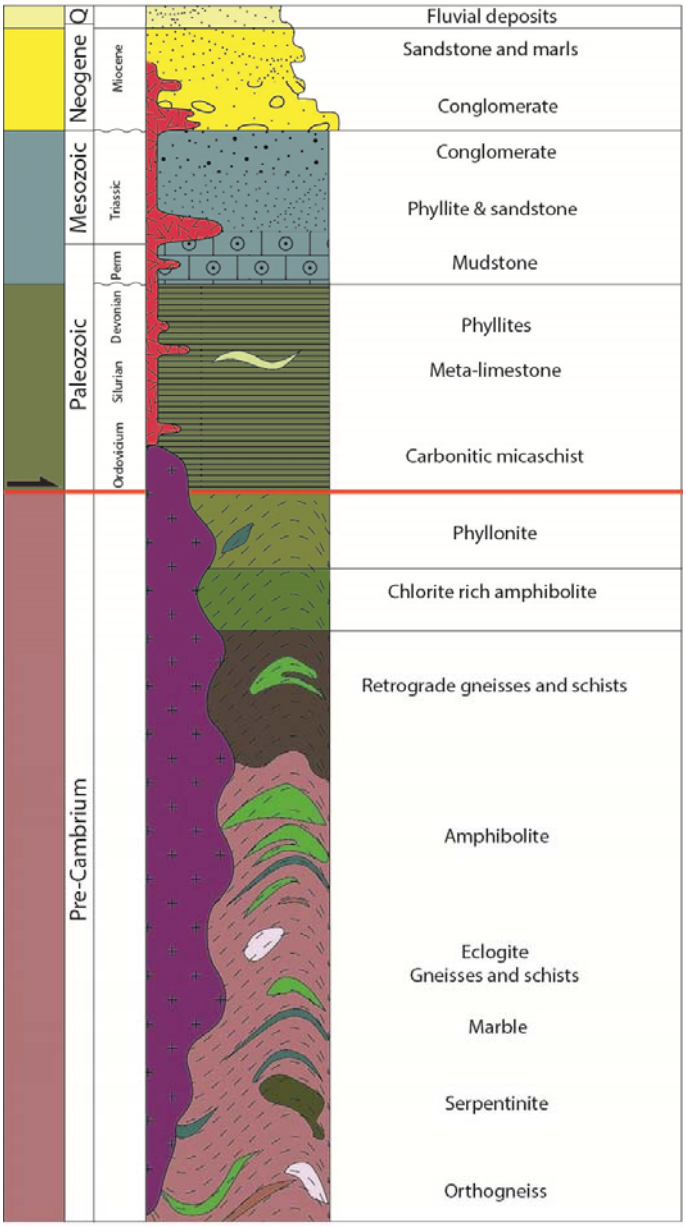

Figure 18: *Tectono-stratigraphic column (Modified after Mioc & Znidarcic, 1977). The numbers 1-5 correspond to the units described in this section.*

Metamorphism

At least two stable mineral assemblages are recognized in the field. A peak metamorphic mineral assemblage, M1, and a retrograde metamorphic facies, M2.

M1 - The M1 mineral assemblage consists of garnet, muscovite, biotite, quartz and feldspar. It represents upper amphibolite facies metamorphism. This high grade metamorphism took place before the D3 phase But its relation to D1 and D2 phases is hard to retrieve from the field data.

M2 - Retrograde greenschist facies metamorphism is recognized by a chlorite overprint. The fact that chlorite seems to define the stretching lineation is an indication for retrograde metamorphic conditions during shearing. The M2 retrograde metamorphism therefore represents Miocene PT –conditions.

More extensive studies of the metamorphic history of the various rock types have been made by optical microscopy. The timing of metamorphic events can be established more precisely by studying the relation between microstructural data and mineral growth. Estimations of PT-conditions can made by analysis of stable mineral assemblages and recrystallization structures. The results of these studies are combined in the chapter 'Microstructural and petrological analysis'.

Field results

Structural analysis has been performed in the Pohorje and Kozjak mountains in a total of 149 stations, dominantly located within the Austroalpine basement (figure 19). Additionally 132 data points from a previous fieldwork (van Greuningen & Haalboom, 2013) were analyzed. Kinematic indicators were used in sections parallel to the stretching lineation to constrain the direction and sense of shear in the region. A first order assessment of the metamorphic grade is obtained in the field in order to better define the relationship between metamorphism and deformation (a more detailed account of this relationship is provided through optical microscopy; section xx). Subsequently an attempt is made to correlate structures in the basement to structures and observations within Miocene sediments, which represent an excellent archive. Hence, aiming to constrain the exhumation and erosion of the metamorphic and igneous rocks in the center of the Pohorje mountains.

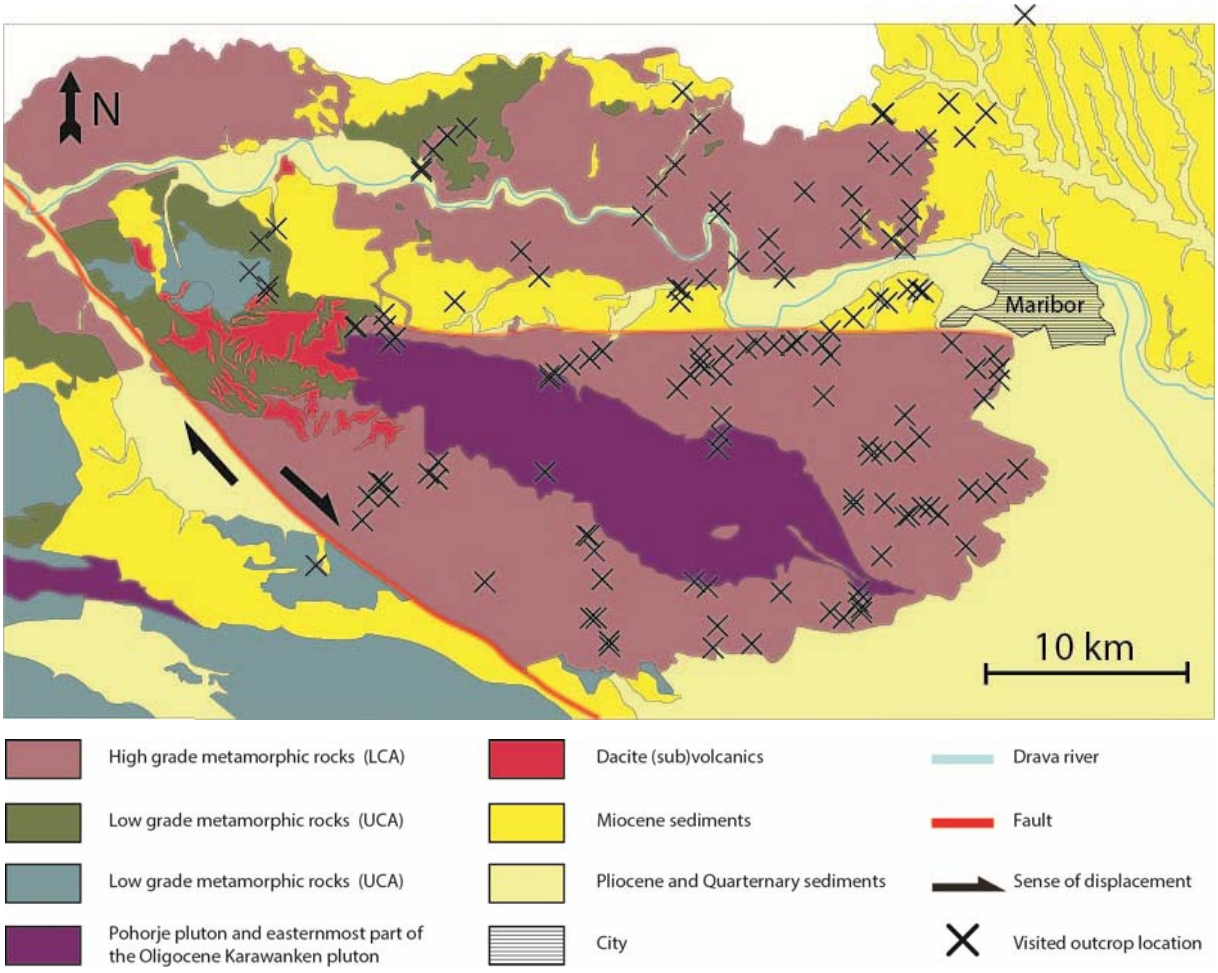

Figure 19: *Simplified map of the Pohorje and Kozjak regions showing the locations of studied outcrops for this research, modified after Mioc and Znidarcic (1977).*

Overprinting relations between different structures allowed for setting up a composite geological history of the area that extends further back than the Miocene events. In the following sections the field results are presented chronologically, starting with the oldest phase of deformation.

D1 - S1 foliation and isoclinal folding

The oldest deformation phase is characterized by a well-developed foliation (S1) and isoclinal folding on a small scale. The S1 foliation is a pervasive foliation and can be observed within all high grade metamorphic rocks in the field area. Generally the dominant foliation observed in an outcrop is the S1 foliation.

The characteristics of S1 depend on rock types. Compositional banding of alternating amphibole rich bands and plagioclase and quartz rich bands, typically creates a well-defined foliation in amphibolites. In most schists and gneisses the S1 foliation is defined by the compositional layering of mica rich and quartz rich layers. The S1 foliation is often a continuous foliation, but can also be a spaced foliation in compositionally layered rocks.

This foliation is axial planar to isoclinal folds, which are most easily seen in quartz veins, and is (sub)parallel to bedding. The isoclinal folds occur on a centimeter to meter scale. The interlimb angle ranges from 15 to 0 degrees, as a result the limbs of quartz veins are roughly parallel to the S1 axial planes (figure 20 a-d).

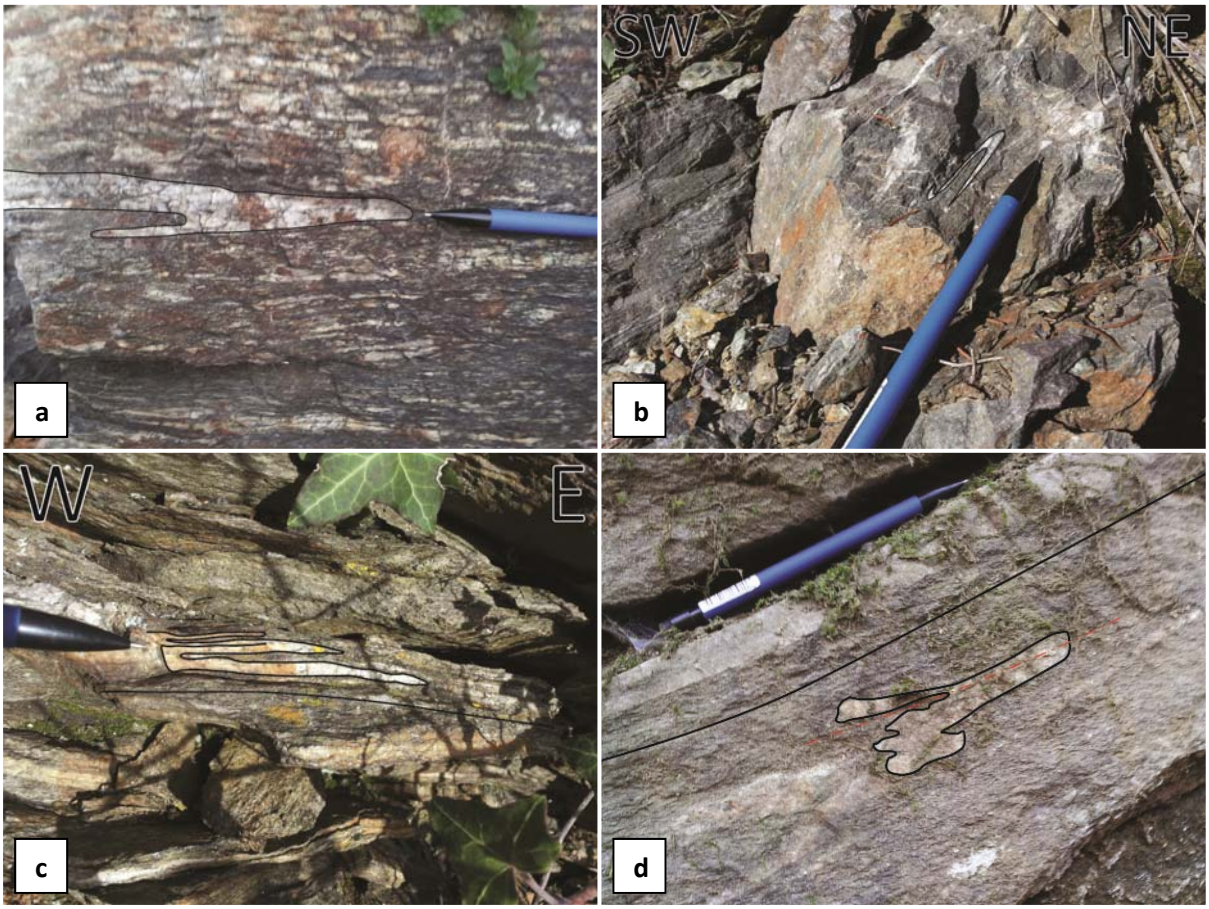

Figure 20: *S1 Foliations and isoclinally folded quartz veins. The axial planes of the isoclinal folds are sub-parallel to the foliation. The folds and pervasive foliation formed during the same deformation phase, D1.* ***A)*** *Isoclinally folded quartz vein in gneiss, location 55.* ***B)*** *Isoclinally folded quartz vein in amphibolite, location 75.* ***C)*** *Isoclinally folded quartz vein in gneiss, location 87.* ***D)*** *Isoclinally folded quartz vein in gneiss, location 127.*

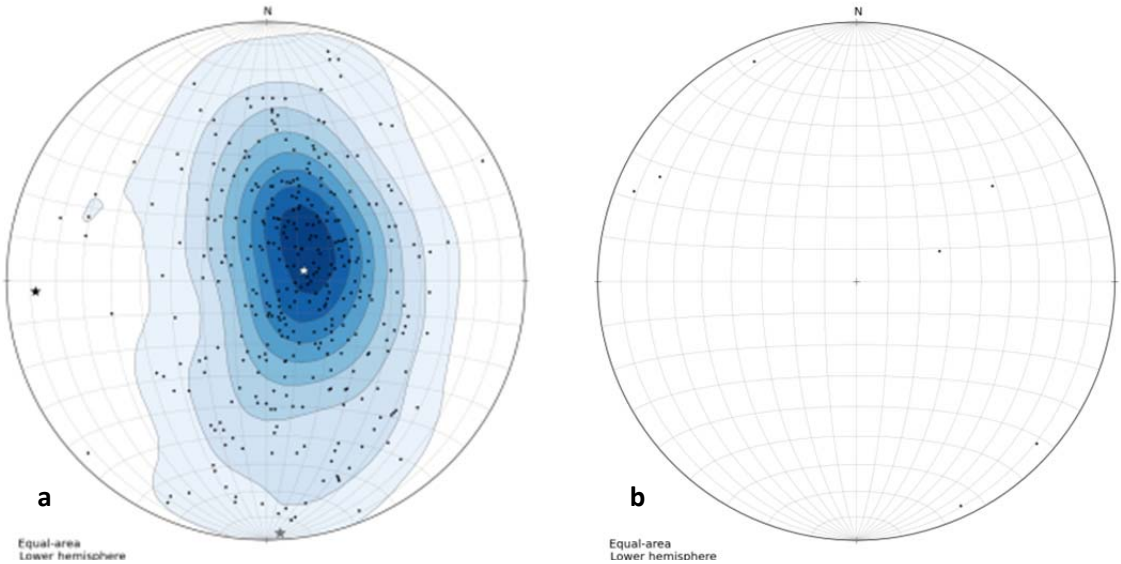

Figure 21: *Lower hemisphere Schmidt net projection of D1 deformation structures.* ***A)*** *Schmidt net projection of the poles to the S1-foliation. Most poles have steep orientations, indicating flat lying foliations. A vague N-S trending girdle can be observed in the data. Combined data from S1 measurements of this field work (n=191), and 168 datapoints from Haalboom & van Greuningen (2013), total (n=359).* ***B)*** *The fold axes of isoclinal folds (n=7).*

Most of the observed isoclinal folds are recumbent folds with gently plunging fold axes (figure 21b).The S1 foliation is usually flat-lying to moderately dipping (figure 3a). The stereographic projection of

the poles to the foliation show that the data plot along a girdle oriented roughly north south. This implies that the S1 foliation is folded along an east west oriented axis.

The isoclinal folding and formation of the S1 foliation is accompanied by stretching parallel to the foliation plane. The same quartz layers that are isoclinally folded with S1 as axial planar foliation, are boudinaged parallel to S1 (figure 22). This pure shear strain behaviour shows that flattening occurred during the D1 deformation phase.

Figure 22: *Quartz vein in gneiss (location 127) folded in the part that is at an angle with the S1 foliation, and boudinaged in the section parallel to the foliation. Red dotted lines are axial planes of the isoclinal folds, parallel to the S1 foliation. Red arrows indicate the direction of shortening, blue arrows indicate the direction of extension. The perpendicular orientation of the shortening and extensional axes are indicative for pure shear strain.*

D2 - S2 foliation and tight folding

The D2 deformation phase is characterized by a second folding phase. These folds typically have a larger wavelength and amplitude than the small scale isoclinal folds of the D1 deformation phase, in outcrops these folds are between several tens of centimeters to several meters wide. The pervasive S1 foliation is folded into asymmetric tight and open folds with occasionally observed refolded, isoclinal folds (D1). (figure 23)

Some outcrops show a second foliation, that is axial planar to the second-generation folds. In contrast to the S1 foliation, this second foliation did not form a pervasive structure.

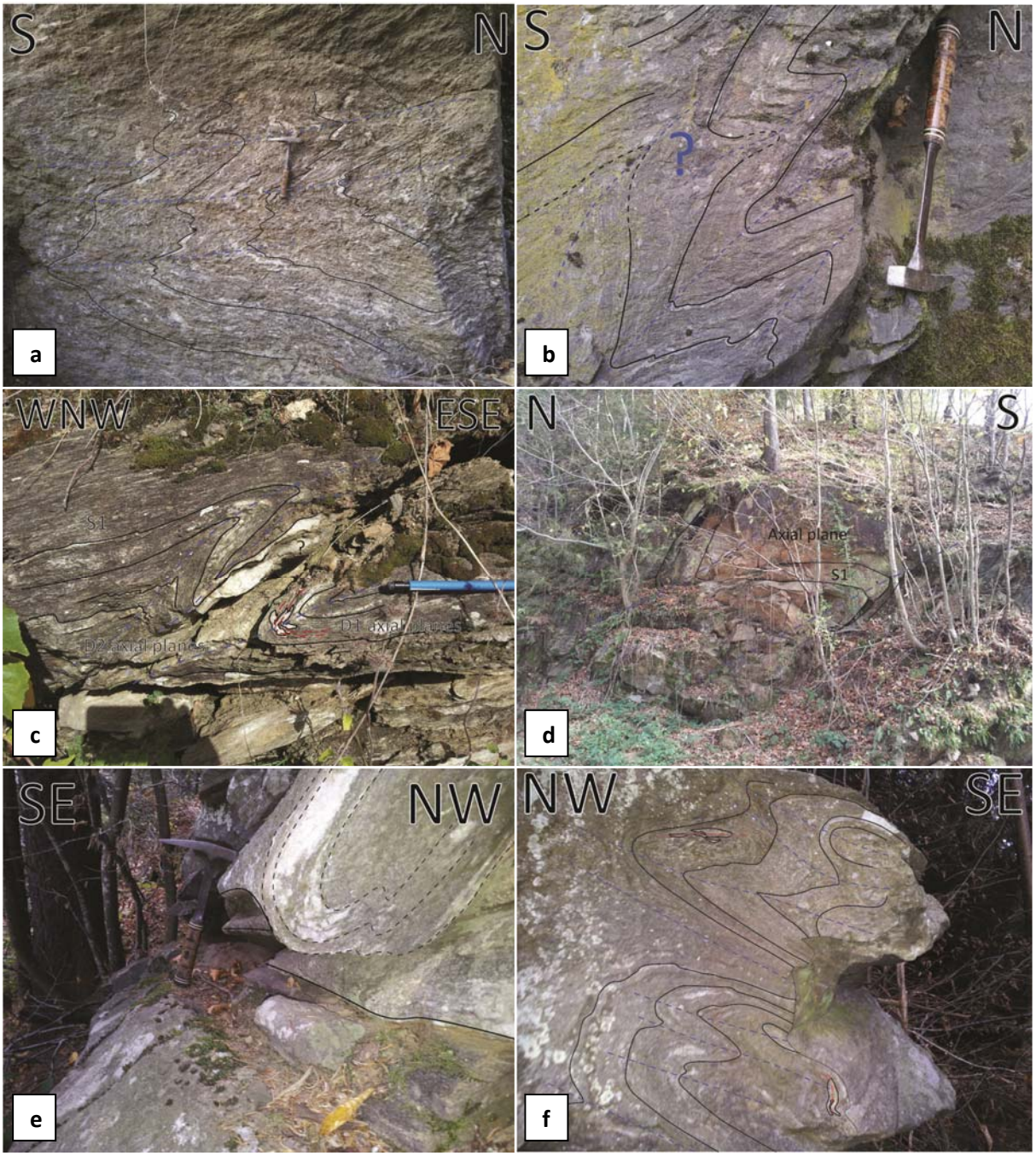

Figure 23: *S2 folds.* ***A)*** *Garnet gneiss with meter scale open to tight folds.* ***B)*** *Tight folds in an amphibolite.* ***C)*** *Tight folds in the hinge of the fold in the lower right an isoclinally folded quartz vein is refolded.* ***D)*** *Larger scale tight folds.* ***E)*** *Tight to isoclinal folds of the D2 phase. The fold axes of several folds are observed through the outcrop on the left of the image.* ***F)*** *Same outcrop as figure e, tight folds refold isoclinally folded quartz veins.*

This second foliation is not observed in every outcrop, and in many instances is only weakly developed. In that case the foliation might only be recognized as an intersection lineation with the S1 foliation (figure 24a & 24b). In some cases however the S2 foliation is the main foliation (figure 24c). In hand specimen scale it can be observed that the S2 foliation developed as a crenulation foliation to the S1 foliation (figure 24d).

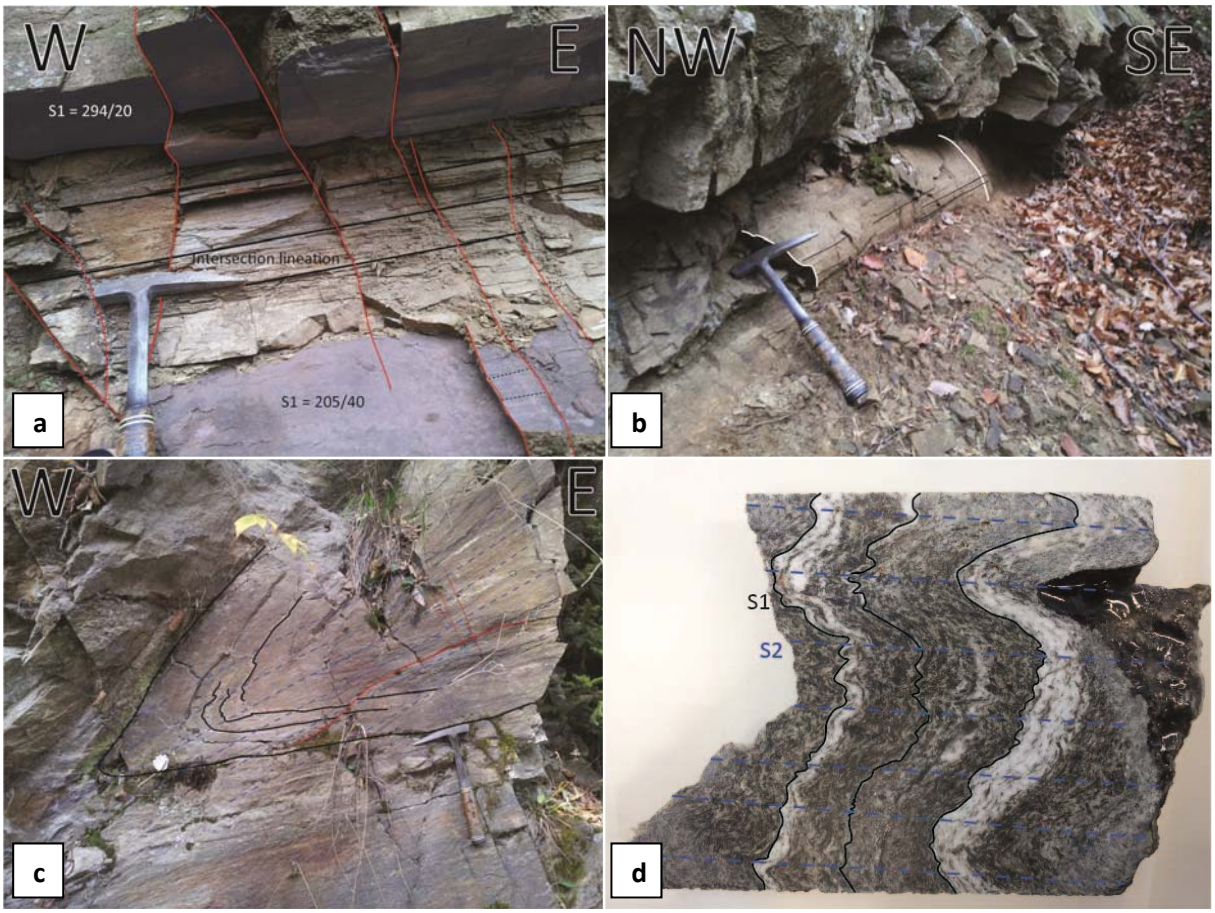

Figure 24: *S2 foliations.* ***A)*** *Gneiss, location 108. Two flanks of a tight fold are observed in upper and lower part of the image, in the center an intersection lineation between the S1 and S2 is observed parrallel to the fold axis of the fold.* ***B)*** *Intersection lineation in the hinge of a fold (location 108)* ***C)*** *A meter scale, tight fold with an axial planar S2 foliation (location 40).* ***D)*** *In this handpiece of amphibolite (location 53) the S2 foliation developed as a crenulation foliation over the S1 foliation. On the scale of the outcrop the S2 foliation was the dominant foliation.*

The fold axes of D2 folds (figure 8) dominantly plunge to the WSW and ENE, showing that folding occurred around a horizontal axis with a general WSW-ENE orientation (Fold axis = 249/21). The axial planes to the D2 folds are gently dipping structures, which implies that D2 folds are flatlying structures. Thus, the D2 folding phase is characterized by recumbent, tight folds with WSW plunging fold axes (figure 23 & 24). The axial planes of these S2 folds are dipping to the NW or to the SW (figure 25). Similar orientations, with one south-dipping group and one north west-dipping group, are observed for the axial planar foliation S2 (figure 26). This distribution of S2 foliations shows that the S2 foliation has been folded during a later phase.

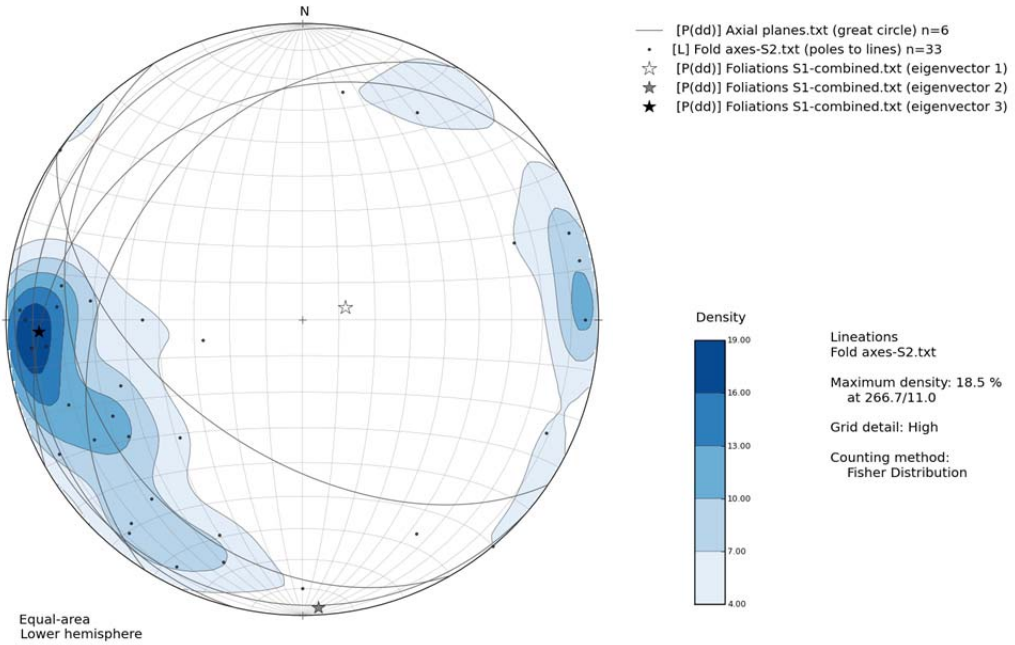

Figure 25: *Fold axes of S2-folds. Fold axes of S2 folds trend WSW-ENE, with the majority of fold axes dipping slightly to the WSW. The maximum density is at 266,7°/11°, which corresponds very well to the σ3-axis of S1 foliations (Eigenvectors S1 are represented by the star symbols). The great circles show the axial planes of S2 folds, generally dipping shallowly to the west. N=6*

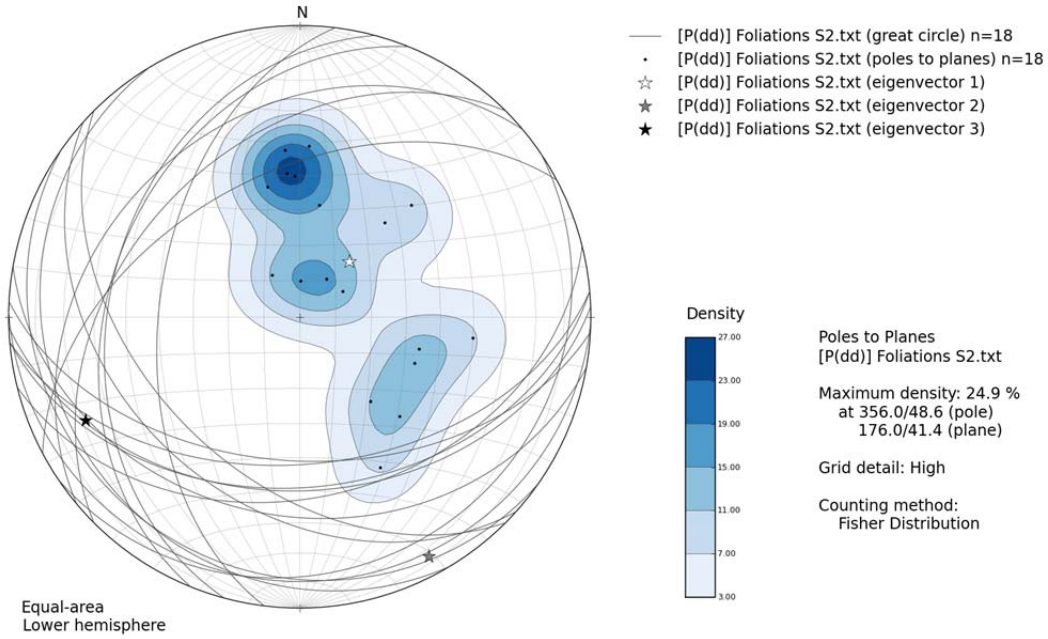

Figure 26: *S2 foliations and poles to planes, showing a bimodal distribution of orientations. One group dipping NW and one group dipping S. Some foliations dip slightly to the west. Evidence that the S2 is also folded along an axis dipping to the WSW. N=18*

D3 – Shearing & folding

The D3 deformation phase is characterized by evident shear structures, that are observed throughout the metamorphic rocks of both the Pohorje and Kozjak mountains. These include mineral stretching lineations, discrete shear zones and even mylonitic foliations (figure 27).

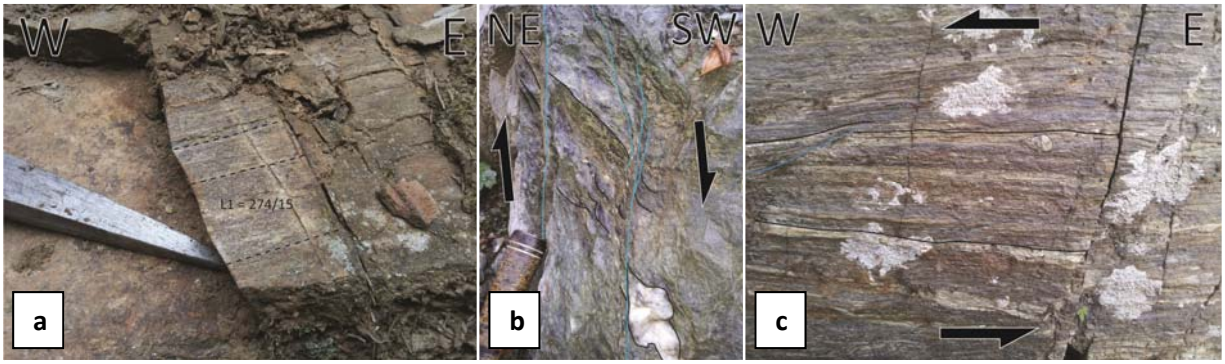

Figure 27: *D3 shear structures.* ***A)*** *Mineral stretching lineations, defined by small mica and elongated feldspar minerals.* ***B)*** *Discrete shear zone, quartz veins turn into the shear zone.* ***C)*** *Mylonitic foliation, sinistral sense of shear is indicated by an asymmetric clast (to the right of the middle) and an C-C' relation (at the left of the figure).*

Mylonites record very high levels of strain, and thus record the locations where strain has localized. Most of the mylonites that developed in the Pohorje area are found in the uppermost parts of the Lower Central Austroalpine unit. The phyllonites, that represent the shallowest part of this nappe, typically have a mylonitic foliation. Outcrops of phyllonite are widespread in the Kozjak mountains. In the Pohorje mountains the occurrence of mylonites can be associated with retrograde metamorphism, and are mostly found along the western and eastern margins of the range.

The S1 foliation is displaced and deformed by D3 shear bands. Similarly, isoclinally folded quartz veins are sheared by D3 shear zones. Stretching lineations associated with D3 deformation are found on the S1 aswell as the S2 foliation planes, associated with kinematic indicators for simple shear.

Stretching lineations are often defined by stretched feldspars, elongated quartz veins and stretched mica (figure 27a). Lineations defined by chlorite are also identified on numerous occasions. The presence of chlorite, overprinting all older structures, in the metamorphic rocks is an indication for retrograde metamorphic conditions.

Most stretching lineations are oriented in an E-W direction and are generally shallow plunging. Although both east- and west plunging stretching lineations are observed, west plunging lineations are dominant (figure 28). Shear bands, asymmetric clasts and veins, sigmaclasts, deltaclasts and strain shadows around porphyroclasts (figure 29) have been used to determine the sense of shear. The analysis of these kinematic indicators shows that the general sense of shear is top to the east (figure 28b & 28c). Deviations from this trend are not uncommon. The opposite direction, top-to-the-west sense of shear is also regularly observed. However, top-to-the-east sense of shear indicators outnumber top-to-the-west indicators significantly in every part of the study area (figure 30), despite the west plunging stretching lineations. Shearbands are most commonly observed, and are typically discontinuous structures with a millimeter to centimeter scale spacing. However, they do not appear in competent lithologies, like quartz veins or coarse grained gneiss. Asymmetric and sigma-type clasts are also frequently observed, which develop from large feldspar clasts, or quartz veins. Strain shadows are frequently observed around garnets.

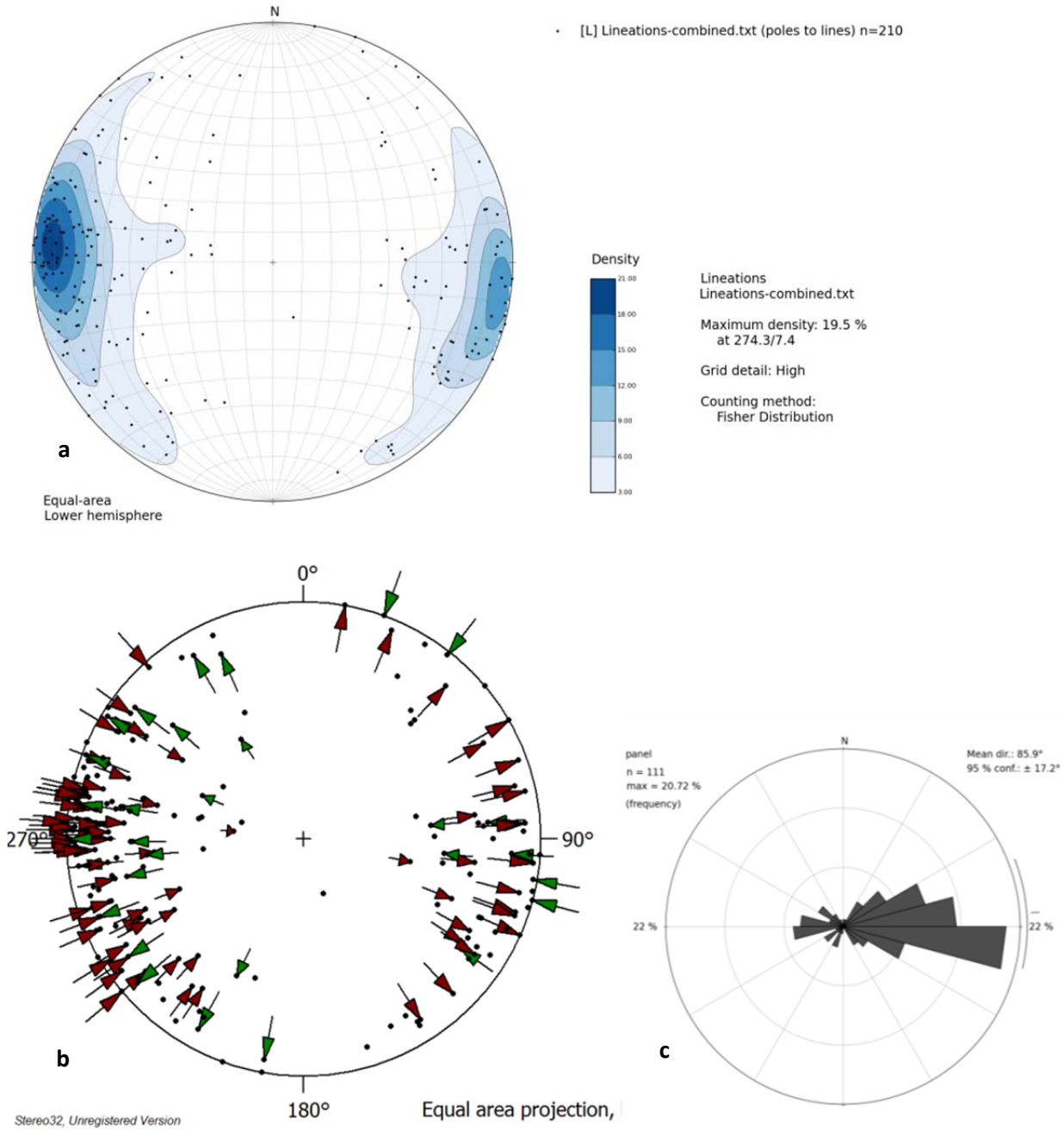

Figure 28: *Stretching lineations and shear sense.* ***A)*** *Stretching lineations (n=210) plunge either to the west or to the east, but dominantly towards the west. The dip angle is typically very low.* ***B)*** *Projection showing the stretching lineations (black dots) and sense of shear (arrows). Multiple measurements with similar values from the same location were averaged, reducing the number of lineation measurements to 188. Green arrows indicate a top-to-the-west sense of shear, whereas red arrows indicate top-to-the-East sense of shear. Also west dipping lineations dominantly have a top-to- the-East sense of shear..* ***C)*** *Rose diagram of the sense of shear. The majority of the data indicates top-to-the-East sense of shear.*

Occasionally small scale asymmetric folding is observed with fold axes approximately perpendicular to the stretching lineations. These Z and S type folds are thought to be related to the D3 shearing, and could be used as an additional kinematic indicator. The fold axes of these asymmetric folds are trending NE-SW, and both show top to the ESE sense of shear, consistent with the regional and local sense of shear derived from other shear sense criteria (figure 29f).

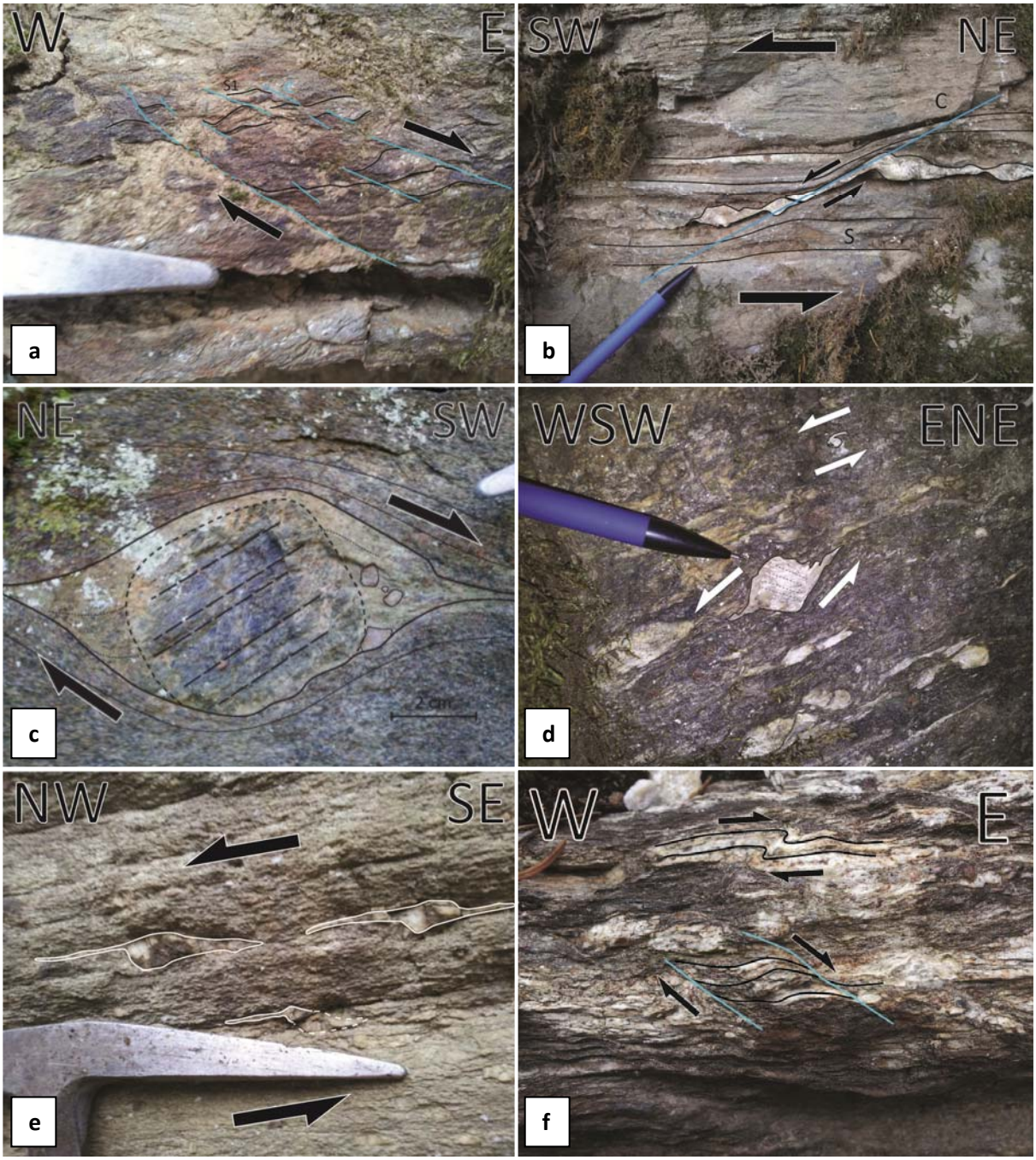

Figure 29: *Shear sense indicators in the Lower Central Austroalpine nappe.* ***A)*** *Shearbands indicating a dextral sense of shear (Micaschist, location 60)* ***B)*** *Sinistral S-C structure and asymmetric clasts (Amphibolite, location 97)* ***C)*** *Dextrally sheared amphibole with strain shadow, amphibolitized eclogite (location 74).* ***D)*** *Feldspar with sheared 'tails' and small delta clast indicating sinistral shear (gneiss, location 98).* ***E)*** *Sigmaclasts indicating sinistral shear (Augengneiss, location 130).* ***F)*** *Shearbands and Z-type fold in gneiss showing used as kinematic indicator for dextral shear (location 49).*

Other than the sense of shear, these outcrops do not have a common denominator, they are not located in similar places nor are they in the same stratigraphic position. They are spread over different areas and different lithological units. In the eastern part of Pohorje also roughly N-S oriented lineations are observed.

The top-to-the-East sense of shear measurements show a variation in direction over the area. In the SW of the Pohorje mountains the stretching lineations are oriented in NW-SE direction, and the main

sense of movement is top to the SE. This orientation is remarkably similar to the trace of the adjacent Lavanttal fault. Further away from the Lavanttal fault, in the eastern and northern part of the Pohorje mountains the sense of shear is due east. In the eastern part of the Kozjak mountains the sense of shear is even top-to-ENE (figure 30).

A few stretching lineations deviate from this trend (locations 130, 131 and 127). These stretching lineations trending NNW-SSE are all located in north eastern part of the Pohorje mountains, in the central part of the antiform that was deducted by Kirst et al. (2011). Therefore, these outcrops represent the deepest levels of the Lower Central Austroalpine unit found in the Pohorje area. The kinematic indicators showing the sense of shear are generally well developed sigmaclasts and not shearbands that are the dominant shear sense indicators in other outcrops. Furthermore, no chlorite overprint has been recognized at these locations. These deviating shear senses are indicated in figure 16 by their purple color.

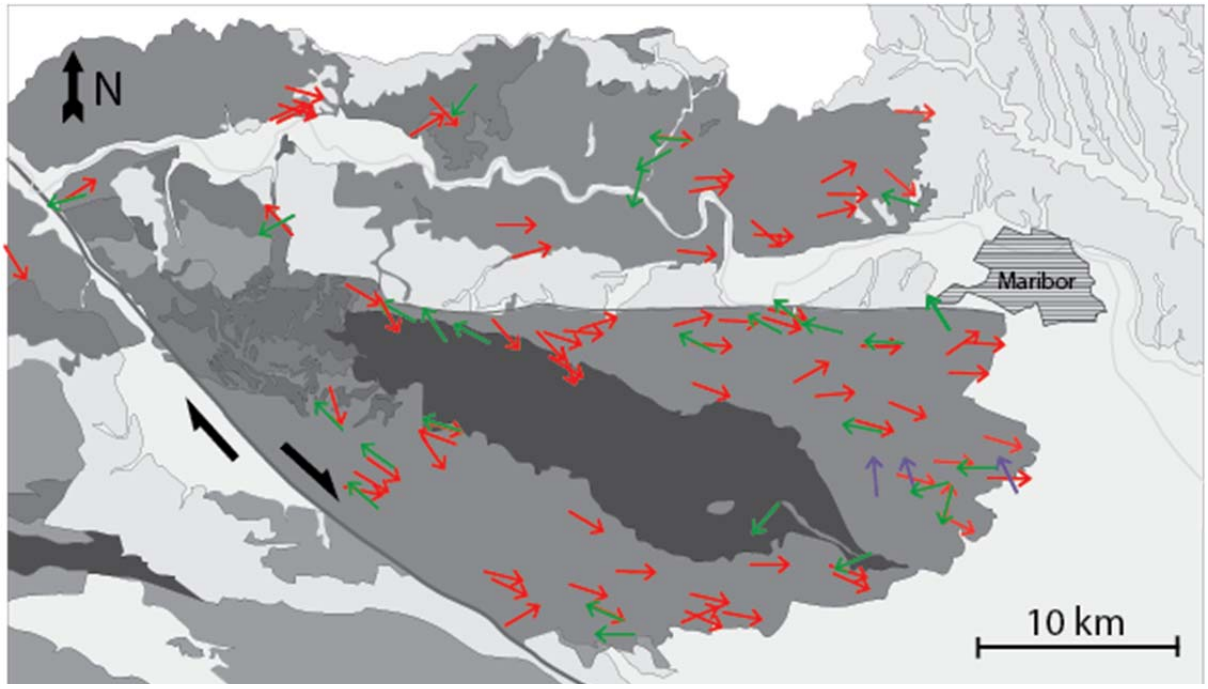

Figure 30: *Map showing the sense of shear in the Pohorje and Kozjak mountains. The dominant sense of shear is top to the east. an important deviation from this trend are locations with top to the west sense of shear. Top to the west sense of shear is observed throughout the area and cannot be specified to certain areas or specific tectono-stratigraphic units.*

Deformation of Pohorje pluton and volcanics

As can be seen in figure 30, some of the shear sense indicators are found within the pluton. The pluton is deformed in its exterior parts close to the metamorphic host rocks. In these parts the granodiorite is foliated and, on this foliation, stretching lineations are observed (Haalboom & van Greuningen, 2013). The sense of shear along these stretching lineations could be determined by analyzing asymmetric feldspar clasts. Stretching lineations are oriented along an E-W trend and plunge either gently to the West or to the East. No dominant sense of shear can be found in the data, as similar numbers of top-to-the-East and top-to-the-West observations were made (figure 31). However, the presence of these D3-structures within the pluton, gives a clear constraint on the timing of the D3 deformation phase.

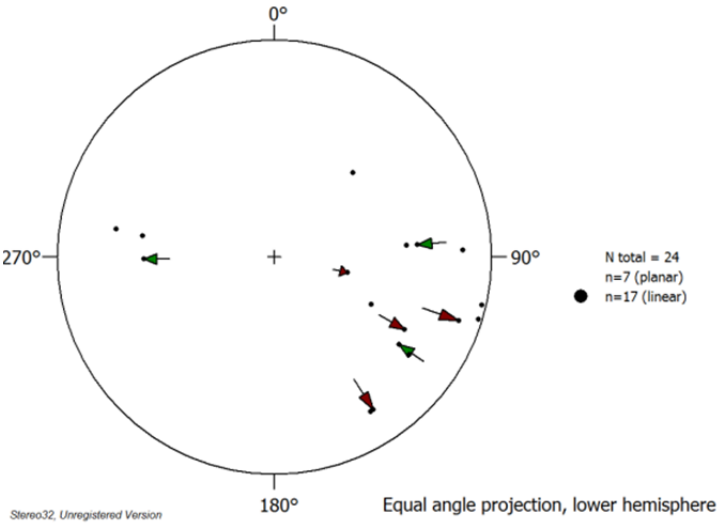

Figure 31: *D3 stretching lineations (n=17) and sense of shear (n=7) obtained from the Pohorje pluton. An E-W trend can be observed in the stretching lineations. The dominant sense of shear is inconclusive, similar amounts of red arrows (top-to-the-East) as green arrows (top-to-the-West) are plotted.*

Another time constraint is linked to observations of deformed dykes and sills. The dykes and sills and dacite subvolcanics in the Pohorje mountains are sometimes deformed by the D3 shearing phase (figure 32a). Other dykes are not deformed and crosscut mylonitic rocks (figure 32b). Shearing related to the D3 deformation phase must have been active during and after the emplacement of the first dykes, however, must have ended before the emplacement of the undeformed dykes.

Figure 32: *Dykes and deformation.*

A) *A white pegmatite vein in orthogneiss is sheared along a subvertical shearplane (location 8).*

B) *Host rocks with a sub horizontal, mylonitic foliation are intruded by several vertical dykes (location 77). The dykes cut the mylonitic foliation and are not deformed.*

Miocene sediments and brittle deformation

The Miocene sedimentary rocks also record D3 deformation. Tilted orientations of the bedding indicate folding of this unit (figure 33a). The associated fold axis, that fits best with the measurements is 285/06.

Faults in Miocene sediments tend to have a steep inclination with respect to the bedding, and given that top-bottom criteria were available, they showed a normal sense of displacement. On several locations mini horst-and-graben structures have formed (figure 33a & 33b). A lot of these normal faults are tilted after faulting. A good example are the rocks from location 20, where the orientation of the bedding is now in an overturned nearly vertical position. North-dipping normal faults are now

gently dipping to the South. These structures have rotated around a flatlying roughly E-W oriented axis. Joints and faults in Miocene sediments can be categorized into two groups. Faults and joints with an ESE-WNW trend, which are found mainly in the Ribnica-Selnica trough, and those with a NNE-SSW trend (figure 34b).

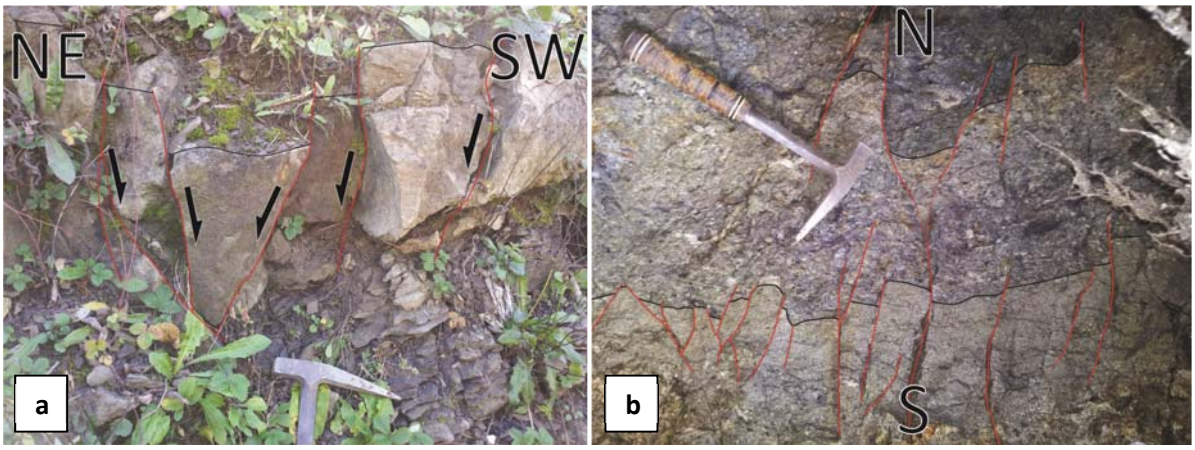

Figure 33: *Faulting in Miocene sediments.* ***A)*** *Small horst-and-graben structure in Miocene sandstones (location 24).* ***B)*** *Small scale horst-and-graben structure in tilted Miocene conglomerates and sandstones (location 24). This picture is rotated 90°, the top is to the right of the image.*

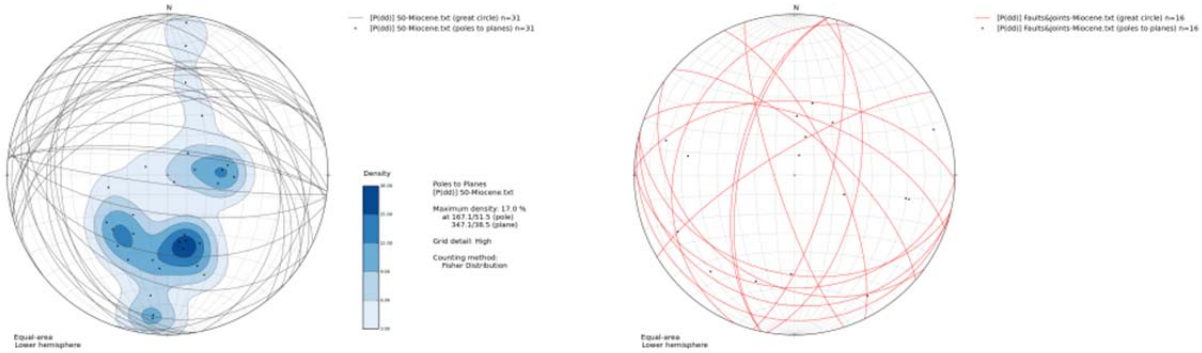

Figure 34: *Miocene sedimentary rock measurements.* ***A)*** *Great circles and poles to the planes of the bedding (S0) of Miocene sedimentary rocks.* ***B)*** *Faults and joints in Miocene rocks can be divided into two groups, one with an ESE-WNW trend, and those with a NNE-SSW trend.*

Summary Field results

The field results allow to differentiate three different deformation phases, D1, D2 and D3 respectively. In the first part of this chapter the main structures of each deformation phase will be summarized, and a mechanism will be proposed for the formation of the deformation structures. In the second part of this chapter the present day structure will be discussed based on cross sections of the area.

D1 – Deformation structures related to D1 are the S1 foliation and isoclinally folded quartz veins. Quartz veins parallel to the foliation are boudinaged, the S1 foliation is flat lying, (sub-)parallel to bedding, and most isoclinal folds are recumbent (figure 3). Therefore it could be interpreted that the main principal stress axes was vertical, and deformation resulted in pure shear strain. This could be the case during burial.

D2 – Tight folds, refolding the S1 foliation, are the most observed structures related to the D2 deformation phase. On several locations a S2 foliation is observed, that developed as an axial plane foliation. Fold axes plunge gently towards the WSW and some to the ENE. S2 recumbent folds typically have flat lying axial planes, dipping to the north-west and south. Several stretching lineations and kinematic indicators show top to the NNW sense of shear. These are observed in rocks that do not seem to be affected by retrograde conditions.

These structures may have resulted from simple shear strain, with top-to-the-NNW sense of shear.

D3 – Within the metamorphic rocks of the Lower Central Austroalpine, the D3 deformation phase is mostly recognized by shear structures. They indicate a dominant top-to-the-East sense of shear. However, abundant top-to-the-West sense of shear indicators are observed as well. The fact that this phase has also affected the Pohorje pluton acts as time constraint. The newly formed foliation in the pluton is folded. The Miocene sediments also record this phase of deformation, a similar direction of folding (Fold axis = 285/06) is observed in the orientation of the bedding of Miocene sedimentary rocks (figure 35) and the refolded S2 foliation planes

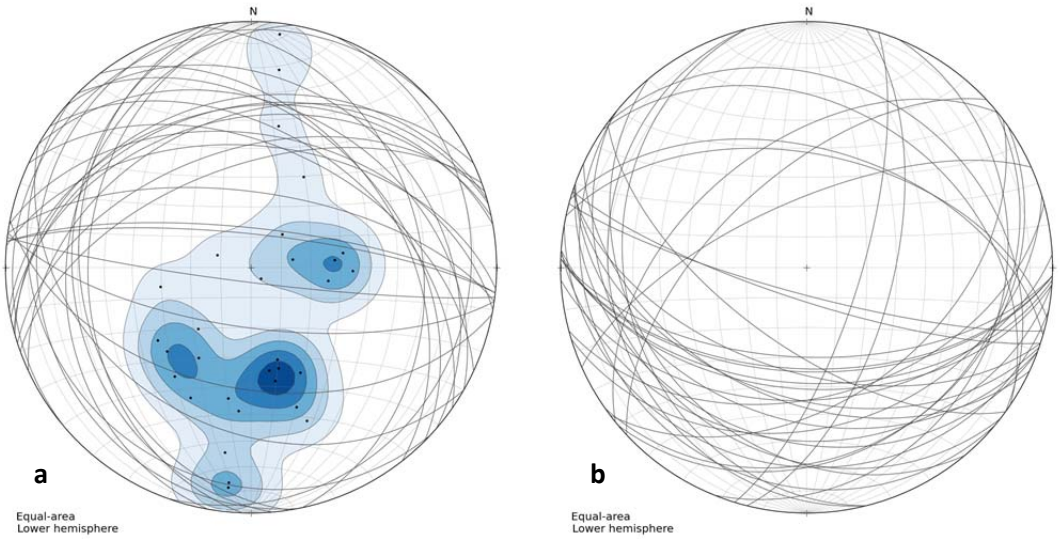

Figure 35: *D3 folding recorded in young rocks.* ***A)*** *Bedding orientations (S0) of Miocene sediments (n=31). These measurements indicate that the Miocene rocks are folded. The fold axis is 285/06.* ***B)*** *Foliations in the pluton (n=36). The orientations appear to be similar to the Miocene bedding plot.*

Faults in the Miocene sediments are rotated by an E-W trending fold axis as well, and therefore are either prefolding or synfolding features.

The granodiorite pebbles and blocks that are found in the deformed Miocene sediments have features indicating a proximal source. Dating of the biotite cooling ages yielded ages similar to those found in the Pohorje pluton (Fodor et al., 2008). Therefore, these pebbles are believed to be derived from the Pohorje pluton.

Several events occurred in the Miocene:

1) Emplacement of the pluton
2) Dominant top-to-the-East sense of shear in the metamorphic basement and the pluton
3) Exhumation of the pluton
4) Deposition of Miocene sediments with pebbles derived from erosion of the pluton
5) Faulting of Miocene sediments
6) N-S folding of the pluton foliation and Miocene sediments.

Microstructural and Petrological Analysis

During two separate fieldworks, oriented samples of rocks have been collected. Nearly all of these oriented samples were derived from the high grade metamorphic unit of the Pohorje and Kozjak mountains. A total of 45 thin sections have been prepared from these oriented samples, to be used for optical microscopy analysis. In most cases a clear stretching lineation was found and measured in the field. The thin sections have been prepared parallel to the stretching lineation and normal to the foliation. Microstructural and petrological analysis is used to infer the kinematics and the relative timing of deformation events, as well as the pressure and temperature conditions at the time of deformation.

Microstructures and Deformation phases

The S1 foliation in most rocks is very well developed, and is derived from the aligned orientation of elongate and platy minerals, the stretching of minerals in the same general direction and compositional layering with different minerals defining distinct bands. In the gneisses, foliations are easy recognizable, as minerals are typically similar in size, and reoriented mica are present (figure 36a). This is not always true for amphibolites and tonalities, which consist of some large equidimensional minerals, amphiboles and feldspars respectively, surrounded by a finer grained groundmass, which obscures foliations on the microscopic scale.

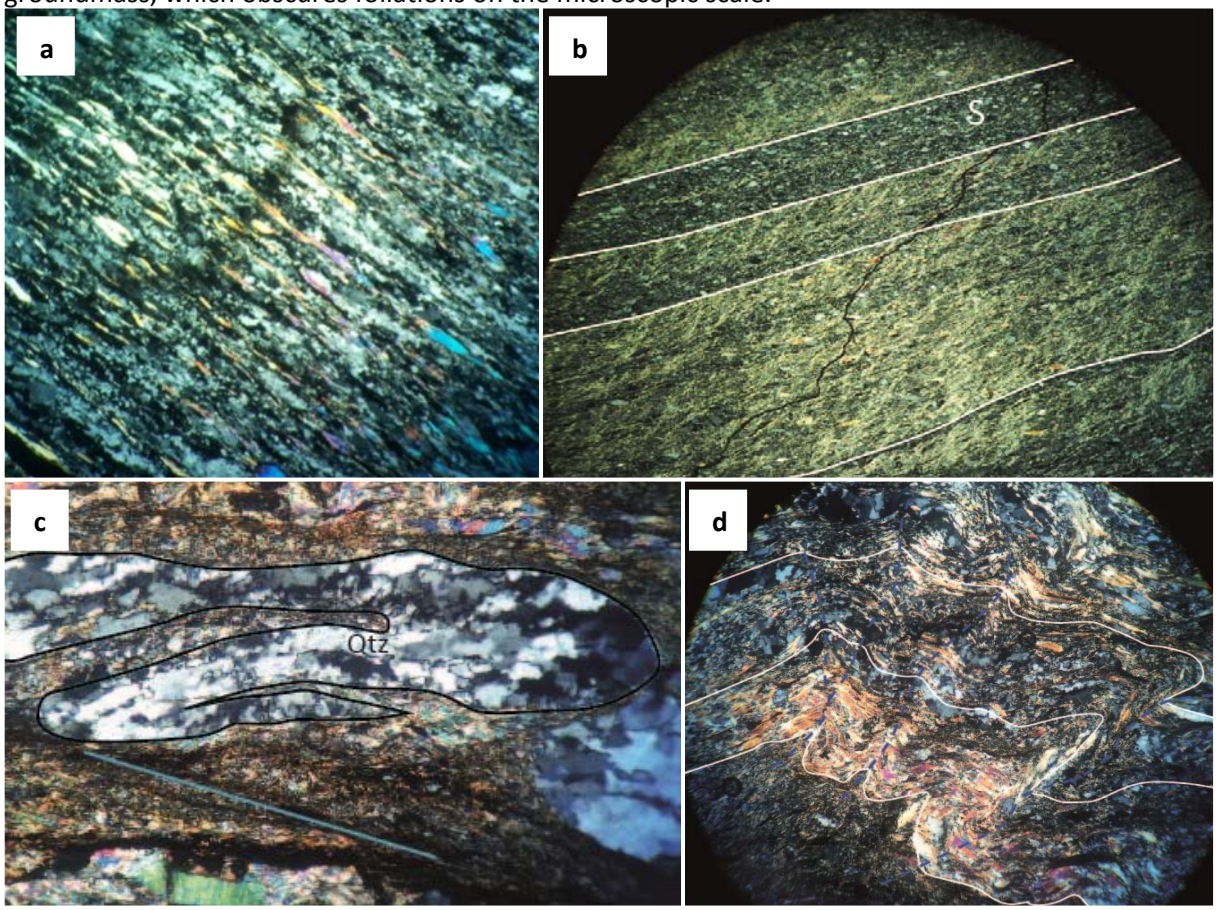

Figure 36: *Foliations in gneisses,* ***A)*** *A gneiss consisting largely of quartz, plagioclase and muscovite shows a clear foliation through the alignment of the mica, width of view 1,5 mm.* ***B)*** *In this gneiss mica and quartz have partly segregated into bands of different composition, width of view 6 mm.* ***C)*** *Two types of folding from the same sample (P21). A) Isoclinally folded quartz vein, the main foliation is axial planar, width of view 1 mm.* ***D)*** *Tight folds affecting the foliation, width of view 5 mm.*

Isoclinally folded quartz veins are also observed in thin sections. These are, just as the macroscopic isoclinal folds often flat lying and the foliation is axial planar to these folds (figure 37a). Also small scale, tight folding (D2) is observed, these folds affect the S1 foliation (figure 37b).

Kinematic criteria related to the D3 shearing event, that are found with microstructural analysis include micro structures as boudins, asymmetric broken clasts (figure 37c), shear bands (figure 37d-37f), strain shadows around porphyroclasts (figure 37a&37b), micafish and asymmetric clasts.

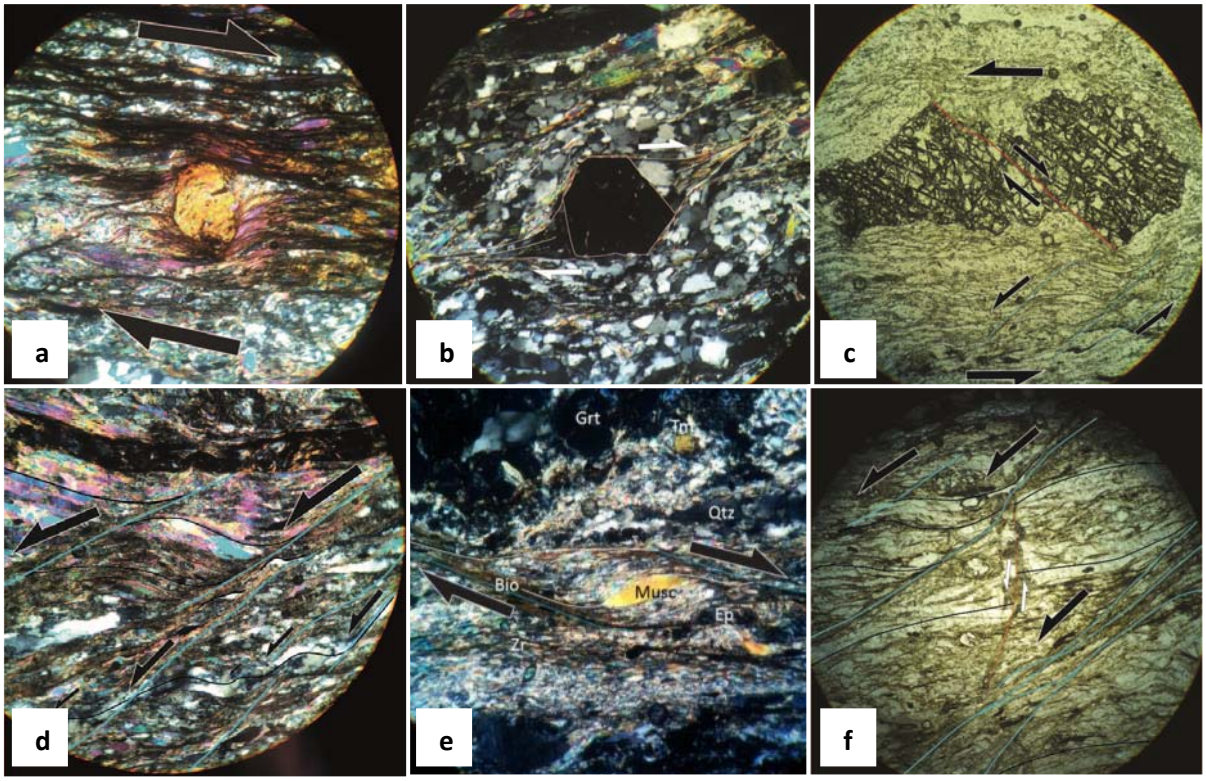

Figure 37: *Kinematic indicators A) strain shadows around a porphyroclast indicating a dextral sense of shear, width of view 1,7 mm. B) Foliation wrapping around a garnet showing a dextral sense of shear, width of view 1,7 mm. C) domino type broken garnet and shearband indicating a dextral sense of shear, width of view 1,7 mm. D) sinistral shearbands, width of view 1,4 mm. E) Dextral shearband, width of view 3,5 mm.F) Sinistral shearbands, width of view 6 mm.*

Using these kinematic indicators the sense of shear could be determined for 32 samples. The distribution of the direction of shear sense is plotted in a rose diagram, clearly demonstrating a dominant top to the east sense of shear (figure 38). The mean direction of these shear senses is top to 93,6°. 6 Out of 32 microstructures however revealed a (roughly) top to the west sense of shear.

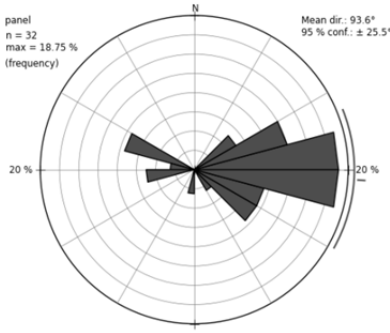

Figure 38: *Rose diagram showing the direction of shear sense of 32 thin sections. A significant majority indicates top to the east sense of shear.*

The deformation phases found in the field can be successfully correlated to structures that developed on the micro scale. In the next section the relation between these deformation events and the metamorphic history of the rocks will be investigated.

Metamorphism

Stable mineral assemblages are key indicators to establish to which metamorphic degree these rocks has been subjected to. In addition, certain recrystallization structures can be used as pressure and temperature indicators. In this section the aim is to constrain the metamorphic history of the rocks. Through careful analysis of the timing of growth of certain indicator minerals, porphyroblast relations and dynamic recrystallization structures the link is established between deformation events and PT-conditions.

UHP Metamorphism

The mineral assemblage of eclogite is observed to consist of garnet, kyanite, omphacite and quartz as the main constituents (figure 39a). Accessory minerals are rutile and apatite. Multi mineral quartz inclusions are found within larger minerals such as omphacite. These might represent coesite retromorphs, with quartz substituting coesite during decompression. Typical radial fractures around these inclusions might have formed due to the increase in volume resulting from the reaction of coesite to quartz (figure 39b). However these findings cannot be regarded as decisive arguments for UHP-metamorphism. However, the findings of exsolution lamellae in the pyroxenes support that this mineral assemblage has experienced UHP metamorphism. The eclogites are typically not foliated as a result of which it is hard to obtain the relative timing of this UHP metamorphism with respect to the deformation phases. However, UHP metamorphism and the formation of eclogites in general is related to subduction. Therefore it seems likely that the timing of the UHP metamorphism is similar to the high grade metamorphic phase in the surrounding host rocks.

Symplectites are present between the minerals (figure 39c). Symplectites typically consist of minerals with slightly different chemical composition then the mineral in the high pressure assemblage. They form under conditions when the high grade assemblage is no longer stable. Therefore, the presence of these symplectites is an indication that the eclogites underwent post-peak pressure metamorphism.

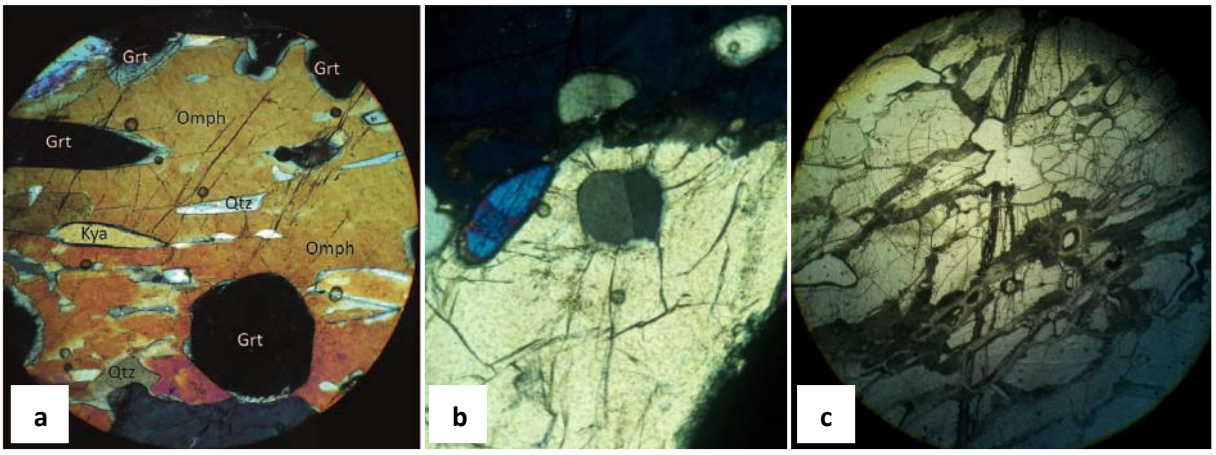

Figure 39: *Eclogite A) Main minerals (XPL), width of view 1,7 mm. B) Two quartz minerals in an inclusion within omphacite (XPL), radial fractures might indicate that coesite used to fill the inclusion, width of view 0,8 mm C) Symplectites clearly surround the minerals in plane polarized light, these symplectites are younger than the fracture that goes from the top to the bottom of the picture, width of view 6 mm*

Peak temperature metamorphism

The gneisses and schists consist largely of quartz, (plagioclase) feldspar, biotite, muscovite and garnet. Accessory minerals are clinozoisite, epidote, staurolite, kyanite, amphiboles, tourmaline

(dravite), titanite, apatite, rutile, zircon, orthopyroxene and opaque minerals (Appendix: Mineral catalogue). A high grade metamorphic mineral assemblage is comprised of biotite, muscovite, garnet, staurolite, kyanite and orthopyroxene. This assemblage represents the highest metamorphic grade found in the metamorphic rocks of the Lower Central Austroalpine nappe. It will be referred to as peak metamorphism, M_{peak}, from now on.

Using the stability field of some indicator minerals the pressure and temperature conditions at which this stable mineral assemblage developed can be defined. The stability fields of several minerals are used in the petrogenetic grid for the KFMASH system, which is suitable for metamorphic rocks of a pelitic origin. The presence of staurolite, kyanite and biotite indicate a narrow range of temperatures and pressures for peak metamorphic conditions. The peak metamorphic temperature ranges between 545°C and 690°C, and pressure between 5 and 15 kbar (figure 40). Assuming a typical lithostatic pressure gradient for crustal rocks of 30 Mpa/km, these pressures can be converted to depths of approximately 18-45 km.

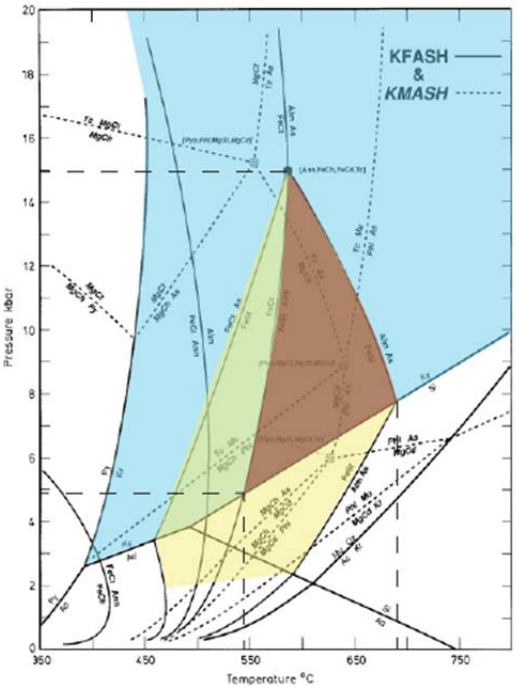

Figure 40: *Petrogenetic grid of the KFMASH-system for pelitic rocks. The stability fields of staurolite (yellow) and kyanite (blue) overlap with the region where garnet and biotite coexist stable together and chlorite and garnet are no longer stable together. The all overlap in the brown area, yielding a small triangle which shows the range of possible PT conditions for this stable mineral assemblage. (Modified after Spears and Cheney, 1989)*

Marbles found in the lower nappe in the Pohorje mountains have most likely experienced similar metamorphic conditions. Microscopical analysis shows that these marbles consist largely (75%) of calcite. Contamination of the protolith carbonate rocks is evident from the additional minerals. The green minerals are identified as zoisite (figure 41a).

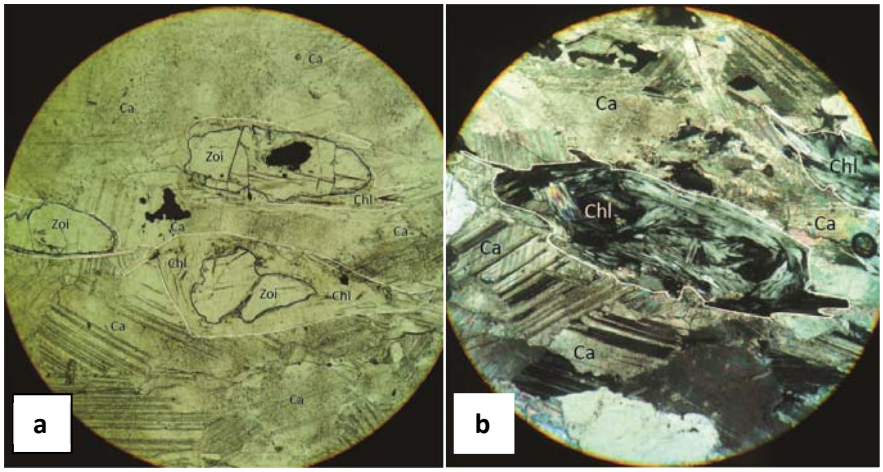

Figure 41: *Marble, location 72.* ***A)*** *Zoisite minerals with rims of chlorite, width of view 6 mm.* ***B)*** *Zoisite pseudomorph, fully replaced by chlorite, width of view 1,7 mm.*

Quartz, actinolite and opaque minerals are present in relatively high concentrations. Additional minerals include titanite and biotite. The presence of zoisite is characteristic for the zoisite zone, a metamorphic zone for calc-silicate rocks, roughly equivalent to the staurolite zone for pelitic rocks. Thus, the marbles represent similar conditions for the peak metamorphism as the gneisses and schists.

The relation between this high grade mineral assemblage and deformation is studied from porhyroblast inclusion patterns and cross cutting relations. Garnet and staurolite porphyroblasts with inclusions are observed (figure 42). The inclusion patterns in both the garnet and the staurolite are straight in the interior of the mineral, however start to curve in the exterior parts of the minerals. The foliation outside the porphyroblasts is wrapping around these minerals. One interpretation is that these porphyroblast first started to grow between two subsequent stages of deformation (inter-tectonic), leading to formation of porhyroblasts with straight inclusion patterns. However growth continued during the second deformation phase causing the syn-tectonic exterior parts of the porphyroblasts.

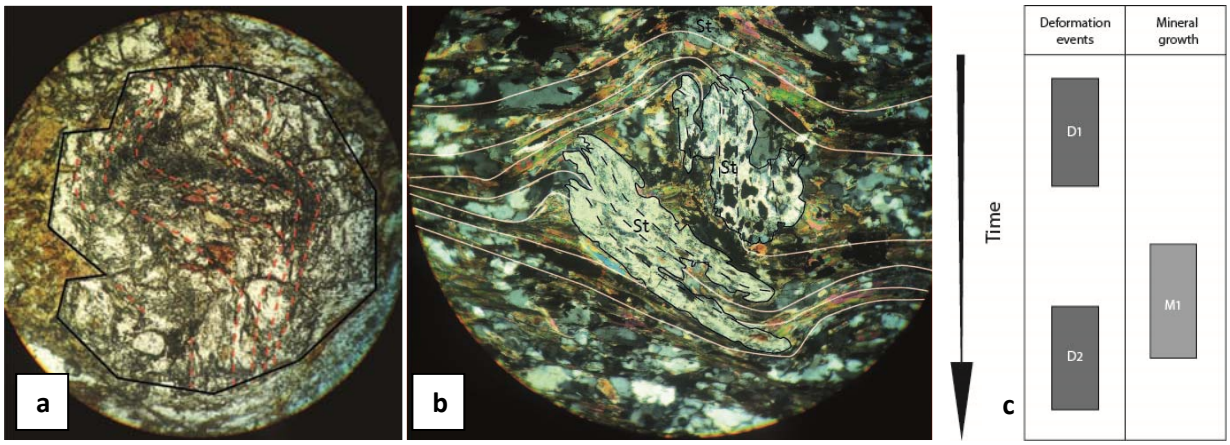

Figure 42: *Porphyroblast relations. A) Garnet with spiral inclusion pattern, the interior part of the inclusions is straight, width of view 1,7 mm.* ***B)*** *Staurolite porphyroblasts with largely straight inclusion patterns, only at the edges the patterns starts to curve, width of view 5 mm.* ***C)*** *Interpretation of the relative timing of deformation and mineral growth involving two deformation phases*

Other interpretations are possible, for instance one where two phases of mineral growth are involved, or one where mineral growth takes place syn-tectonic, however with rotation of the minerals starting close before the end of growth.

Linking these relations between peak metamorphism and deformation with earlier described deformation phases we see that, all possible models include a phase of deformation starting before the stage of mineral growth. Thus, the formation of this mineral assemblage (M_{peak}) post-dates the formation of a primary foliation (D1). Furthermore, the assemblage is older than the tight folding phase (D2), as is observed by the folding of large muscovite minerals that formed during the high grade metamorphism. (figure 36d & figure 43). The shearing event (D3) postdates the mineral growth, as strain shadows evolved around garnets and associated minerals (figure 37a & 37b) and muscovites and biotites are clearly sheared by shear bands (figure 37d & 37e).

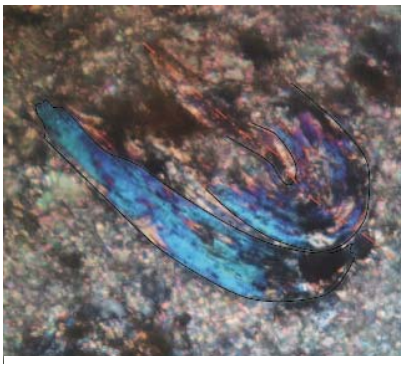

Figure 43: *Folded mica crystal, width of view 0,5 mm.*

Retrograde conditions

During a later stage, crystallization takes place of epidote, clinozoisite and chlorite. Euhedral minerals of epidote and clinozoisite are observed that overgrow the foliation made up by biotite and muscovite (figure 44a & figure 44b). Most minerals of the high grade mineral assemblage are still (meta)stable, however, biotite is replaced by chlorite (figure 44c). This second mineral assemblage is characteristic for greenschist or epidote-amphibolite facies metamorphism. The growth of these minerals therefore represent retrograde metamorphic reactions. The thin sections show that some areas are shielded from this retrograde metamorphism, sample 87 for instance contains bands rich in kyanite and staurolite. Other bands, separated by mica-rich bands, contain little to no kyanite and staurolite, but do contain vast amounts of chlorite. This effect is regarded by the author as evidence for the importance of fluid availability during retrograde metamorphic reactions. This phase of mineral growth pre-dates the D3 shearing event. Large chlorite minerals associated with this phase are sheared by D3 shear bands (figure 44d), and epidote minerals are broken (figure 44a).

Zoisite minerals in marbles often have a reaction rim of chlorite (figure 41a). In some instances pseudomorphs of zoisite are present, that are completely filled with chlorite (figure 41b).The chlorite replacing the rims of zoisite minerals is indicative for a retrograde metamorphic overprint.

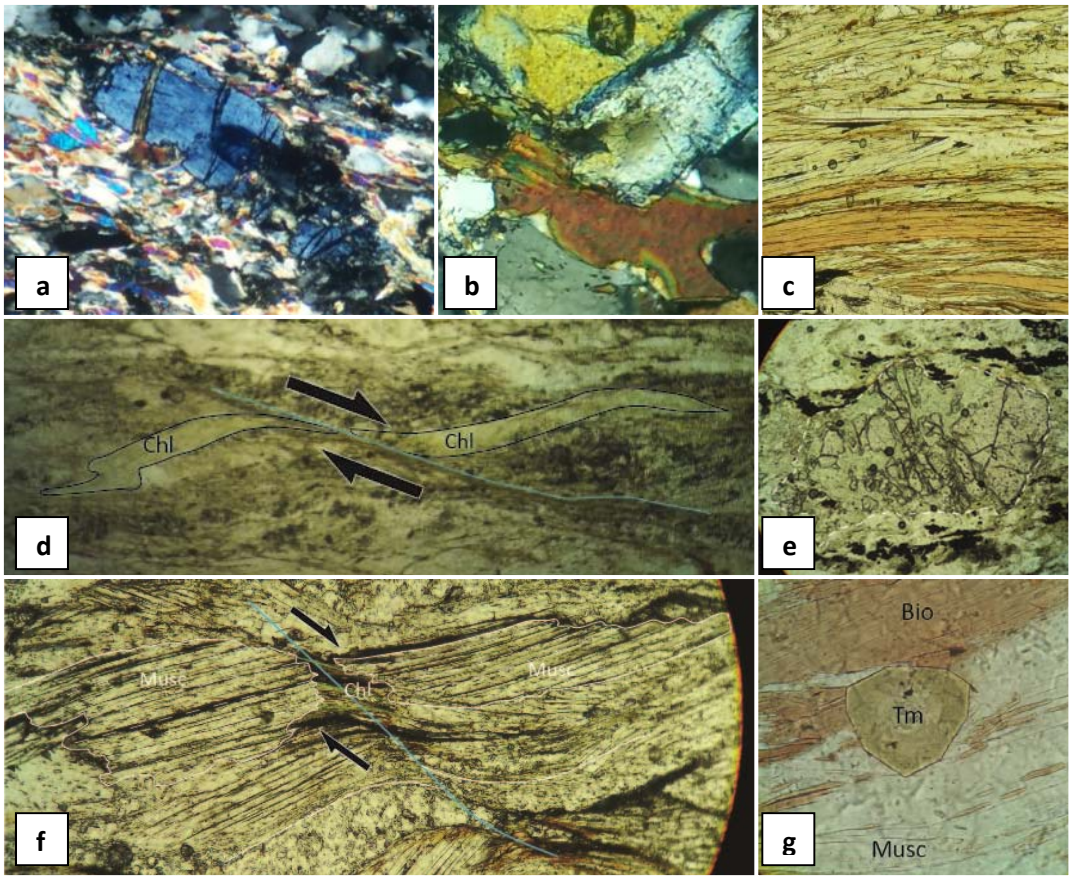

Figure 44: *Mineral growth and timing. A) Epidote growing over the muscovite foliation, this mineral has broken during deformation and chlorite has grown between the fragments, width of view 0,8 mm. B) Clinozoisite growing over biotite, width of view 0,5 mm. C) Chlorite replacing biotite, width of view 0,3 mm. D) Chlorite crystal sheared, width of view 4 mm. E) Broken garnet with chlorite filling the gaps, width of view 1,2 mm. F) chlorite has grown on the shearplane displacing a muscovite crystal, width of view 1,4 mm. G) Tourmaline growing over a biotite and muscovite microstructure, width of view 1 mm.*

Metamorphic conditions during D3 shearing

The deformation related to the shearing event is represented on the micro scale by brittle fracturing of minerals like garnet and shear along shear bands. At these locations space is created for new minerals to grow. In nearly all instances chlorite grows in these places (figure 44e & 44f). This is thought to indicate that lower greenschist facies conditions prevailed during this deformation.

It has been observed that the gneisses, schists and amphibolites of the Pohorje and Kozjak mountains, as well as the Pohorje pluton, show dynamic recrystallization microstructures of quartz and plagioclase minerals. The dominant recrystallization mechanism provides information on the temperature conditions during deformation (Stipp et al., 2002).

Quartz

Quartz is present in nearly all rock samples and is found throughout the groundmass of the rock as well as in quartz veins. Both types of quartz show typical recrystallization structures. Recrystallized quartz grains are often elongated and aligned (figure 45a) In addition to this grain shape orientation, occasionally a clear lattice preferred orientation (LPO) has formed. This LPO is observed by using a gypsum plate on the microscope.

It has been observed that usually all of the quartz is recrystallized, and grain sizes are roughly similar. If old crystals still exist they contain a network of subgrains. These structures indicate that progressive subgrain rotation has caused dislocation walls to eventually become new recrystallized grain boundaries. The analysis of the thin sections indicates that subgrain rotation (SGR) is the dominant recrystallization mechanism for quartz in most rocks.

However, subgrain rotation is not the only recrystallization mechanism that has affected quartz. Large crystals with highly lobate shapes are found, for instance in recrystallized quartz veins from location 96 (figure 45b). These amoeboid shapes and relatively large grain size indicate that grain boundary migration (GBM) is the recrystallization mechanism here.

Bulging grain boundaries are also observed, indicating that bulging as a recrystallization process also takes place. These bulging grain boundaries are found for instance in a quartz vein where subgrain recrystallization dominates (figure 45c). Thus, it is observed that several recrystallization mechanisms have often affected the same sample.

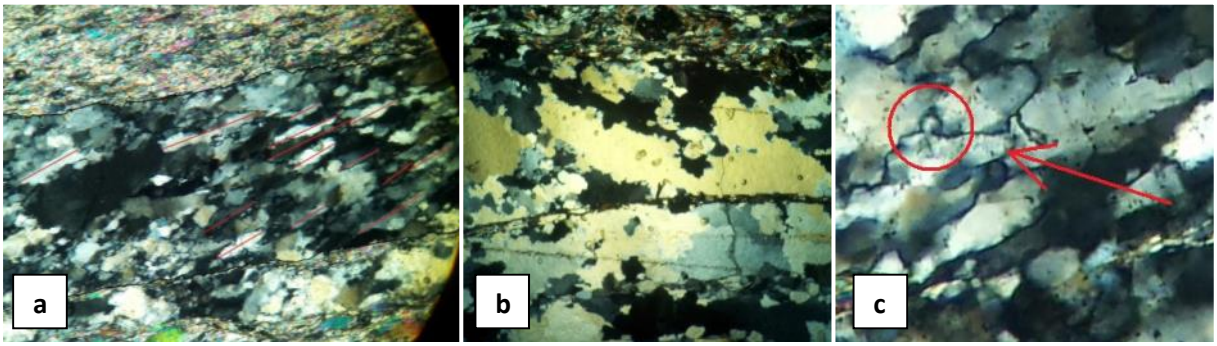

Figure 45: *Quartz dynamic recrystallization structures, A) A vein with almost fully recrystallized quartz. The dominant process of dynamic recrystallization is progressive subgrain rotation (SGR). The large dark grey quartz mineral with undulatory extinction is a remnant from before recrystallization, width of view 5 mm. B) Quartz vein with highly mobile quartz grain boundaries. The dominant process acting here was grain boundary migration (GBM), width of view 3 mm. C) A bulging grain boundary is observed 'frozen' in the structure at the verge of forming a new recrystallized grain. The process is called grain boundary bulging (BLG), width of view 0,2 mm.*

Plagioclase and the Pohorje pluton

Plagioclase feldspars (Plag) are present within most gneisses and schists, and are the main minerals showing dynamic recrystallization in the granodiorite pluton.

In the thin sections of the rocks from the pluton, it was observed that plagioclase commonly only features partial recrystallization, in contrast to quartz. Characteristic for this partial recrystallization is a bimodal distribution of grain size, with large old plagioclase crystals and small new, recrystallized crystals. The small new minerals form rims around large old minerals (figure 46a & figure 46b), such a structure is characteristic for bulging recrystallization, where small new crystals form and accumulate between the relicts of old grains. Bulging is the dominant recrystallization mechanism for plagioclase in the surrounding metamorphics too, although recrystallization by subgrain rotation is also observed.

The recrystallized grain size of plagioclase is smaller than the recrystallized grain size of quartz, and the new plagioclase crystals do not show a strong preferred orientation of aligned grains (figure 46c).

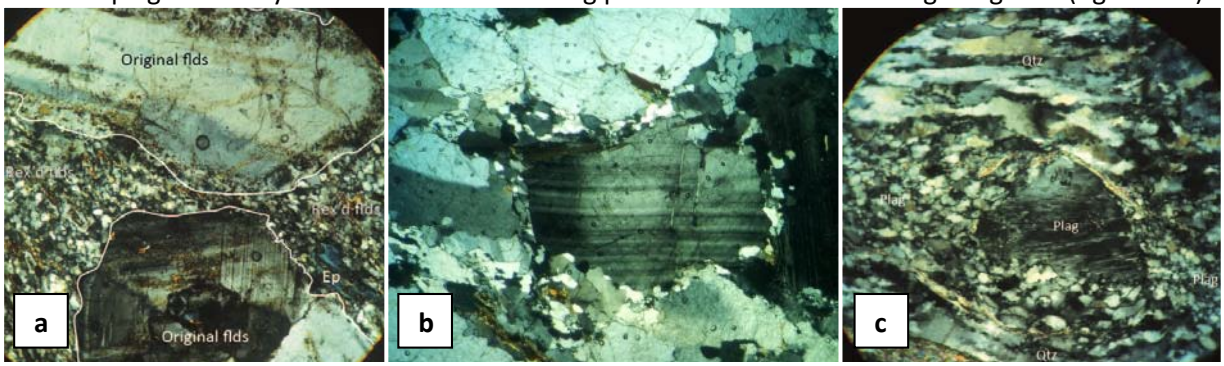

Figure 46: *Dynamic recrystallization of (plagioclase) feldspar.* ***A)*** *Large feldspars with concentric zonation are found in the tonalite pluton. The fine grained mass around these feldspars originated from the dynamic recrystallization (BLG) of the large feldspars, width of view 5 mm.* ***B)*** *Core-and-mantle structure in tonalite, resulting from BLG recrystallization, width of view 3,5 mm.* ***C)*** *Recrystallized grain size varies for quartz and feldspar; quartz (top and bottom) fully recrystallized by SGR, leading to a larger grainsize and clear preferred orientation, whereas partial recrystallization by BLG of plagioclase (center) led to a smaller recrystallized grain size without clear orientation, width of view 4 mm.*

Late stage deformation and mineral growth

Calcite veins are present in at least one sample, sample P15 from location p63. These calcite veins are very small, < 1 mm in width, and occur in conjugate sets. The veins are straight and apparently not folded, nor show any obvious signs of deformation. On a microscopic level however, twinning of the calcite crystals shows that these veins must have been submitted to deformation. The twins in calcite are used as a temperature gauge. Cross hatched 'thick' twins are the most abundant type of twinning, which is characteristic for type 2 twins. Type 3 curved and intersecting twins are also observed (figure 47).

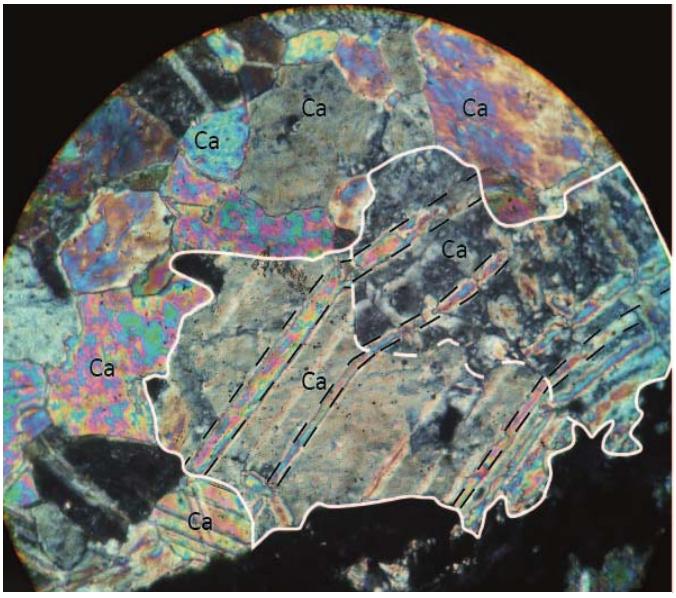

Figure 47: *Calcite twinning. Thick twins that occasionally bend are type 2 to type 3 twins, width of view 1,6 mm.*

The latest phase of mineral growth observed in the thin sections is the growth of tourmaline. Zoned and unzoned tourmaline crystal typically show euhedral crystal habits growing over all other foliations and microstructures (figure 44g). No signs of deformation postdating the growth of tourmaline are found. Thus, the formation and modest deformation of calcite veins and the growth of tourmaline represent the latest events that affected the metamorphic rocks already at shallow depths.

Implications on temperature conditions

The upper limit for the temperature is given by the fact that minerals like garnet and amphiboles do not show dynamic recrystallization structures. So the upper temperature limit is around 700°C (figure 48).

Dynamic recrystallization structures have been observed in quartz and feldspars. Dynamic recrystallization structures develop in feldspar at temperatures higher than 400 degrees (figure 48). Higher temperatures for the crystal plasticity of plagioclase are also given, T greater than 500 to 550 °C (e.g. Voll 1976; Tullis 1983). As only partially recrystallized feldspar structures are observed, and grain boundary bulging is the dominant process, temperatures related to the dynamic recrystallization of feldspar are maximally 600°C.

Dynamic recrystallization of quartz is dominated by GBM for temperatures above approximately 400 °C, between ~400-~330°C SGR dominates, and below 330°C bulging dominates. All these recrystallization processes are observed and provide a temperature range for the deformation of the quartz in these rocks. It appears that amoeboid crystal structures related to GBM, are surrounded by small crystals and 'bulging' grain boundaries, possibly related to bulging recrystallization. Therefore, it is observed that low temperature recrystallization structures overprint higher temperature structures.

Type 2 to type 3 calcite twins indicate temperatures of approximately 200°C (Passchier & Trouw, 2005).

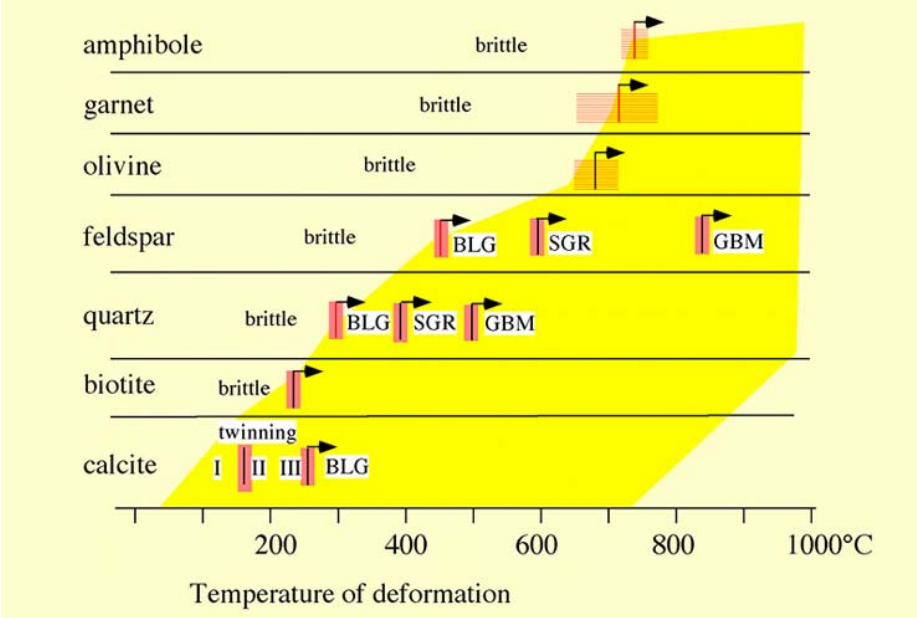

Figure 48: *Temperature dependence of recrystallization mechanisms for different minerals. (Passchier & Trouw, 2005)*

Summary metamorphic events and timing

1. In Eclogites, Eclogite facies metamorphism is represented by the stable mineral assemblage of kyanite, omphacite, garnet and quartz. Microstructures possibly indicate UHP-metamorphism.

2. M_{peak} is the highest grade of metamorphic rocks found in the gneisses and schists of the LCA unit. M_{peak} is characterized by minerals like garnet, staurolite, kyanite and mica's. This mineral assemblage represents an upper amphibolite facies metamorphism (585°C < T < 695°C, 0,53 < P < 1,19 Gpa). Zoisite zone metamorphism in marbles indicates similar conditions. Symplectites in eclogite may have started growing already during this phase.

   Porphyroblasts show that this phase postdates the D1 deformation phase.

3. An episode in which chlorite, epidote and clinozoisite grow, representing retrograde epidote-amphibolite facies metamorphism in gneisses and schists. Furthermore, this phase is recognized in marbles by a chlorite overprint of zoisite.

   D2 deformation postdates the first two phases of metamorphism. The relation between D2 deformation and the epidote-amphibolite facies metamorphism could not be constrained.

4. A syn-tectonic phase of chlorite growth, characteristic for greenschist facies conditions occurs during D3 shearing. This phase is also recognized in the pluton, demonstrated by solid state dynamic recrystallization structures found in samples from the pluton. Temperatures as high as 500°C are indicated by GBM in quartz veins and BLG in feldspars of the pluton. These structures are overprinted by lower temperature dynamic recrystallization structures.

5. Modest deformation of calcite veins as shown by type 2 calcite twins, record the lowest temperatures (<200 °C) in the area. Together with post-tectonic growth of tourmaline, these are the youngest events in the Pohorje region.

Discussion

Profiles and present 3D structure

Based on the maps (Sheet Slovenj Gradec (Mioc and Znidarcic, 1987) and sheet Maribor (Mioc and Znidarcic, 1987)) and the combined structural data from this research and from Haalboom & van Greuningen (2013), two cross-sections have been constructed.

Profile A is oriented WNW-ESE over the center of the Pohorje mountains. It stretches from several kilometers from the western margin of the Pohorje mountains in the West to the Mura basin in the East (figure 49).

Profile B is oriented NNW-SSE over the Pohorje and Kozjak mountains. The northern boundary of the profile is located close to the border between Slovenia and Austria, which corresponds roughly to the boundary between the Kozjak mountains and the Styrian basin. In the south the profile extends until just south of the Lavanttal fault (figure 49).

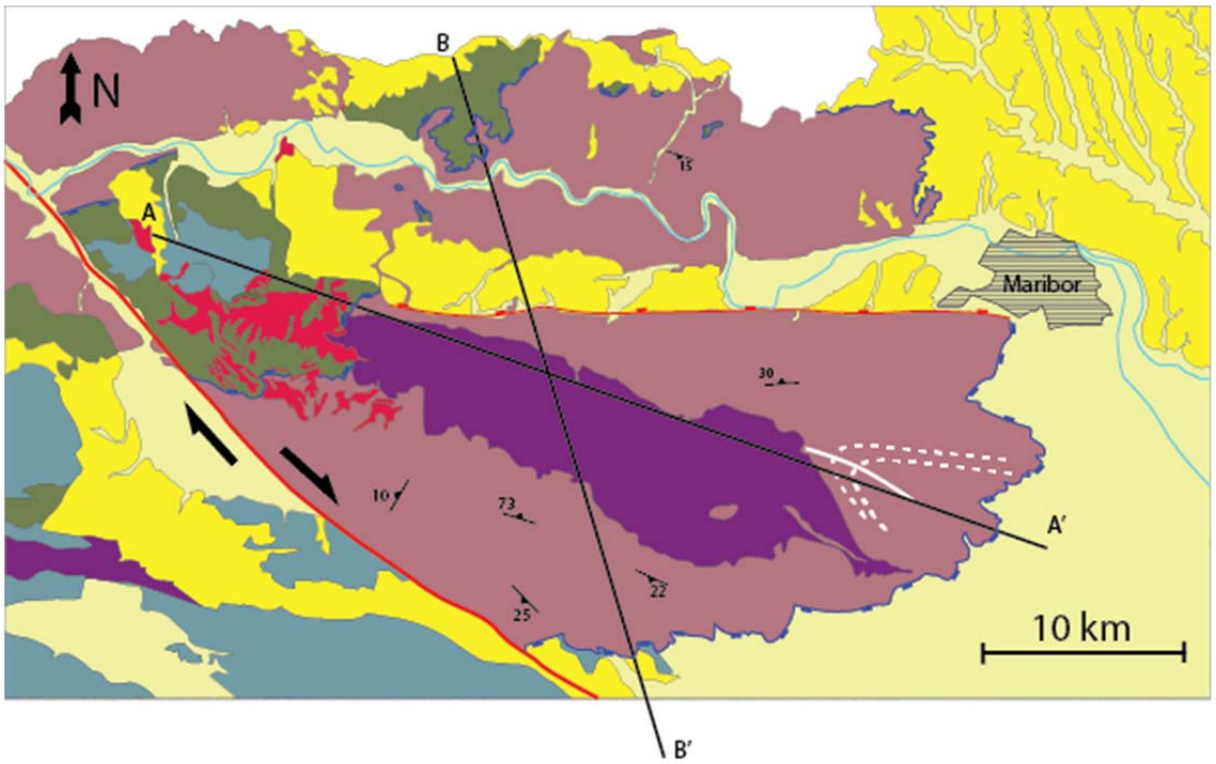

Figure 49: *The geological map of the Pohorje and Kozjak mountains shows the traces of both profiles. Average values of the S1 foliation orientation are represented by strike-dip symbols. The trace of the Pohorje antiform is shown in white. Furthermore the Lavanttal fault is indicated, as is the normal fault that is the Southern boundary of the Ribnica-Selnica trough. The nappe contact is indicated by the blue line with dents. The nappe contact is thought to be reactivated as a low angle detachment and this feature is stressed in the map. The Eastern margins of the Pohorje and Kozjak mountains in contact with the Mura basin are also identified as features resulting from movement along the same low angle detachment. Dents point in to the footwall. Modified after Mioc & Znidarcic.*

The solid black lines at the topography of the profiles represent measurements of the S1 foliation. The dip angle of the black lines is the apparent dip, corrected for the orientation of the profiles.

Based on these measurements the dotted lines are constructed that represent the foliation of the rocks. However, the S1 foliation is folded on a smaller scale by the tight S2 folds. Therefore, the dotted line more likely represents the general orientation of the S2 foliation, which is axial planar to S2 folds and is only refolded during the D3 phase.

Profile BB' shows that foliations in the South of the Pohorje Mountains dip to the South and North of the pluton dip to the North. The other profile (profile AA') shows foliations dipping gently to the West. This westward plunging antiformal shape has been described for the Pohorje mountains by various authors (Kirst et al., 2010, Janak et al., 2006). The Pohorje pluton is situated in the core of this antiform. Some steep orientations of the S1 foliations South of the pluton might be explained by the existence of asymmetric, parasitic folds (profile BB'). In figure 50 the main structure is reconstructed in 3D.

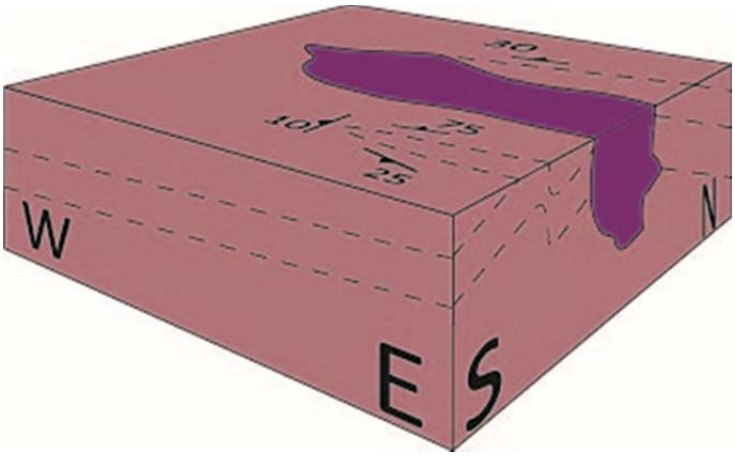

Figure 50: *3D Schematic representation of the S1 foliations of the Pohorje block. They form a large scale, west plunging antiformal structure with smaller scale asymmetric folds. The Pohorje tonalite intrusion occupies the center of the antiformal structure.*

Tectonic structures

In profile BB' the majority consists of Lower Central Austroalpine gneisses and schists (pink). For simplicity, only some amphibolite lenses are indicated with a bright green color (figure 51).

In the Northern part of profile BB', the Kozjak mountains, a part of the Upper Central Austroalpine nappe is present. Here, mainly Paleozoic basement rocks of the UCA are found (green). In the South the Mesozoic cover rocks of the UCA are observed (blue). The thrust contact between both nappes is indicated by the red line. This nappe contact runs over the top of the present day topography of the Pohorje Mountains and has eroded away in large parts. The red arrows indicate the sense of movement along this nappe contact during Cretaceous thrusting with a top to the NW motion, in present day coordinates (figure 51).

The nappe contact is interpreted to be reactivated as a low angle detachment with top to the E sense of displacement, as is indicated by the blue displacement symbols. The low angle detachment is

thought to have been active during the Early Miocene. The authors view this low angle detachment as the primary and most significant mechanism to explain the observed Ottnangian-Lower Badenian (~18,5-16 Ma) exhumation of the Pohorje pluton and surrounding LCA metamorphics.

In profile AA', the retrograde metamorphic overprint of high grade metamorphic rocks or diaphthorite rocks are observed to be concentrated in the westernmost and easternmost parts of the LCA nappe, in the places closest to the old nappe contact. This is taken as a strong indication that the nappe contact was reactivated during retrograde conditions. During deformation the low angle detachment may have acted as a pathway for fluids, making the surrounding rocks more susceptible for retrograde metamorphism. Profile AA' shows a significant portion of Upper Central Austroalpine nappe rocks in the western part of the Pohorje Mountains. In the eastern part no rocks of the UCA nappe are present. Thus, these shallower parts of the nappe stack are concentrated in the west.

The foliation in the basement rocks of this Upper Central Austroalpine nappe is discordant to the foliation of the Lower Central Austroalpine rocks below the nappe contact. The top-to-the-east sense of displacement along the low angle detachment, that reactivated the Cretaceous nappe contact, is nearly perpendicular to the direction of view and is indicated by the blue arrows. The UCA rocks are interpreted to be a rotated block from above the detachment. Its approximate shape is outlined by the dashed lines. More of these UCA blocks might be expected to be present below the sedimentary fill of the Mura basin.

The low angle detachment is offset by younger structures. The normal faults bordering the Ribnica-Selnica trough crosscut the low angle detachment. Also the Lavanttal fault is thought to crosscut the low angle detachment (Profile A), as the Lavanttal fault was mainly active during the Late Miocene (Wölfler et al., 2010).

Pluton & Volcanics

Both profiles show the intruded tonalite-granodiorite pluton. The shape of the pluton in-depth is difficult to determine and its geometry is based on the extrapolation of surface structures like foliation planes to depth. The elongated shape of the pluton is inferred from the surface expression of the pluton. It is thought that the pluton already had an elongated shape during the intrusion, however, the elongated shape might be amplified by extensional deformation during post-intrusion D3 shearing. The fact that deformation was localized along the edges of the pluton, and has not affected the center of the pluton, gives the impression that the elongated shape is an original feature of the pluton and not purely the result of deformation. This interpretation is shared by other authors (Fodor et al., 2008).

Fodor et al. (2008) concluded that the eastern part of the pluton crystallized at greater depths than the western part of the pluton. Therefore it is likely that a possible feeder dyke of the pluton is situated in the east. Profile A passes through the edge of the pluton, therefore it most likely does not crosscut such a feeder dyke. Thus, the cross section geometry of the pluton is chosen not to show the feeder dyke, giving it a shape slightly different from the general idea of pluton geometries with feeder dykes. In the summary figure (figure 54) a more general shape with feeder dyke is adopted. Another clue for the shape from the pluton is the distribution of (sub)volcanics. The dacite dykes are thought to be genetically linked to the pluton. Their occurrence west of the pluton may hint that the pluton underlies these rocks at depth.

Fodor et al. (2008) recognized that two generations of dykes are present, the first generation of deformed dykes and a second generation of undeformed dykes. This is confirmed by this research. In profile A these two generations are displayed by different shades of pink. The first generation is deformed by shearing along the low angle detachment, whereas the second generation crosscuts the detachment. Thus, the ages of these different generations of dykes can be used to constrain the age of deformation.

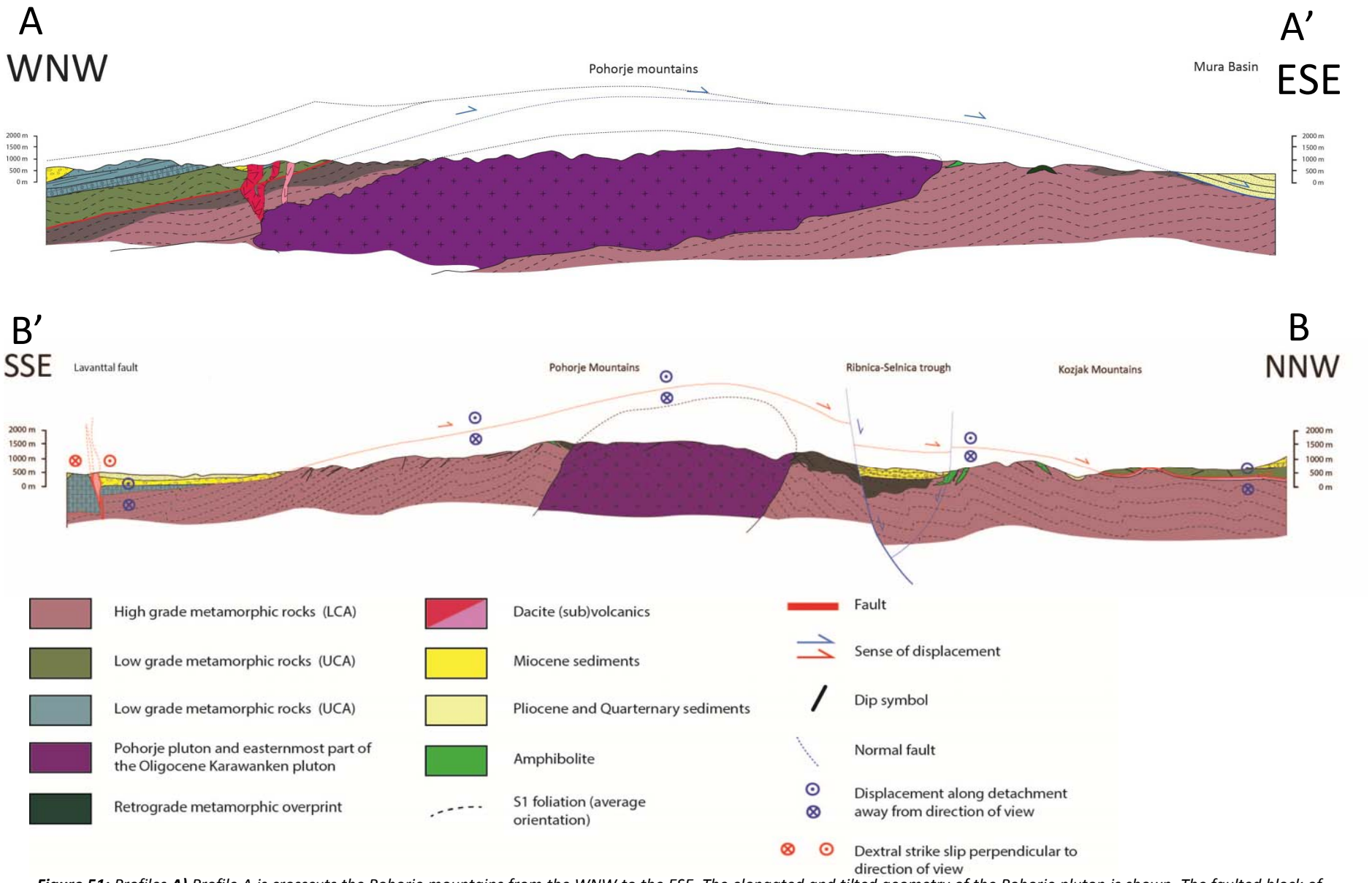

Figure 51: *Profiles **A)** Profile A is crosscuts the Pohorje mountains from the WNW to the ESE. The elongated and tilted geometry of the Pohorje pluton is shown. The faulted block of UCA rocks lies unconformably on the LCA. The nappe contact in between is reactivated as low angle detachment and rocks of the LCA in its vicinity are retromorphosed. Two generations of subvolcanics and dykes exist. **B)** The original nappe contact (red) is displayed, and blue displacement symbols indicate the later movement during the reactivation as low angle detachment. In this NNW-SSE profile the Ribnica-Selnica trough can be observed as well as the anriformal shape of the Pohorje mountainswith the pluton in the center. The Lavantall faulton the left crosscuts the detachment.*

Geological history

Figure 52 shows the relative and absolute ages of the major tectonic events in the Eastern Alps and the Pannonian basin, as well as some dated events in the Pohorje mountains. The most important deformation phases and metamorphic events recognized in the Pohorje and Kozjak mountains in this research are correlated to this recorded events. The rationale behind these correlations is made in the following chapters.

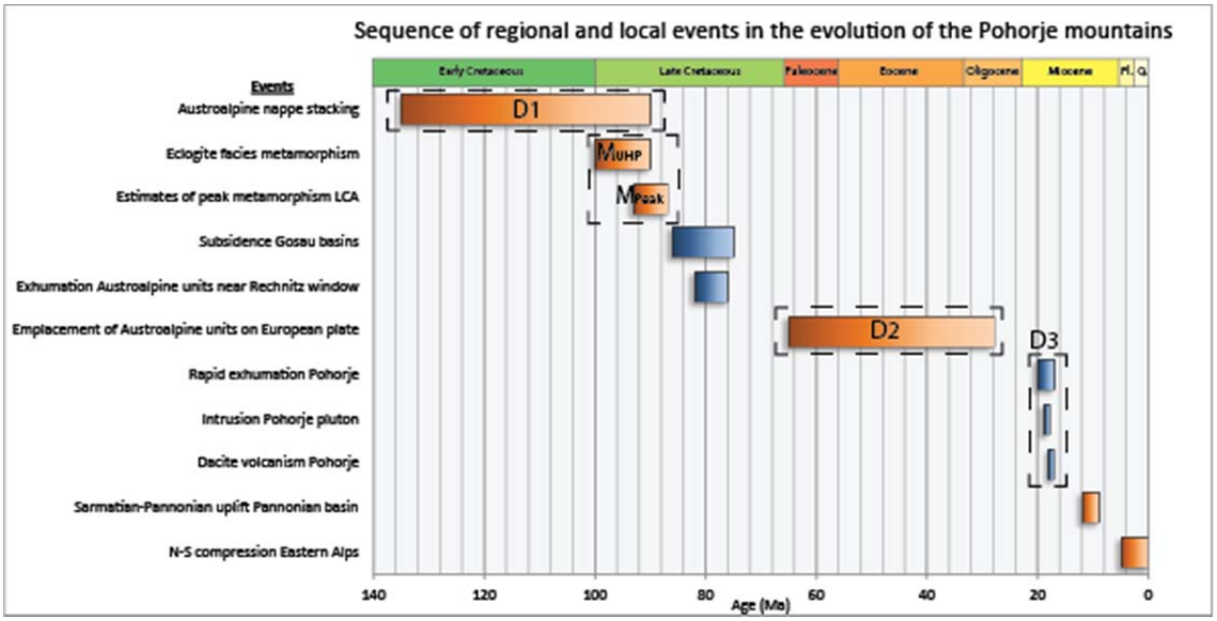

Figure 52: *Event chart linking the major tectonic and magmatic events of the Eastern Alps the Pannonian basin with the Pohorje and Kozjak mountains. Absolute ages are based on literature, more extensive background can be found in the introduction. 1. (Schmid et al., 2008) 2.&3. (Thöni et al., 2002, Miller et al., 2005, Janak et al., 2006) 4.&5. (Willingshofer et al., 1999 and references therein, Kurz et al., 2002, Cao et al., 2013) 6. (Schuster et al., 1998 and references therein, Schmid et al., 1996) 7., 8. & 9. (Fodor et al., 2008, Hendrikx et al., 2010, Trajanova et al., 2008, Steininger et al., 1988, Sachsenhofer et al., 1998), 10. & 11. (Horvath et al., 2006, Bada et al., 2001, Harzhauser & Piller, 2004, Sölva et al., 2005)*

Pre Miocene evolution

Isoclinal folding is observed in the high-grade metamorphic basement of the Lower Central Austroalpine nappe but also in the low-grade metamorphic rocks of the Upper Central Austroalpine basement. Janak et al. (2004), concluded that the low grade metamorphism of the upper nappe took place during the Variscan orogeny. Therefore, It seems plausible that the isoclinal folding of the low grade metamorphic rocks is related to this Variscan metamorphic event as well.

The D1 deformation phase in the high grade metamorphic rocks could also be related to this mountain building event. A second option however is that the isoclinal folding and formation of the S1 foliation is coupled to the HP Cretaceous metamorphism event that affected the Lower Central Austroalpine nappe in the Pohorje mountains, during the Eoalpine orogenic phase (Neubauer et al., 2000, Schmid et al., 2004). In this case the age of the D1 deformation phase should be Late Cretaceous, as the intracontinental subduction and accompanied UHP metamorphism took place around 93-87 Ma (Janak et al., 2006, Thöni et al., 2002). This later model is favored by the author, largely because it can be expected that subduction to great depths is likely to be associated with ductile deformation structures, that would possibly overprint older Variscan structures. The UCA

nappe did not subduct during the Eoalpine orogenic phase. As a result the Variscan deformation may have escaped overprinting during the Cretaceous. In this case, isoclinal folding in the UCA does not originate from the same deformation phase as the isoclinal folding in the LCA.

Extensional shear structures in the Pohorje mountains are commonly related to the Miocene extension and exhumation, based on retrograde conditions during this phase and the deformation in the pluton that can be used as a time marker. However, a relatively small patch of sedimentary rocks was assigned a Cretaceous age by Mioc and Znidarcic (1977). These Cretaceous sediments are in contact with the Triassic rocks of the UCA, and could imply that subsidence affected the Pohorje region in the Cretaceous. This subsidence might be the only link to this extensional phase that is well documented in other parts of the Eastern Alps (Willingshofer et al., 1999 and references therein, Kurz et al., 2002, Cao et al., 2013).

The top-to-the-NNW oriented shear sense indicators and associated recumbent, tight folds and axial planar S2 foliation of the D2 phase are linked to the Tertiary orogenic phase of the Alps (Neubauer et al., 2000, Schmid et al., 2008). This phase is related to the Paleogene closure of the Alpine neotethys that led to the NNW directed emplacement of the Austroalpine nappe stack onto the European plate (Schuster et al., 1998 and references therein, Schmid et al., 1996). Aside from the similarity in direction of displacement, the relative timing of the D2 event coincides with the relative timing of this Tertiary orogenic phase, after the high grade metamorphism and before the intrusion of the Pohorje pluton in the Early Miocene. The major part of the PTt-path (before the merger with the purple path) has lapsed by this time (figure 53).

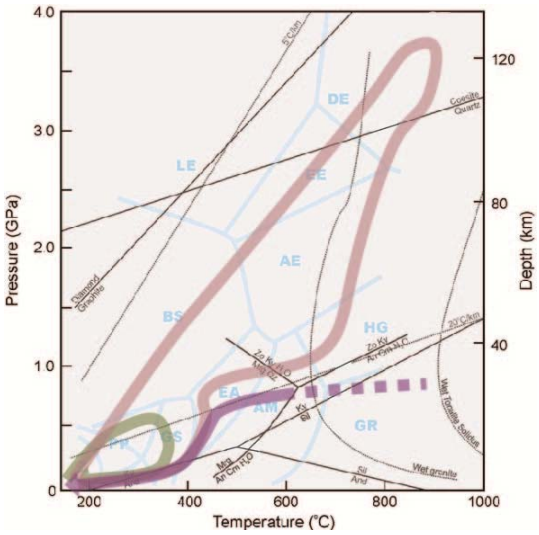

Figure 53: *PTt-path. Green path shows the Variscan metamorphism (rough estimate) that is possibly observed in Upper Central Austroalpine rocks. Pink path represents LCA basement rocks. Purple path represents the pluton.*

Exhumation of the Pohorje mountains

The timing of D3 deformation corresponds to the timing of Miocene exhumation of the pluton and surrounding metamorphics. D3 shear structures in the pluton and the deformation of dykes that are slightly younger than the age of the pluton, namely ~17-16 Ma (Trajanova et al., 2008), constrain the age of deformation and support the interpretation that D3 deformation structures are related to the mechanisms governing the rapid exhumation shortly after emplacement of the pluton (Fodor et al., 2008).

The presence of newly grown chlorite on shear planes and in between broken garnets indicates retrograde metamorphic conditions prevailed during this deformation event. The PT conditions for this phase, derived from the retrograde mineral assemblage and dynamic recrystallization structures typically fall in the range of the greenschist metamorphic facies. Dynamic recrystallization structures that represent lower temperatures overprint a higher temperature structure, which is regarded as an additional indication for exhumation during the D3 phase.

The D3 shear structures are generally flatlying, E-W oriented stretching lineations and associated kinematic indicators with a dominant top-to-the-east sense of shear. From profile 2 an open antiform can be observed from east to west across the Pohorje mountains; In the west foliations dip dominantly to the west and in the east foliations are flat lying to slightly dipping. A mechanism that is known to fit with these characteristics, a consistent sense of shear over both sides of a dome shape, is a low angle detachment. Therefore, a conceptual model in which shear deformation is concentrated along a single low angle detachment with top to the east sense of shear is proposed. The advantages and limitations of this model will be discussed in the next paragraphs. Furthermore the model will be compared to pre-existing, alternative models for the exhumation of the Pohorje mountains.

At this point, it should be noted that various deviating sense of shear measurements are observed. Numerous measurements reveal a top-to-the-west sense of shear along stretching lineations with a similar trend as the top-to-the-east kinematic indicators. The mechanism responsible for these opposite measurements is not yet explained. The model put forward by Fodor et al. (2008) features west directed low angle detachments at the western margin of the Pohorje Mountains and east directed low angle detachments at the eastern margin of this small range. This model does not propose an elegant solution for the differential amounts of exhumation between the western and eastern part of the pluton. Furthermore, this model predicts that the sense of shear is dominantly top-to-the-west in the western part of the Pohorje mountains and dominantly top-to-the-east in the eastern part of the Pohorje mountains. This is not supported by field data that reveal a dominant top-to-the-east sense of shear throughout the Pohorje and Kozjak mountains. For these reasons a more asymmetric mechanism is proposed to better fit the observations.

However, the proposed model of footwall exhumation by an east directed low angle detachment fault does not inherently explain the presence of top-to-the-west sense of shear indicators. A possible explanation could be that the top-to-the-West sense of shear is of a slightly different age, but no indication for this age difference can be given. Alternatively, these kinematic indicators formed simultaneously as a conjugate set at the onset of shearing.

The second explanation is based on the assumption that both top-to-the-west and top-to-the-east shear bands were active simultaneously. It has been documented that both synthetic and antitethic

shear bands can develop in a sub-simple shear domain (Simpson & De Poar, 1993). It has been proposed for low angle detachments, that extensional crenulation cleavages, described as shear bands in this report, develop as conjugate sets at the onset of deformation. Only during a later phase the synthetic set of shear bands becomes dominant (Zheng et al., 2004). In this scenario the top-to-the-west shearbands (antithetic) are related to and formed simultaneously with the top-to-the-east shearbands (synthetic). The synthetic shearbands may be underdeveloped with respect to the antithetic shearbands in some outcrops.

The D3 shear structures are found throughout the high-grade metamorphic unit (Lower Central Austroalpine) and are also found within the low grade metamorphic rocks of the Upper Central Austroalpine nappe. This makes it difficult to assign a specific location to the detachment. However, the strain is not distributed equally across the fieldwork area, as is evidenced by the observations of mylonites, which are found mainly in the western- and easternmost parts of the Pohorje mountains. Likewise, the phyllonite unit, which outcrops extensively in the Kozjak mountains and represents the highest part of the Lower Central Austroalpine nappe, shows more intensive shear structures. The same holds for the retrograde metamorphic overprint, which is more intensive within the upper levels of the Lower Central Austroalpine unit, near the contact with the Upper Central Austroalpine unit. These areas were mapped separately as a retrograde unit by Mioc and Znidarcic (1977). Colletini (2011) showed that low angle normal faults act as preferential pathways for fluid flow. As fluids are often required for retrograde metamorphic reactions to proceed, this characteristic makes the rock that is part of or close to a low angle detachment prone to a retrograde metamorphic overprint.

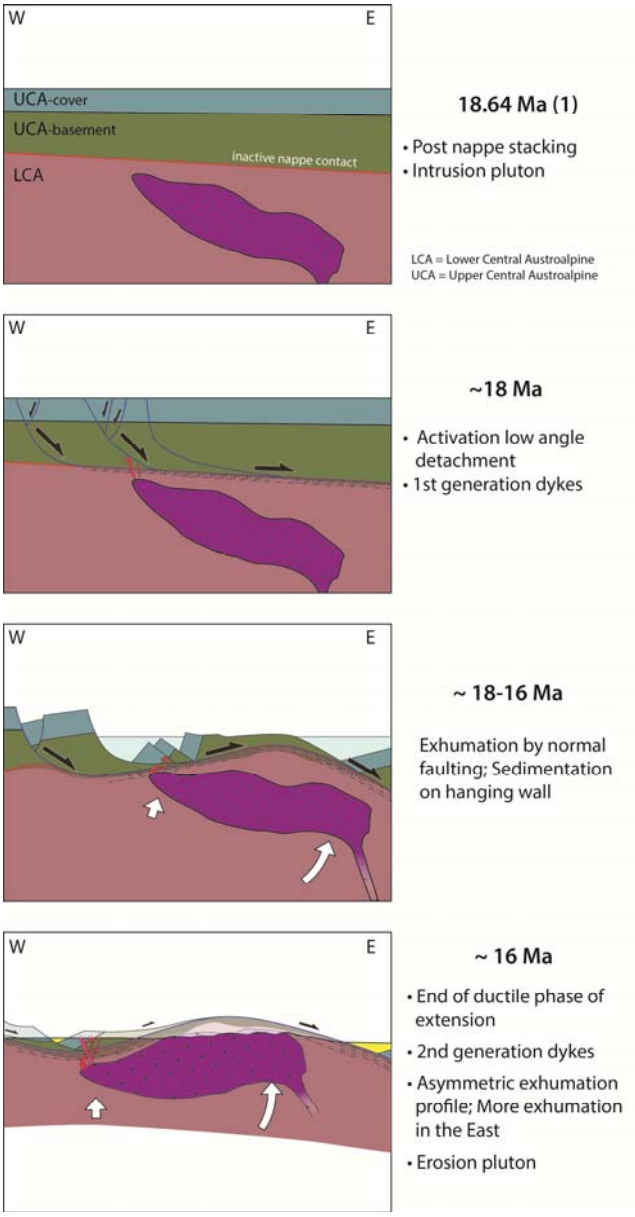

Figure 54: *Conceptual model of the Miocene exhumation history of the Pohorje pluton. Localized deformation above the detachment causes differential uplift of the footwall. Simultaneous with this differential uplift active volcanism takes place in the western part of the Pohorje mountains and sedimentation in the basins.*

Combining these findings we propose that the low angle detachment is located at the boundary between the high grade rocks of the Lower Central Austroalpine and the low grade rocks of the Upper Central Austroalpine (figure 54), in other words; the low angle extensional detachment reactivated the nappe contact (Janak et al., 2006, Szafian et al., 1999).

At the contact between the Lower and Upper Austroalpine nappes, the rocks are completely cataclastic and multiple discrete faults occur within this zone (figure 2- Brittle deformation). It can be argued that faulting in the brittle regime is the equivalent of the shear structures and mylonites in the ductile domain of the low angle detachment, and thus reveals the localization of deformation along the nappe contact.

The model describes exhumation of the high-grade metamorphic rocks of the LCA within the footwall of an East-directed low angle detachment fault. Fodor et al. (2008) showed that different amounts of exhumation have affected the western and the eastern part of the pluton, using Al-in Hornblende barometry. Samples, now at the surface, from the western part of the pluton yielded pressures of 3-4 kbar, whereas the sample from the eastern part of the pluton yielded higher pressures of 6-7 kbar. This implies that the eastern part of the pluton crystallized at greater depths (16-19 km) than the western part of the pluton, that crystallized at 8-11 km depth. Therefore differential exhumation must have exhumed the eastern part of the pluton 8 km more than the western part of the pluton. This asymmetric exhumation is confirmed by older K-Ar ages in the host rocks in the western part of the Pohorje mountains, by the close proximity of structurally higher nappes of the UCA (Fodor et al., 2008) and the difference of $^{40}Ar/^{39}Ar$ cooling ages between the western and eastern part of the pluton (Hendrikx et al., 2010). Differential amounts of uplift are typically observed in exhumed footwalls of low angle normal faults (Kurz et al., 2002, Lister & Baldwin, 1993). This is a characteristic feature of metamorphic core complexes and is believed to result from the upward bowing of the original detachment due to isostatic compensations resulting from lateral variations in the amount of upper crustal thinning (Lister & Davis, 1989) (figure 55).

Entirely different views on the Karpatian exhumation of the Pohorje mountains exist as well. For instance, Pischinger et al. (2008) introduced their view on the exhumation of the Pohorje mountains assigning an important role to the Ribnica-Selnica through. These authors suggest, based on fault-slip analysis, that the faults bordering the through were already active as dextral strike slip faults during the Ottnangian-Karpatian. They argue that north directed normal displacement along these faults and other E-trending faults along the margin of the Koralm complex occurred as early as the Karpatian (~17-16 Ma), simultaneously with the phase of rapid exhumation of the Pohorje mountains and subsidence in the southern Styrian basin. Therefore Pischinger et al. (2008) conclude that this phase is most likely responsible for the exhumation of the Pohorje mountains.

However, this view is not supported by the kinematic data described in this report. Furthermore, it cannot explain the differential amount of exhumation between the eastern and western part of the pluton (Fodor et al., 2008, Hendrikx & Brautigam, 2010). Thus, this alternative model is regarded less valid than models that relate the exhumation to E-W extension.

The Pohorje Mountains: a metamorphic core complex?

The style of exhumation of the Pohorje Mountains resembles in many ways the exhumation observed in metamorphic core complexes. Metamorphic core complexes are exhumed in the footwall of a low angle detachment, from below an extending upper crust (Lister & Davis, 1989, Coney & Harms, 1984). This tectonic style of exhumation is associated with a characteristic style of deformation structures. Furthermore, as the footwall is uplifted through the crust during the evolution of this system, a succession of deformation structures and retrograde metamorphism

reflect progressively shallower environments. Lastly, core complexes are commonly associated with igneous activity. In this section these features will be discussed to assess whether the Pohorje mountains qualify as a core complex, sensu Lister & Davis (1989).

Structural evidence

The low angle detachment that separates the footwall and hanging wall is thought to be nearly horizontal in the deeper parts of the fault. In this stage the mylonitization of the rocks starts. The sense of shear along the low angle detachment is the same along its length. Brittle extensional faults dominate the hanging wall. As a result the mylonitized zones bowes upward due to isostatic compensations. The result is an antiformal structure, in the center of which the footwall is exposed from below the hanging wall. The sense of shear of the mylonites is the same on both sides of the antiformal structure. However as a result of the bowing upwards, motion along the detachment is unfavourable along tilted parts. Therefore, active displacement along mylonites shifts in the direction of motion along the fault (Lister & Davis, 1989) (figure 55).

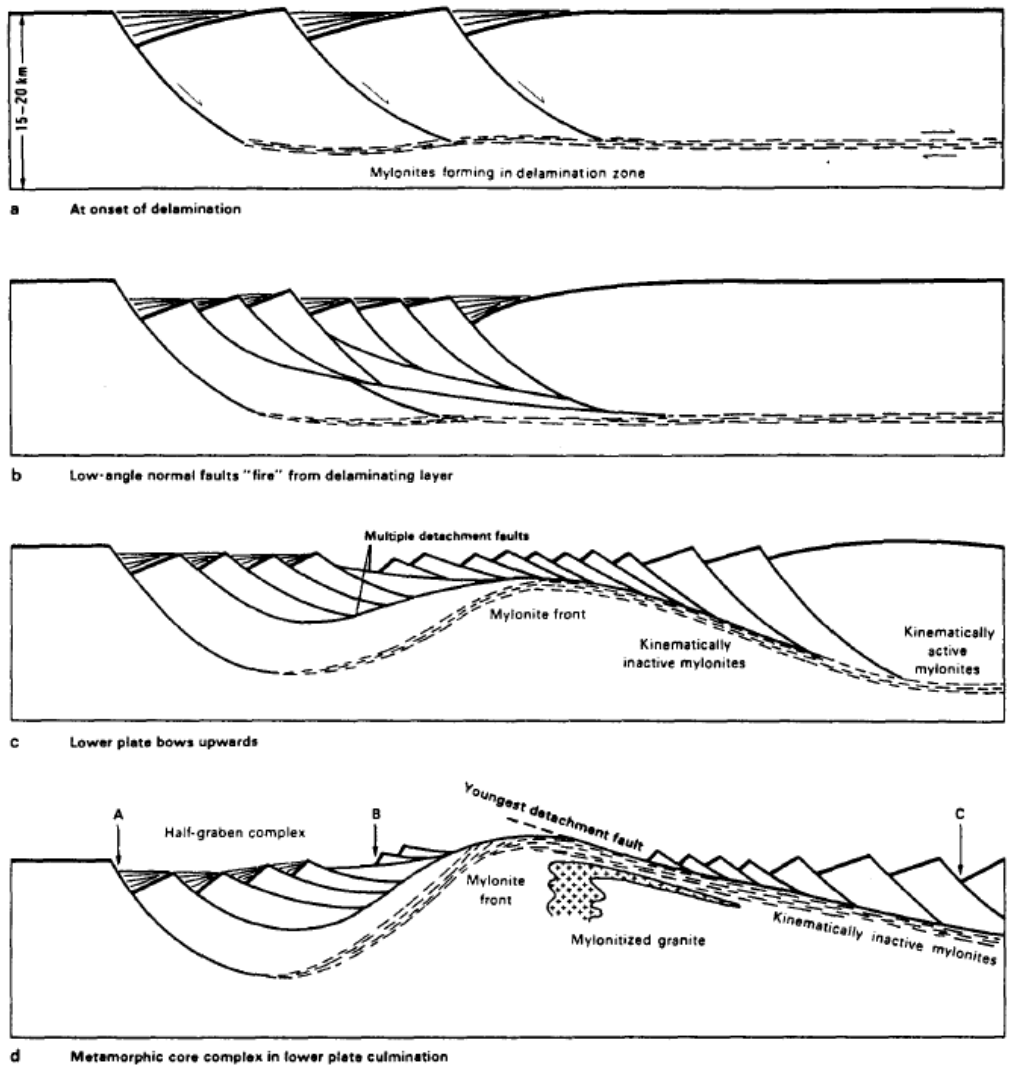

Figure 55: *Evolution of a metamorphic core complex (after Lister & David, 1989).*

In the Pohorje mountains the rocks of the LCA nappe represent the footwall and the UCA represents the hanging wall. Ductile deformation in general and mylonites reveal a dominant top to the east sense of shear. Profile AA' (figure 51) shows that an antiformal shape can also be observed in a

WNW-ESE cross section through the Pohorje mountains. The sense of shear is dominantly top-to-the-east on both sides of this structure. A shift in activity along this mylonite zone has not been observed during this research.

Metamorphism and overprinting relations

Lister & David (1989) proposed that the uppermost part of the footwall is deformed under a range of conditions during exhumation from considerable depths to the surface. Mylonitization in a relatively wide zone occurs under amphibolite facies conditions. Discrete, narrower zones overprint this zone under greenschist conditions slightly closer to the surface. When rocks are exhumed above the brittle-ductile boundary cataclasis of the rocks affects an even narrower zone until a discrete fault develops at the shallowest levels (Lister & David, 1989).

In the Pohorje mountains several features indicate that the conditions during deformation changes from ductile conditions to more shallow and brittle conditions. Ductile deformation structures that formed under retrograde greenschist conditions are found in a very thick zone, but is more intense near the contact between the LCA and UCA units. Furthermore, dynamic recrystallization structures show that lower temperature structures (BLG) overprint higher temperature structures (SGR). Also brittle structures are observed like a cataclastic zone at the contact between the nappes (Appendix; stop 82). Young N-S trending normal faults crosscut older ductile structures and indicate east directed extension in the same direction as the ductile extensional structures (Fodor et al., 2008). Thus a succession of deformation with the same sense of shear but representing progressively shallow depths is present in the Pohorje mountains. Although amphibolite facies metamorphism related to extensional tectonics are not observed in the Pohorje mountains (maximum temperatures around 500 °C), this sequence of overprinting relations is otherwise very similar to those observed in metamorphic core complexes.

Magmatism

The Pohorje pluton has long been considered to represent the easternmost expression of Periadriatic intrusions. Fodor et al. (2008) showed that the Miocene intrusion age of the Pohorje pluton makes it highly unlikely that this pluton is related to the Oligocene age Periadriatic intrusions. But, the age of intrusion is very similar to the age of rapid exhumation in the Pohorje Mountains, suggesting a causal relation between extension and magmatism.

The relation between magmatism and core complex formation has been described extensively in the literature (Lister & David, 1989, Lister & Baldwin, 1993, Coney & Harms, 1984, Charles et al., 2011, Denèle et al., 2011). Some authors favor a model with a pre-existing fault that governs exhumation before intrusion of granitic plutons. In this model the intrusion of the granite pluton may be the result of local decompression and partial melting. An opposing view on core complex formation is that the intrusion of melt and resulting heating of the country rocks weakens the crust, after which deformation along low angle detachments is initiated. In this model the formation of a core complex is driven by the intrusion (Lister & Baldwin, 1993).

A clue that extension may have preceded the intrusion of the pluton in the Pohorje mountains comes from Eggenburgian (~19 Ma) apatite fission track ages in detrital apatites (Sachsenhofer et al., 1998). These might indicate that uplift related to extension may have occurred slightly before the intrusion of the pluton. Furthermore the heating of Karpatian sediments indicated by vitrinite reflectance data shows a very high heat flow during the Karpatian. The heat flow can be significantly increased due to

magmatism. If deposition of transgressive sediments on Austroalpine basement preceded magmatism it would imply that deformation preceded the pluton and not vice versa. However, Sachsenhofer et al. (1998) could convincingly correlate the heating to the slightly younger dacitic volcanism in the western part of the Ribnica-Selnica trough and pointed out that only the heat of rapidly exhumed Austroalpine basement is also enough to create the required heat flows to explain the observations. Therefore, the relation between magmatism and deformation is still obscured although and intimate and genetic link is suspected.

Post Karpatian events

After the initial phase of rapid extension and subsidence during the Karpatian, tectonic activity slowed down (Gross et al., 2007). Continuous sedimentation is recorded in the eastern Styrian basin, north east of the Pohorje and Kozjak mountains, until the latest Sarmatian, earliest Pannonian (Gross et al., 2007). In the Pannonian, from 9 Ma onwards, the stress regime in the Pannonian basin changed from E-W extension to E-W compression (Peresson & Decker, 1997) as a result of far field intraplate stresses related to renewed west directed subduction of the European plate below the Carpathian arc. The exact timing for this change in stress regime is debated and might not have occurred simultaneously throughout the basin. Latest compression in the Carpathians was recorded at 11 Ma (Matenco et al., 2010). Local inversion of extensional structures, marking a compressional phase, has been recorded from 11-8 Ma (Horvath et al., 2006, Bada et al., 2001). Unconformities in the Vienna and Styrian basins, marking uplift in the western parts of the Pannonian basin, occurred slightly earlier between 12,3 and 12,1 Ma, during the Sarmatian (Harzhauser & Piller, 2004). In the Pohorje mountains apatite fission track ages of 11,1 – 9,8 Ma (Hendrickx et al., 2010) might be related with this phase of inversion. These apatite fission track ages do not vary from east to west over the pluton. This symmetry is in contrast with the earlier asymmetric exhumation, implying that a different process than exhumation along a low angle detachment has accommodated the later pulses of exhumation.

During this period, inversion of E-W extensional structures is recorded (Gosar, 2005, Pischinger et al., 2008) and N-S extension in and around the Styrian basin is observed (Peresson & Decker, 1997). This N-S extension could be related to the normal faulting of the Ribnica-Selnica trough. The exhumation could be the result of footwall uplift.

Several authors have recognized a Late Miocene to Pliocene deformation phase associated with NNW-SSE compression in the Pohorje Mountains (Fodor et al., 2008, Solva et al., 2005) and in the adjacent Mura basin just to the East of the Pohorje Mountains (Gosar et al., 2005).

The antiformal structure of the Pohorje mountains is thought to be related to this phase of N-S shortening. A northward shift of the Drava river basin is documented for this time (Solva et al., 2005). Combined geomorphological-tectonic research shows that until the latest Miocene the Drava river flowed through the western part of the Ribnica-Selnica trough, whereas today the Drava river channel crosscuts the Kozjak mountains 1 km to the north and only enters the trough just west of Selnica. Solva et al. (2005) relate this northward shift to asymmetric uplift and doming of the Pohorje-Kozjak area during compression starting around the Miocene-Pliocene boundary.

We recorded that S2 foliations are folded around a WSW plunging fold axis that could very well correspond to this phase of deformation. The foliations within the pluton and the orientations of the bedding of Miocene sediments can only be affected by deformation younger than Karpatian age.

Both are clearly folded during N-S to NNE-SSW shortening. Although this orientation is slightly different from the orientation described in the area, we suggest that these structures can be assigned to this phase of inversion.

The updoming during this phase is likely to be associated with the latest phase of uplift and erosion in the Pohorje mountains, especially in the central part of the mountain range. The occurrence of rocks without retrograde overprint containing kinematic indicators that are correlated to the older D2 deformation phase suggests that these rocks were only partly affected by the shearing of the D3 phase. Only during this later phase, erosion of the central part of the newly formed dome structure exposed these rocks at the surface.

Although coeval N-S shortening and E-W extension of the D3 phase is mechanically viable and probably has occurred, the attribution of the doming of the Pohorje mountains to the D3 phase does not fit with the timing of exhumation. Therefore, it might be more convenient to establish a D4 deformation phase that describes the folding into an antiformal structure and related deformation.

Regional implications

The transition from the Eastern Alps to the Pannonian basin is characterized in other areas by exhumation along low angle detachments. The Rechnitz window, for instance, is situated in a setting where low angle normal faults have resulted in the exhumation of a metamorphic core (Cao et al., 2013). The same genesis could be applicable to the Algyo block mentioned earlier.

Similar mechanisms of Miocene exhumation have been proposed for the Medvednica mountains in Croatia (Beniest et al., 2013). The Fruska Gora metamorphic core of northern Bosnia was exhumed as the footwall below a low angle detachments from 28 Ma onwards and later by normal faults (Toljic et al., 2013). This Oligocene age is slightly older than the Early Miocene ages proposed for most of the other structures. But it can be concluded that core complex formation affected the wider Eastern Alpine and Pannonian basin area. This phase typically predates the rift style extension during the middle Miocene. These core complexes, like the Pohorje metamorphic core complex, thus record the onset of a change in tectonic style. It is likely that older flatlying structures are more easily reactivated as low angle detachments than it would be to create new structures. Therefore, an early phase of extension along low angle detachments might be explained by the reactivation of existing weaknesses in the thick Alpine crust.

The driving forces between this shift in tectonic regime remain rather enigmatic. However, the importance of both the tensile stresses related to the rollback of the subducted European lithosphere along the Carpathian arc and compressional forces related to the indentation of Adria in the Eastern Alps should not be underestimated.

Summary & Conclusions

1. At least three deformation phases can be distinguished in the Pohorje area. The D1 isoclinal folding phase, that is most likely to be related with Cretaceous stacking of Austroalpine nappes. The D2 tight folding phase, that is related to the Paleogene emplacement of the Austroalpine nappes onto the European foreland. And the D3 phase that accommodated the exhumation of the high-grade metamorphic rocks and the pluton.
2. The high grade metamorphism of the Lower Central Austroalpine nappe is related to deep subduction at the culmination of the D1 phase during the Late Cretaceous.
3. Field observations and microstructural analysis can relate the D3 shear structures to retrograde conditions. D3 solid state deformation of the Pohorje pluton and Karpatian to Badenian age sediments containing eroded plutonic material, constrain the Karpatian age of this deformation phase.
4. E-W oriented stretching lineations and kinematic indicators (D3) reveal a dominant top to the East sense of shear. A low angle detachment with top-to-the-East sense of shear has governed the exhumation of the Pohorje pluton and the surrounding amphibolite facies metamorphic rocks as a footwall complex. The Pohorje mountains classify as a Cordilleran type metamorphic core complex.
5. The low angle detachment reactivated the Cretaceous nappe contact, between the LCA and UCA.
6. The Miocene exhumation of the Pohorje and Kozjak mountains in the footwall of a low angle detachment is characteristic for other small ranges (Medvednica Mountains, Rechnitz Window, Fruska Gora) at the transition between the Eastern Alps and the Pannonian basin.
7. In regions where extension and lateral extrusion affects a mountain range, sub horizontal pre-existing weakness zones, f.i. nappe contacts may be reactivated as low angle normal faults. This leads to the exhumation of metamorphic rocks in the footwall of these low angle faults. Extruded regions between strike slip faults do not behave as rigid blocks, but rather deform by similar mechanisms as described in this paper.

Acknowledgements

First and above all I would like to thank Inge van Gelder for her guidance during the first days in the field, for the numerous suggestions and improvements of the final text, for her close involvement during the process and in general for all the positive feedback and good moments. I would like to thank Ernst Willingshofer for the wise remarks at critical moments, the approachable attitude and good discussions. I could not wish for better supervision! Furthermore, I would like to thank Suzanne van Greuningen and Sabine Haalboom for letting me use their samples and data, for helping me with practical stuff regarding my field work and for advising me the best accommodation possible. I would like to thank Otto Stiekema and his collegues from the rock preparation lab at Utrecht University for making the thin sections. I am grateful to Herman van Roermund and Martin Drury for the useful discussions on metamorphic grade of eclogites and meta-pelitic rocks.

References

Bada, G., Horváth, F., Cloetingh, S., Coblentz, D.D. and Tóth, T. (2001), Role of topography-induced gravitational stresses in basin inversion: The case study of the Pannonian basin. Tectonics, vol. 20-3, pg. 343-363.

Beniest, A., Matenco, L., Willingshofer, E. and van Gelder, I.E. (2013), From orogenic buildup to extensional unroofing: The evolution of the Adria – Europe collisional zone in the Medvednica Mountains of Croatia. Master thesis, Utrecht University.

Cao, S.Y., Neubauer, F., Bernroider, M., Liu, J.L. and Genser, J. (2013), Structures, microfabrics and textures of the Cordilleran-type Rechnitz metamorphic core complex, Eastern Alps. Tectonophysics, vol. 608, pg. 1201-1225.

Collettini, C. (2011), The mechanical paradox of low-angle normal faults: Current understanding and open questions. Tectonophysics, vol. 510, pg. 253-268.

Coney, P.J. and Harms, T.A. (1984), Cordilleran metamorphic core complexes: Cenozoic extensional relics of Mesozoic compression. Geology, vol. 12, pg. 550-554.

Denèle, Y., Lecomte, E., Jolivet, L., Lacombe, O., Labrousse, L., Huet, B. and Le Pourhiet, L. (2011), Granite intrusion in a metamorphic core complex: The example of the Mykonos laccolith (Cyclades, Greece). Tectonophysics, vol. 501, pg. 52-70.

Dunkl, I. and Demény, A. (1997), Exhumation of the Rechnitz Window at the border of the Eastern Alps and Pannonian Basin during Neogene extension. Tectonophysics, vol. 272, pg. 197-211.

Fodor, L.I., Gerdes, A., Dunkl, I., Koroknai, B., Pècskay, Z., Trajanova, M., Horváth, P., Vrabec, M., Jelen, B., Balogh, K. and Frisch, W. (2008), Miocene emplacement and rapid unroofing of the Pohorje pluton at the Alpine-Pannonian-Dinaridic junction, Slovenia. Swiss Journal of Geosciences, vol. 101, pg. 255-271.

Frisch, W., Dunkl, I. and Kuhleman, J. (2000), Post-collisional orogen-parallel large-scale extension in the Eastern Alps. Tectonophysics, vol. 327, pg. 239-265.

Froitzheim, N., Plašienka, D. and Schuster, R. (2008), Alpine tectonics of the Alps and Western Carpathians. Geol. Soc. London Special Publications, Tectonic Aspects of the Alpine-Dinaride-Carpathian System, 978-1-86239-252-6.

Gosar, A. (2005), Geophysical and structural characteristics of the pre-Tertiary basement of the Mura Depression (SW Pannonian Basin, NE Slovenia). Geologica Carpathica, vol. 56-2, pg. 103-112.

Gross, M., Fritz, I., Piller, W.E., Soliman, A., Harzhauser, M., Hubmann, B., Moser, B., Scholger, R., Suttner, T.J. and Bojar, H.-P. (2007), The Neogene of the Styrian basin – Guide to Excursions. Joannea Geol. Paläont., vol. 9, pg. 117-193.

Haalboom, S., Willingshofer, E.W. and van Gelder, I.E. (2013), Miocene exhumation of the Pohorje Pluton in the Eastern Alps in relation to Indentation of Adria and lateral extrusion towards the Pannonian Basin. Master thesis, Utrecht University.

Hamor, G., Ravasz-baranyai, L., Balogh, K. and Arva-Sos, E. (1980), Radiometric ages of the Miocene rhyolite tuff horizons in Hungary. Máfi Evi JeIentise 1978-ról, 65-73 [in Hungarian with English abstract].

Harzhauser, M. and Piller, W.E. (2004), Integrated stratigraphy of the Sarmatian (Upper Middle Miocene) in the western Central Paratethys. Stratigraphy, vol. 1-1, pg. 65-86.

Hendrikx, J., Brautigam, K., Wijbrans, J., Foeken, J. and Andriesen, P. (2010), Rapid and uneven cooling of the Pohorje pluton in NE Slovenia during the Miocene. Master thesis, Vrije Universiteit Amsterdam.

Horváth, F., Bada, G., Szafián, P., Tari, G., Ádám, A. and Cloetingh, S. (2006), Formation and deformation of the Pannonian Basin: constraints from observational data. Geological Society, London, Memoirs, vol. 32, pg. 191-206

Janák, M., Froitzheim, N., Lupták, B., Vrabec, M. and Krogh Ravna, E.J. (2004), First evidence for ultrahigh-pressure metamorphism of eclogites in Pohorje, Slovenia: Tracing deep continental subduction in the Eastern Alps. Tectonics, vol. 23, TC5014, doi: 10.1029/2004TC001641.

Janák, M., Froitzheim, N., Vrabec, M., Krogh Ravna, E.J. and De Hoog, J.C.M. (2006), Ultrahigh-pressure metamorphism and exhumation of garnet peridotite in Pohorje, Eastern Alps. Journal of metamorphic Geology, vol. 24, pg. 19-31.

Kirst, F., Sandmann, S., Nagel, T.J., Froitzheim, N. and Janák, M. (2010), Tectonic evolution of the southeastern part of the Pohorje Mountains (Eastern Alps, Slovenia). Geoligica Carpathica, vol. 61, pg. 451-461.

Kurz, W., Fritz, H., Tenczer, V. and Unzog, W. (2002), Tectonometamorphic evolution of the Koralm Complex (Eastern Alps): constraints from microstructures and textures of the 'Plattengneis' shear zone. Journal of Structural Geology, vol. 24, pg. 1957-1970.

Lister, G.S. and Baldwin, S.L. (1993), Plutonism and the origin of metamorphic core complexes. Geology, vol. 21, pg. 607-610.

Lister, G.S. and Davis, G.A. (1989), The origin of metamorphic core complexes and detachment faults formed during the Tertiary continental extension in the northern Coloradi River region, U.S.A.. Journal of Structural Geology, vol. 11, pg. 65-94.

Luth, S., Willingshofer, E., Sokoutis, D. and Cloetingh, S. (2013), Does subduction polarity change below the Alps? Inferences from analogue modelling. Tectonophysics, vol. 582, pg. 140-161.

Matenco, L., Krézsek, C., Merten, S., Schmid, S., Cloetingh, S. and Andriessen, P. (2010), Characteristics of collisional orogens with low topographic build-up: an example from the Carpathians. Terra Nova, vol. 22, pg. 155-165.

Mioč, P. 1978: Geology of the sheet Slovenj Gradec L 33–55 1:100000. Federal Geological Survey of Yugoslavia, Belgrade, 74 pp.

Mioč, P. & Žnidarčič, M. 1977: Geological map of the sheet Slovenj Gradec, L33–55, 1:100000. Federal Geological Survey of Yugoslavia, Belgrade.

Neubauer, F., Genser, J. and Handler, R. (2000), The Eastern Alps: Result of a two-stage collision process. Miit. Österr. Geol. Ges., vol. 92, pg. 117-134.

Passchier, C.W. and Trouw, R.J.A. (2005), Microtectonics, 2nd edition. Springer Berlin Heidelberg New York, ISBN-10: 3-540-64003-7, ISBN-13: 978-3-540-64003-7.

Peresson, H. and Decker, K. (1997), Far-field effects of Late Miocene subduction in the Eastern Carpathians: E-W compression and inversion of structures in the Alpine-Carpathian-Pannonian region. Tectonics, vol. 16-1, pg. 38-56.

Pisschinger, G., Kurz, W., Übleis, M., Egger, M., Fritz, H., Brosch, J.F. and Stingl, K. (2008), Fault slip analysis in the Koralm Massif (Eastern Alps) and consequences for the final uplift of "cold spots" in Miocene times. Swiss Journal of Geosciences, vol. 101-0, pg. 235-254.

Ratschbacher, L., Frisch, W., Neubauer, F., Schmid, S.M. and Neugebauer, J. (1989), Extension in compressional orogenic belts: The eastern Alps. Geology, vol. 17, pg. 404-407.

Sachsenhofer, R.F., Dunkl, I., Hasenhüttl, C. and Jelen, B. (1998), Miocene thermal history of the southwestern margin of the Styrian Basin: vitrinite reflectance and fission-track data form the Pohorje/Kozjak area (Slovenia). Tectonophysics, vol. 297, pg. 17-29.

Sassi, R., Mazzoli, C., Miller, C. and Konzett, J. (2004), Geochemistry and metamorphic evolution of the Pohorje Mountain eclogites from the easternmost Austroalpine basement of the Eastern Alps (Northern Slovenia). Lithos, vol. 78, pg. 235-261.

Schmid, S.M., Pfiffner, O.A., Froitzheim, N., Schönborn, G. and Kissling, E. (1996), Geophysical-geological transect and tectonic evolution of the Swiss-Italian Alps. Tectonics, vol. 15-5, pg. 1036-1064.

Schmid, S.M., Bernoulli, D., Fügenschuh, B., Matenco, L., Schefer, S., Schuster, R., Tischler, M. and Ustaszewski, K. (2008), The Alpine-Carpathian-Dinaridic orogenic system: correlation and evolution of tectonic units. Swiss Journal of Geosciences, vol. 101, pg. 139-181.

Schmid, S.M., Fügenschuh, B., Kissling, E. and Schuster, R. (2004), Tectonic map and overall architecture of the Alpine orogen. Eclogae Geologicae Helveticae, vol. 97, pg. 93-117.

Simpson, C. and De Poar, D.G. (1993), Strain and kinematic analysis in general shear zones. Journal of Structural Geology, vol. 15-1, pg. 1-20.

Sölva, H., Stüwe, K. and Strauss, P. (2005), The Drava river and the Pohorje mountain range (Slovenia): geomorphological interactions. Mitt. Naturwiss. Ver. Steiermark, vol. 134, pg. 45-55.

Spear,F.S., and Cheney, J.T. (1989), A petrogenetic grid for pelitic schists in the system SiO_2 - Al_2O_3 - FeO - MgO - K_2O - H_2O. Contributions to Mineralogy and Petrology, vol. 134, pg. 17-32.

Steininger, F., Müller, C. and Rögl, F. (1988), Correlation of Central Paratethys, Eastern Paratethys, and Mediterranean Neogene stages. In: Royden, L.H. & Horváth, F. (Eds.): The Pannonian Basin. American Association of Petroleum Geologists Memoir, vol. 45, pg. 79–87.

Stipp, M., Stünitz, H., Heilbronner, R. and Schmid S.M. (2002), Dynamic recrystallization of quartz: correlation between natural and experimental conditions. Geological Society, London, Special Publications, vol. 200, pg. 171-190.

Szafián, P., Tari, G., Horváth, F. and Cloetingh, S. (1999), Crustal structure of the Alpine-Pannonian transition zone: a combined seismic and gravity study. Int. Journ. Earth Sciences, vol. 88, pg. 98-110.

Tari, G., Dövenyi, P., Dunkl, I., Horvath, F., Lenkey, L., Stefanescu, M., Szafián, P. and Tóth, T. (1999), Lithospheric structure of the Pannonian basin derived from seismic, gravity and geothermal data. Geological Society, London, Special Publications, vol. 156, pg. 215-250.

Thöni, M. (2002), Sm-Nd isotope systematics in garnet from different lithologies (Eastern Alps): age results, and an evaluation of potential problems for garnet Sm-Nd chronometry. Chemical Geology, 185, 255–281.

Toljic, M., Matenco, L., Ducea, M.N., Stojadinovic, U., Milivojevic, J. and Deric, N. (2013), The evolution of a key segment in the Europe-Adria collision: The Fruska Gora of northern Serbia. Global and Planetary Change, vol. 103, pg. 39-62.

Trajanova, M., Pécskay, Z. and Itaya, T. (2008), K-Ar geochronology and petrography of the Miocene Pohorje Mountains batholith (Slovenia). Geologica Carpathica, vol. 59-3, 247-260.

Tullis, J. and Yund, R.A. (1985), Dynamic recrystallization of feldspar: A mechanism for ductile shear zone formation. Geology, vol. 13, pg. 238-241.

Ustaszewski, K., Schmid, S.M., Fügenschuh, B., Tischler, M., Kissling, E. and Spakman, W. (2008), A map-view restoration of the Alpine-Carpathian-Dinaridic system for the Early Miocene. Swiss J. Geosci., vol. 101-1, pg. 273-294.

Voll, G. (1976), Recrystallization of quartz, biotite and feldspar from Erstfeld to the Levantine Nappe, Swiss Alps, and its geological significance. Schweiz. mineral. Petrogr. Mitt., vol. 56, pg. 641-647.

Vrabec, M. (2010), Garnet peridotites from Pohorje: Petrography, geothermobarometry and metamorphic evolution. Geologija, vol.53, pg. 21-36.

Willingshofer, E., Neubauer, F. and Cloetingh, S. (1999), the significance of Gosau-type basins for the Late Cretaceous tectonic history of the Alpine-Carpathian belt. Phys. Chem. Earth (A), vol. 24-8, pg. 687-695.

Wölfler, A., Kurz, W., Danišík, M. and Rabitsch, R. (2010), Dating of fault zone activity by apatite fission track and apatite (U-Th)/He thermochronometry: a case study from the Lavanttal fault system (Eastern Alps). Terra Nova, vol. 22, pg. 274-282.

Zheng, Y., Wang, T., Ma, M. and Davis, G.A. (2004), Maximum effective moment criterion and the origin of low-angle normal faults. Journal of Structural Geology, vol. 26, pg. 271-185.